TEXAS INSTRUMENTS

LM25149 超低 I$_Q$、アクティブ EMI フィルタ内蔵、42V 同期整流降圧 DC/DC コントローラ

1 特長

- 機能安全対応
  - 機能安全システムの設計に役立つ資料を利用
- 2 つの EMI 低減機能を内蔵
  - 低周波数での EMI 性能を向上させるアクティブ EMI フィルタ
  - 低周波数帯域と高周波数帯域にわたる EMI 性能を向上させる選択可能なデュアル・ランダム・スペクトラム拡散 (DRSS)
  - EMI を平均 25dBµV 低減
  - 外部差動モード入力フィルタのサイズを 50% 低減、システム・コストを低減
  - CISPR 32 Class B 要件に対して最適化
- 多用途の同期整流降圧 DC/DC コントローラ
  - 3.5V～42V の広い入力電圧範囲
  - 精度 1% の固定 3.3V、5V、12V 出力または可変出力 (0.8V～36V)
  - 最大接合部温度：150℃
  - シャットダウン・モード電流：2.3µA
  - 無負荷時スリープ電流：9.5µA
  - 最大 2 フェーズをスタック可能
  - 周波数フォールドバックによる高度なドロップアウト
- スイッチング周波数：100kHz～2.2MHz
  - SYNC In および SYNC Out 機能
- 堅牢な設計用の本質的な保護機能
  - ヒカップ・モードによる過電流の内部保護
  - ENABLE および PGOOD 機能
  - VCC、VDDA、ゲート駆動の UVLO 保護
  - 内部または外部ループ補償
  - ヒステリシス付きのサーマル・シャットダウン保護
- LM25149 と WEBENCH® Power Designer

2 アプリケーション

- ビル・オートメーション
- 産業用輸送
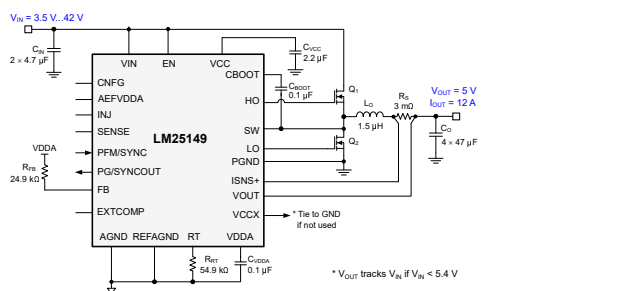- ワイヤレス・インフラ
- 試験 / 測定機器

3 概要

LM25149 は、大電流、シングル出力のアプリケーション向けに対応した、42V の超低静止電流 (I$_Q$) の同期整流降圧 DC/DC コントローラです。本コントローラはピーク電流モード制御アーキテクチャを採用しているため、ループ補償が簡単、過渡応答が高速であり、負荷およびライン・レギュレーションが非常に優れています。LM25149 は、大電流アプリケーション向けに高精度の電流共有を行う、インターリーブ・デュアル位相モードで設定できます。必要に応じて最低 3.5V の V$_{IN}$、ほぼ 100% のデューティ・サイクルで動作できます。

LM25149 は、アクティブ EMI フィルタとデュアル・ランダム・スペクトラム拡散 (DRSS) という 2 つの独自の EMI 低減機能を備えています。アクティブ EMI フィルタは、DC 入力バス上のすべてのノイズまたはリップル電圧を検出し、逆位相のキャンセル信号を注入することで、妨害を低減します。DRSS は、低周波数の三角変調と高周波のランダム化変調を組み合わせ、それぞれ低い周波数帯域と高い周波数帯域にわたって EMI を低減します。このハイブリッド手法は、業界標準の EMC テストで規定されている複数分解能帯域幅 (RBW) 設定に適合します。
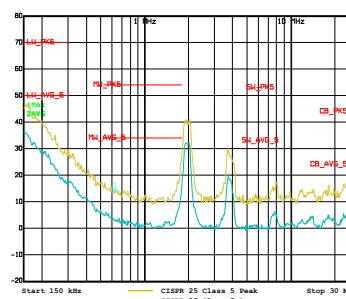
製品情報

部品番号	パッケージ[(1)]	本体サイズ (公称)
LM25149	VQFN (24)	3.5mm × 5.5mm

(1) 利用可能なすべてのパッケージについては、このデータシートの末尾にある注文情報を参照してください。

代表的なアプリケーション回路図

CISPR 25 EMI 性能 (150kHz～30MHz)

English Data Sheet: SNVSBV5

Table of Contents

4 Revision History

資料番号末尾の英字は改訂を表しています。 その改訂履歴は英語版に準じています。

Changes from Revision A (April 2021) to Revision B (December 2021)	Page
• ドキュメントのステータスを事前情報から量産データに変更.. 1	

5 概要 (続き)

LM25149 の追加機能として、最大 150℃の接合部温度での動作、ユーザー選択可能なダイオード・エミュレーションによる軽負荷時消費電流の低減、オープンドレインのパワー・グッド・フラグによるフォルト報告と出力監視、高精度イネーブル入力、プリバイアスされた負荷への単調なスタートアップ、内蔵 VCC バイアス電源レギュレータとブートストラップ・ダイオード、内蔵 3ms ソフト・スタート時間、自動回復機能付きサーマル・シャットダウン保護があります。

LM25149 コントローラは、熱特性が強化された 3.5mm × 5.5mm の 24 ピン VQFN パッケージで供給されます。放熱特性を改善するため露出パッドが付属しています。.

6 Pin Configuration and Functions
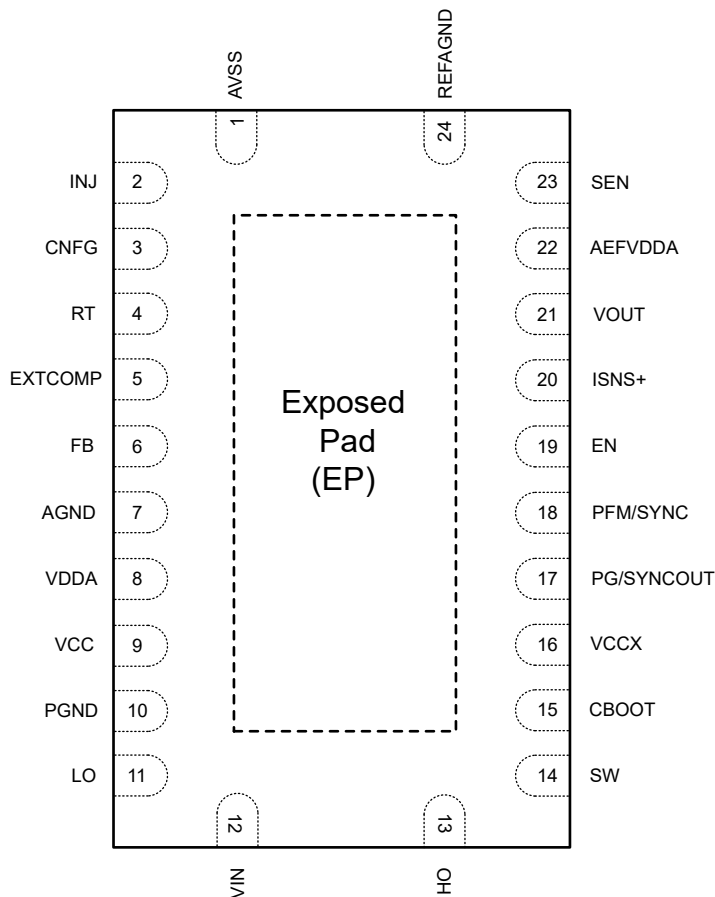
Connect the exposed pad to AGND and PGND on the PCB.

図 6-1. 24-Pin VQFN RGY Package (Top View)

表 6-1. Pin Functions

PIN		I/O[1]	DESCRIPTION
NO.	NAME		
1	AVSS	G	Active EMI bias ground connection
2	INJ	O	Active EMI injection output
3	CNFG	1	Connect a resistor to ground to set primary/secondary, spread spectrum enable/disable, or interleaved operation. After start-up, CNFG is used to enable AEF.
4	RT	I	Frequency programming pin. A resistor from RT to AGND sets the oscillator frequency between 100 kHz and 2.2 MHz.
5	EXTCOMP	O	The output of the transconductance amplifier. If used, connect the compensation network from EXTCOMP to AGND.

Product Folder Links: *LM25149*

表 6-1. Pin Functions (continued)

PIN		I/O[1]	DESCRIPTION
NO.	NAME		
6	FB	I	Connect FB to VDDA to set the output voltage to 3.3 V. Connect FB using a 24.9 kΩ or 49.9 kΩ to VDDA to set the output voltage to 5 V or 12 V, respectively. Install a resistor divider from VOUT to AGND to set the output voltage setpoint between 0.8 V and 36 V. The regulation voltage at FB is 0.8 V.
7	AGND	G	Analog ground connection. Ground return for the internal voltage reference and analog circuits
8	VDDA	O	Internal analog bias regulator. Connect a ceramic decoupling capacitor from VDDA to AGND.
9	VCC	P	VCC bias supply pin. Connect ceramic capacitors between VCC and PGND.
10	PGND	G	Power ground connection pin for low-side power MOSEFT gate driver
11	LO	O	Low-side power MOSFET gate driver output
12	VIN	P	Supply voltage input source for the VCC regulators
13	HO	O	High-side power MOSFET gate driver output
14	SW	P	Switching node of the buck regulator and high-side gate driver return. Connect to the bootstrap capacitor, the source terminal of the high-side MOSFET, and the drain terminal of the low-side MOSFET.
15	CBOOT	P	High-side driver supply for bootstrap gate drive
16	VCCX	P	Optional input for an external bias supply. If V_{VCCX} > 4.3 V, VCCX is internally connected to VCC and the internal VCC regulator is disabled.
17	PG/SYNCOUT	P	An open-collector output that goes low if V_{OUT} is outside the specified regulation window. The PG/SYNCOOUT pin of the primary controller in dual-phase mode provides a 180° phase-shifter SYNCOUT signal.
18	PFM/SYNC	I	Connect PFM/SYNC to VDDA to enable diode emulation mode. Connect PFM to GND to operate the LM25149 in forced PWM (FPWM) mode with continuous conduction at light loads. PFM can also be used as a synchronization input to synchronize the internal oscillator to an external clock.
19	EN	I	An active-high precision input with rising threshold of 1 V and hysteresis current of 10 µA. If the EN voltage is less than 0.5 V, the LM25149 is in shutdown mode, unless a SYNC signal is present on PFM/SYNC.
20	ISNS+	I	Current sense amplifier input. Connect the ISNS+ to the inductor side of the external current sense resistor (or to the relevant sense capacitor terminal if inductor DCR current sensing is used) using a low-current Kelvin connection.
21	VOUT	I	Output voltage sense and the current sense amplifier input. Connect VOUT to the output side of the current sense resistor (or to the relevant sense capacitor terminal if inductor DCR current sensing is used).
22	AEFVDDA	P	Active EMI bias power. Connect a ceramic capacitor between AEFVDDA and AVSS.
23	SENSE	I	Active EMI sense input
24	REFAGND	G	Active EMI reference ground

(1)   P = Power, G = Ground, I = Input, O = Output

Product Folder Links: *LM25149*

7 Specifications

7.1 Absolute Maximum Ratings

Over the recommended operating junction temperature range of –40℃ to 150℃ (unless otherwise noted). [(1)]

		MIN	MAX	UNIT
Output voltage	VOUT, ISNS+ to AGND	–0.3	36	V
	VOUT to ISNS+	–0.3	0.3	V
Input voltage	VIN to PGND	–0.3	47	V
	SW to PGND	–0.3	47	V
	SW to PGND, transient < 20 ns	–2		V
	CBOOT to SW	–0.3	6.5	V
	CBOOT to SW, transient < 20 ns	–5		V
	HO to SW	–0.3	V_{HB} + 0.3	V
	HO to SW, transient < 20ns	–5		V
	LO to PGND	–0.3	V_{VCC} + 0.3	V
	LO to PGND, transient < 20 ns	–1.5		V
	EN to PGND	–0.3	47	V
	VCC, VCCX, VDDA, PG, FB, PFM/SYNC, RT, EXTCOMP to AGND	–0.3	6.5	V
	AEFVDDA to AVSS	–0.3	5.5	V
	INJ to REFAGND	–0.3	5.5	V
	SEN to REFAGND	0.3	47	V
	REFAGND to AVSS	-0.3	0.3	V
	CNFG to AGND	–0.3	5.5	V
Operating junction temperature, T_J		–40	150	°C
Storage temperature, T_{stg}		–55	150	°C

(1) Stresses beyond those listed under *Absolute Maximum Ratings* may cause permanent damage to the device. These are stress ratings only, which do not imply functional operation of the device at these or any other conditions beyond those indicated under the *Recommended Operating Conditions*. Exposure to absolute-maximum-rated conditions for extended periods may affect device reliability.

7.2 ESD Ratings

			VALUE	UNIT
$V_{(ESD)}$	Electrostatic discharge	Human-body model (HBM), per ANSI/ESDA/ JEDEC JS-001 [(1)]	±2000	V
		Charged device model (CDM), per ANSI/ESDA/ JEDEC JS-002 [(2)]	±750	

(1) JEDEC document JEP155 states that 500-V HBM allows safe manufacturing with a standard ESD control process.
(2) JEDEC document JEP157 states that 250-V CDM allows safe manufacturing with a standard ESD control process.

Product Folder Links: *LM25149*

7.3 Recommended Operating Conditions

Over operating junction temperature range junction temperature range of –40℃ to 150℃ (unless otherwise noted)

		MIN	NOM	MAX	UNIT
V_{IN}	Input supply voltage range	3.5		42	V
V_{OUT}	Output voltage range	0.8		36	V
	SW to PGND	–0.3		42	V
	CBOOT to SW	–0.3	5	5.25	V
	FB, EXTCOMP, RT to AGND	–0.3		5.25	V
	EN to PGND	–0.3		42	V
	VCC, VCCX, VDDA to PGND	–0.3	5	5.25	V
	VOUT, ISNS+ to PGND	–0.3		36	V
	PGND to AGND	–0.3		0.3	V
	AEFVDDA to AVSS	–0.3		5	V
	INJ to REFAGND	–0.3		5	V
	SEN to REFAGND	–0.3		36	V
	REFAGND to AVVS	–0.3		0.3	V
	CNGF to AGND	–0.3		5.5	V
T_J	Operating junction temperature	–40		150	°C

7.4 Thermal Information

THERMAL METRIC[1]		LM25149 is a 42-V	UNIT
		RGY (VQFN)	
		24 PINS	
$R_{\theta JA}$	Junction-to-ambient thermal resistance	37.3	°C/W
$R_{\theta JC(top)}$	Junction-to-case (top) thermal resistance	32	
$R_{\theta JB}$	Junction-to-board thermal resistance	15.5	
Ψ_{JT}	Junction-to-top characterization parameter	1.2	
Ψ_{JB}	Junction-to-board characterization parameter	15.5	
$R_{\theta JC(bot)}$	Junction-to-case (bottom) thermal resistance	5.6	

(1)   For more information about traditional and new thermal metrics, see the *Semiconductor and IC Package Thermal Metrics* application report.

7.5 Electrical Characteristics

T_J = –40°C to 150°C. Typical values are at T_J = 25°C and V_{IN} = 12 V (unless otherwise noted).

PARAMETER		TEST CONDITIONS	MIN	TYP	MAX	UNIT
SUPPLY (VIN)						
I_{Q-VIN1}	VIN shutdown current	V_{EN} = 0 V		2.3	3.8	µA
I_{Q-VIN2}	VIN standby current	Non-switching, 0.5 ≥ V_{EN} ≤ 1 V		124		µA
I_{SLEEP1}	Sleep current, 3.3 V	1.03 V ≤ V_{EN} ≤ 42 V, V_{VOUT} = 3.3 V, in regulation, no-load, not switching, V_{PFM}/SYNC = 0 V		9.5	19.7	µA
I_{SLEEP2}	Sleep current, 5.0 V	V_{EN} = 5 V, V_{VOUT} = 5.0 V, in regulation, no-load, not switching, $V_{PFM/SYNC}$ = 0 V		9.9	19.9	µA
ENABLE (EN)						
V_{SDN}	Shutdown to standby threshold	V_{EN} rising		0.5		V
$V_{EN-HIGH}$	Enable voltage rising threshold	V_{EN} rising, enable switching	0.95	1.0	1.05	V
I_{EN-HYS}	Enable hysteresis	V_{EN} = 1.1 V	–12	–10	–8	µA
INTERNAL LDO (VCC)						
$V_{VCC-REG}$	VCC regulation voltage	I_{VCC} = 0 mA to 100 mA	4.7	5	5.3	V
$V_{VCC-UVLO}$	VCC UVLO rising threshold		3.3	3.4	3.5	V
$V_{VCC-HYST}$	VCC UVLO hysteresis			148		mV

T_J = –40°C to 150°C. Typical values are at T_J = 25°C and V_{IN} = 12 V (unless otherwise noted).

PARAMETER		TEST CONDITIONS	MIN	TYP	MAX	UNIT
$I_{VCC-REG}$	Internal LDO short-circuit current limit		115	170		mA
INTERNAL LDO (VDDA)						
$V_{VDDA-REG}$	VDDA regulation voltage		4.75	5	5.25	V
$V_{VDDA-UVLO}$	VDDA UVLO rising	V_{VCC} rising, V_{VCCX} = 0 V	3	3.2	3.3	V
$V_{VDDA-HYST}$	VDDA UVLO hysteresis	V_{VCCX} = 0 V		120		mV
R_{VDDA}	VDDA resistance	V_{VCCX} = 0 V		5.5		Ω
EXTERNAL BIAS (VCCX)						
$V_{VCCX-ON}$	VCCX$_{(ON)}$ rising threshold		4.1	4.3	4.4	V
$V_{VCCX-HYST}$	VCCX hysteresis voltage	V_{VCCX} = 5 V		130		mV
R_{VCCX}	VCCX resistance	V_{VCCX} = 5 V		2		Ω
REFERENCE VOLTAGE						
V_{REF}	Regulated FB voltage		795	800	808	mV
OUTPUT VOLTAGE (VOUT)						
$V_{OUT-3.3V-INT}$	3.3-V output voltage setpoint	R_{FB} = 0 Ω, V_{IN} = 3.8 V to 42 V , internal COMP	3.267	3.3	3.333	V
$V_{OUT-3.3V-EXT}$	3.3-V output voltage setpoint	R_{FB} = 0 Ω, V_{IN} = 3.8 V to 42 V, external COMP	3.267	3.3	3.33	V
$V_{OUT-5V-INT}$	5-V output voltage setpoint	R_{FB} = 24.9 kΩ, V_{IN} = 5.5 V to 42 V, internal COMP	4.95	5.0	5.05	V
$V_{OUT-5VEXT}$	5-V output voltage setpoint	R_{FB} = 24.9 kΩ, V_{IN} = 5.5 V to 42 V, external COMP	4.95	5.0	5.05	V
$V_{OUT-12V-INT}$	12-V output setpoint	R_{FB} = 48.7 kΩ, V_{IN} = 24 V to 42 V, internal COMP	11.88	12	12.12	V
$V_{OUT-12V-EXT}$	12-V output setpoint	R_{FB} = 48.7 kΩ, V_{IN} = 24 V to 42 V, external COMP	11.88	12	12.12	V
$R_{FB-OPT1}$	5-V output select		23	25	27	kΩ
$R_{FB-OPT2}$	12-V output select		47	50	53	kΩ
ERROR AMPLIFIER (COMP)						
$g_{m-EXTERNAL}$	EA transconductance, external compensation	FB to EXTCOMP	1020	1200		µS
$g_{m-INTERNAL}$	EA transconductance, internal compensation	FB to EXTCOMP, EXTCOMP 100 kΩ to VDDA		30		µS
I_{FB}	Error amplifier input bias current				75	nA
$V_{COMP-CLAMP}$	COMP clamp voltage	V_{FB} = 0 V		2.1		V
$I_{COMP-SRC}$	EA source current	$V_{EXTCOMP}$ = 1 V, V_{FB} = 0.6 V		180		µA
$I_{COMP-SINK}$	EA sink current	$V_{EXTCOMP}$ = 1 V, V_{FB} = 1 V		180		µA
R_{COMP}	Internal compensation	EXTCOMP 100 kΩ to VDDA		400		kΩ
C_{COMP}	Internal compensation	EXTCOMP 100 kΩ to VDDA		50		pF
$C_{COMP-HF}$	Internal compensation	EXTCOMP 100 kΩ to VDDA		1		pF
PULSE FREQUENCY MODULATION (PFM/SYNC)						
V_{PFM-LO}	PFM detection threshold low		0.8			V
V_{PFM-HI}	PFM deception threshold high				2.0	V
V_{ZC-SW}	Zero-cross threshold			–5.5		mV
V_{ZC-DIS}	Zero-cross threshold disable	PFM=VDDA, 1000 SW cycles after first HO pulse		100		mV
$F_{SYNCIN3}$	Frequency sync range	R_{RT} = 10 kΩ, ±20 % of the nominal oscillator frequency	1.74		2.70	MHz
$t_{SYNC-MIN3}$	Minimum pulse-width of external synchronization signal		20		250	ns
$t_{SYNCIN-HO}$	Delay from PFM faling edge to HO rising edge			45		ns
$t_{PFM-FILTER}$	SYNCIN to PFM mode		13		45	µs
DUAL RANDOM SPREAD SPECTRUM (DRSS)						
Δf_C	Modulation frequency percentage change			7		%

Submit Document Feedback

Product Folder Links: *LM25149*

T_J = –40°C to 150°C. Typical values are at T_J = 25°C and V_{IN} = 12 V (unless otherwise noted).

PARAMETER		TEST CONDITIONS	MIN	TYP	MAX	UNIT
f_m	Modulation frequency		8.2		16.2	kHz
SWITCHING FREQUENCY						
V_{RT}	RT pin regulation voltage	10 kΩ < R_{RT} < 100 kΩ		0.5		V
F_{SW1}	Switching frequency 1	R_{RT} = 97.6 kΩ to GND		0.220		MHz
F_{SW2}	Switching frequency 2	V_{IN} = 12 V, R_{RT} = 9.09 kΩ to GND	1.98	2.2	2.42	MHz
F_{SW3}	Switching frequency 3	R_{RT} = 220 kΩ to GND		100		kHz
$SLOPE_1$	Internal slope compensation 1	R_{RT} = 9.09 kΩ		600		mV/µs
$SLOPE_2$	Internal slope compensation 2	R_{RT} = 97.6 kΩ		50		mV/µs
$t_{ON(min)}$	Minimum on-time			50		ns
$t_{OFF(min)}$	Minimum off-time			90		ns
POWER GOOD (PG)						
V_{PG-UV}	Power Good UV trip level	Falling with respect to the regulated voltage	90%	92%	94%	
V_{PG-OV}	Power Good OV trip level	Rising with respect to the regulation voltage	108%	110%	112%	
$V_{PG-UV-HYST}$	Power Good UV hysteresis	Fallinge with respect to the regulated output		3.6%		
$V_{PG-OV-HYST}$	Power Good OV hysteresis	Rising with respect to the regulation voltage		3.4%		
$t_{-PG-RISING-DLY}$	OV filter time	V_{OUT} rising		25		µs
$t_{-PG-FALL-DLY}$	UV filter time	V_{OUT} falling		25		µs
V_{PG-OL}	PG/SYNC voltage	Open collector, $I_{PG/SYNC}$ = 2 mA			0.8	V
SYNCHRONIZATION OUTPUT (PG/SYNCOUT)						
$V_{SYNCOUT-LO}$	SYNCO-LO low-state voltage	R_{CONFIG} = 54.9 kΩ or 71.5 kΩ to VDDA (primary), $I_{PG/SYNCOUT}$ = 2 mA			0.8	V
$V_{SYNCOUT-HO}$	SYNCO-HO high-state voltage	R_{CONFIG} = 54.9 kΩ or 71.5 kΩ to VDDA (primary), $I_{PG/SYNCOUT}$ = 2 mA.	2.0			V
$t_{SYNCOUT}$	Delay from HO rising edge to SYNCOUT (PGOOD pin in primary mode)	V_{PFM} = VDDA, F_{SW} set by R_{RT} = 100 kΩ		2.1		µs
STARTUP (Soft Start)						
t_{SS-INT}	Internal fixed soft-start time		1.9	3	4.6	ms
BOOT CIRCUIT						
$V_{BOOT-DROP}$	Internal diode forward drop	I_{CBOOT} = 20 mA, VCC to CBOOT	0.63	0.8		V
I_{BOOT}	CBOOT to SW quiescent current, not swwitching	V_{EN} = 5 V, $V_{CBOOT-SW}$ = 5 V	3.0		4.2	µA
$V_{BOOT-SW-UV-R}$	CBOOT to SW UVLO rising threshold	$V_{CBOOT-SW}$ rising		2.83		V
$V_{BOOT-SW-UV-F}$	CBOOT to SW UVLO falling threshold	$V_{CBOOT-SW}$ falling		2.5		V
$V_{BOOT-SW-UV-HYS}$	CBOOT to SW UVLO hysteresis			0.05		V
V_{HO-LOW}	HO low-state output voltage	I_{HO} = 100 mA		38		mV
HIGH-SIDE GATE DRIVER (HO)						
$V_{HO-HIGH}$	HO high-state output voltage	I_{HO} = –100 mA, , $V_{HO-HIGH}$ = V_{CBOOT} – V_{HO}		106		mV
V_{HO-LOW}	HO low-state output voltage	I_{HO} = 100 mA		50		mV
$t_{HO-RISE}$	HO rise time (10% to 90%)	C_{LOAD} = 2.7 nF		7		ns
$t_{HO-FALL}$	HO fall time (90% to 10%)	C_{LOAD} = 2.7 nF		7		ns
I_{HO-SRC}	HO peak source current	V_{HO} = V_{SW} = 0 V, V_{CBOOT} = V_{VCCX} = 5 V		2.2		A
$I_{HO-SINK}$	HO peak sink current	V_{VCCX} = 5 V		3.2		A
LOW-SIDE GATE DRIVER (LO)						
V_{LO-LOW}	LO low-state output voltage	I_{LO} = 100 mA		50		mV
$V_{LO-HIGH}$	LO high-state output voltage	I_{LO} = –100 mA		130		mV
$t_{LO-RISE}$	LO rise time (10% to 90%)	C_{LOAD} = 2.7 nF		7		ns
$t_{LO-FALL}$	LO fall time (90% to 10%)	C_{LOAD} = 2.7 nF		7		ns
I_{LO-SRC}	LO peak source current	V_{HO} = V_{SW} = 0 V, V_{CBOOT} = V_{VCCX} = 5 V		2.2		A
$I_{LO-SINK}$	LO peak sink current	V_{VCCX} = 5 V		3.2		A
ADAPTIVE DEADTIME CONTROL						
t_{DEAD1}	HO off to LO on deadtime			20		ns

Product Folder Links: *LM25149*

T_J = –40°C to 150°C. Typical values are at T_J = 25°C and V_{IN} = 12 V (unless otherwise noted).

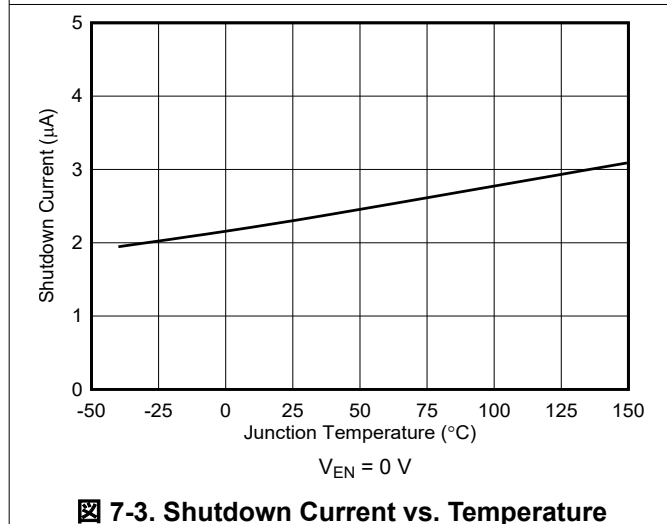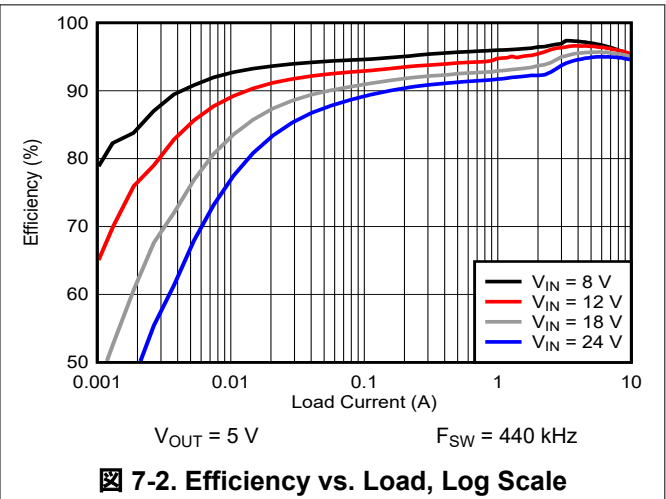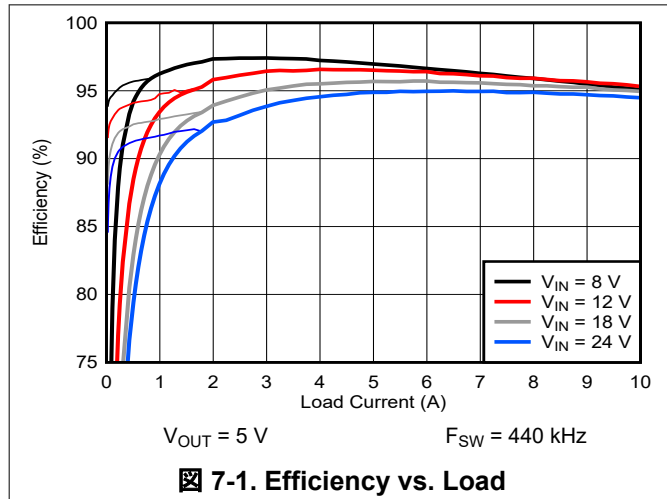| PARAMETER		TEST CONDITIONS	MIN	TYP	MAX	UNIT
t_{DEAD2}	LO off to HO on deadtime			20		ns
INTERNAL HICCUP MODE						
HIC_{DLY}	Hiccup mode activation delay	$V_{ISNS+} - V_{VOUT}$ > 60 mV		512		cycles
HIC_{CYCLES}	HICCUP mode fault	$V_{ISNS+} - V_{VOUT}$ > 60 mV		16384		cycles
OVERCURRENT PROTECTION						
V_{CS-TH}	Current limit threshold	Measured from ISNS+ to VOUT	49	60	73	mV
$t_{DELAY-ISNS+}$	ISNS+ delay to output			65		ns
G_{CS}	CS amplifier gain		9.0	10	10.8	V/V
$I_{BIAS-ISNS+}$	CS amplifier input bias current			15		nA
CONFIGURATION						
$R_{CNFG-OPT1}$	Primary, no spread spectrum		28.7	29.4	31	kΩ
$R_{CNFG-OPT2}$	Primary, with spread spectrum		40.2	41.2	43.2	kΩ
$R_{CNGF-OPT3}$	Primary, interleaved, no spread spectrum		53.6	54.9	57.6	kΩ
$R_{CNFG-OPT4}$	Primary, interleaved, with spread spectrum		69.8	71.5	73.2	kΩ
$R_{CNFG-OPT5}$	Secondary		87	90.9	93.1	kΩ
THERMAL SHUTDOWN						
T_{J-SD}	Thermal shutdown threshold [1]	Temperature rising		175		°C
T_{J-HYS}	Thermal shutdown hysteresis [1]			15		°C

(1)   Specified by design. Not production tested.

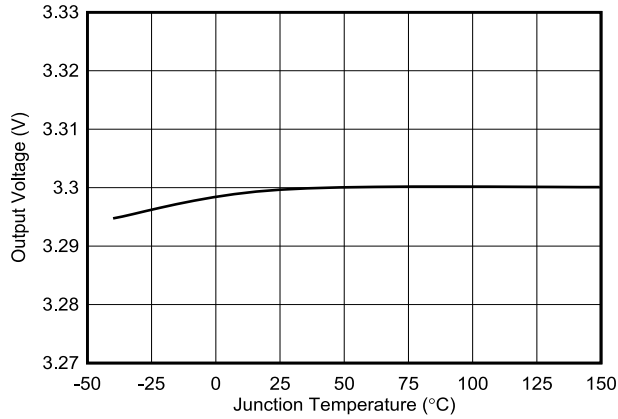## 7.6 ACTIVE EMI Filter

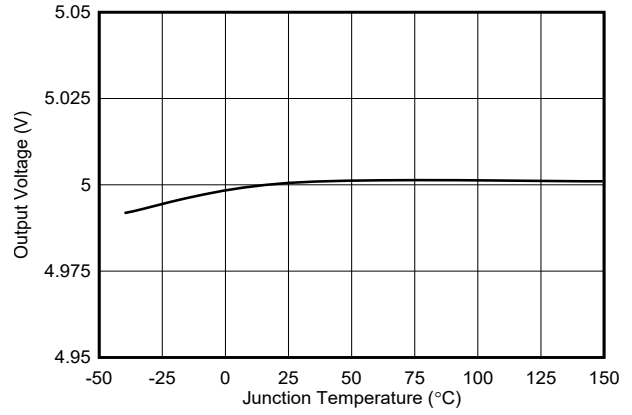T_J = –40°C to 150°C, $V_{AEFVDDA}$ = 5 V (unless otherwise noted).

PARAMETER		TEST CONDITIONS	MIN	TYP	MAX	UNIT
Active EMI Filter						
$V_{AEF-UVLO-R}$	Voltage AEF UVLO rising threshold			4.15		V
$V_{AEF-UVLO-F}$	Voltage AEF UVLO falling threshold			3.5		V
$V_{AEF-HYST}$	Voltage AEF UVLO hysteresis			650		mV
A_{OL}	DC gain				68	dB
f_{BW}	Unity gain bandwidth			300		MHz
$V_{AEF-HIGH}$	AEF voltage rising threshold	Enable AEF (CNFG pin)			2.0	V
$V_{AEF-LOW}$	AEF voltage falling threshold	Disable AEF (CNFG pin)	0.8			V
$V_{AEF-REF}$	AEF reference voltage			2.5		V

7.7 Typical Characteristics

V_{OUT} = 5 V F_{SW} = 440 kHz

図 7-1. Efficiency vs. Load

V_{OUT} = 5 V F_{SW} = 440 kHz

図 7-2. Efficiency vs. Load, Log Scale

V_{EN} = 0 V

図 7-3. Shutdown Current vs. Temperature

0.5 V ≤ V_{EN} ≤ 1 V

図 7-4. Standby Current vs. Temperature

V_{VOUT} = 3.3 V   1.03 V ≤ V_{EN} ≤ 42 V

図 7-5. Sleep Current vs. Temperature

V_{VOUT} = 5 V   1.03 V ≤ V_{EN} ≤ 42 V

図 7-6. Sleep Current vs. Temperature

Product Folder Links: *LM25149*
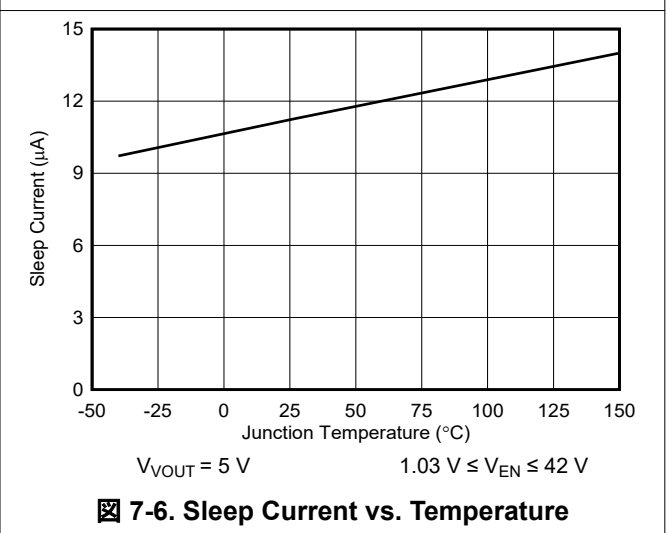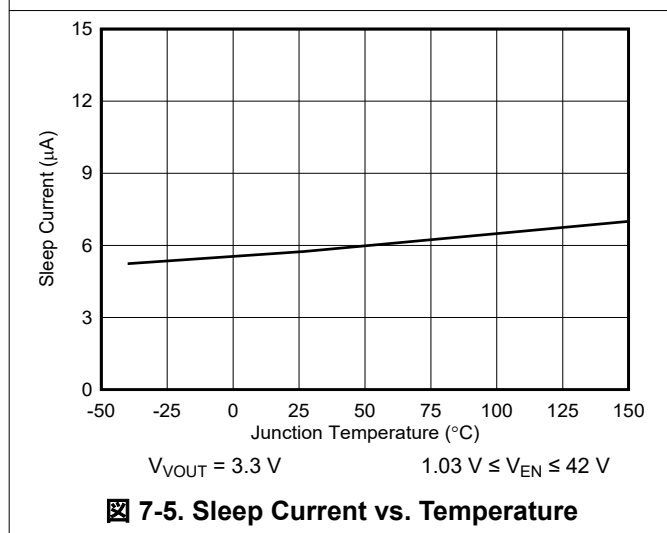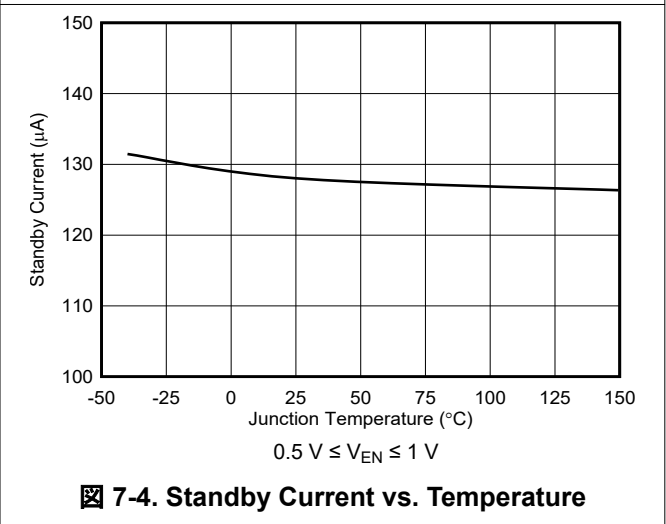
図 7-7. Fixed 3.3-V Output Voltage vs. Temperature

図 7-8. Fixed 5-V Output Voltage vs. Temperature
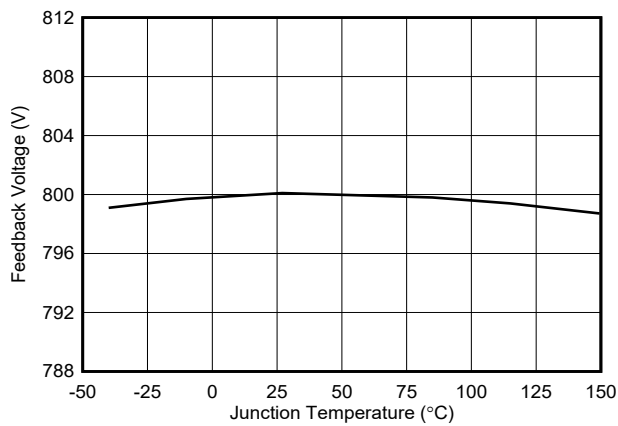
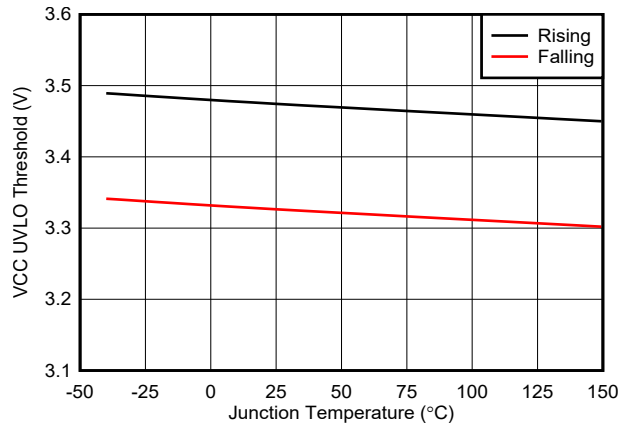図 7-9. Feedback (FB) Voltage vs. Temperature
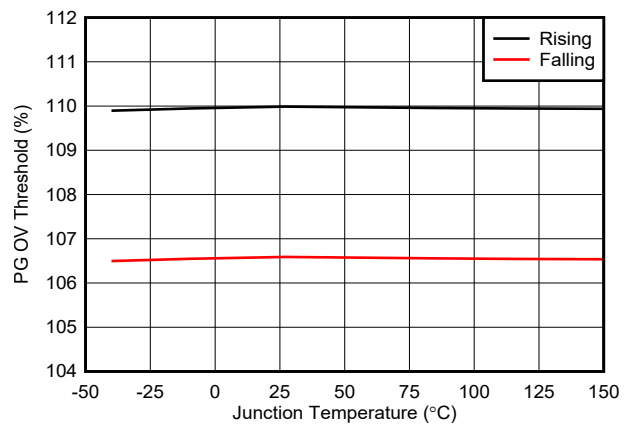
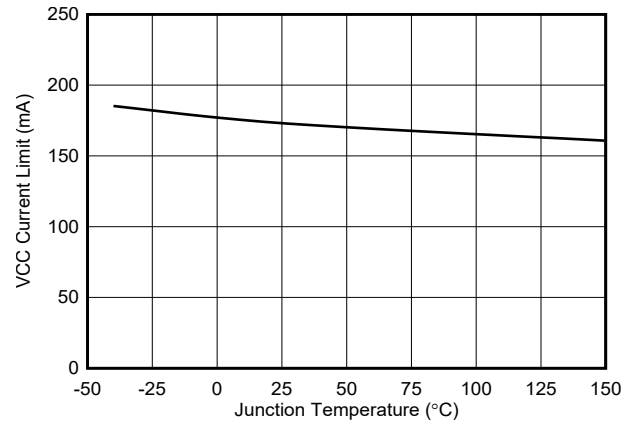

図 7-10. PG OV Thresholds vs. Temperature
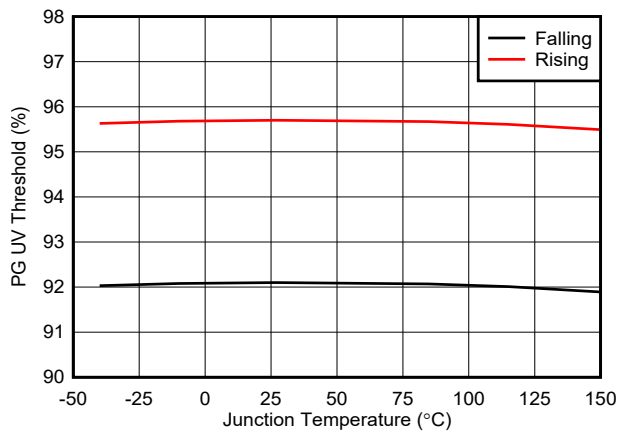
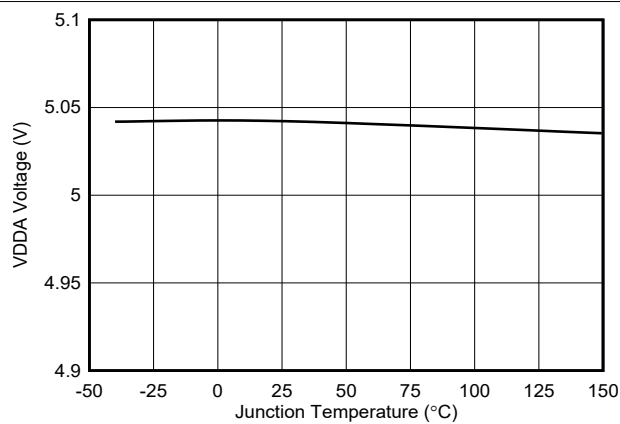図 7-11. PG UV Thresholds vs. Temperature
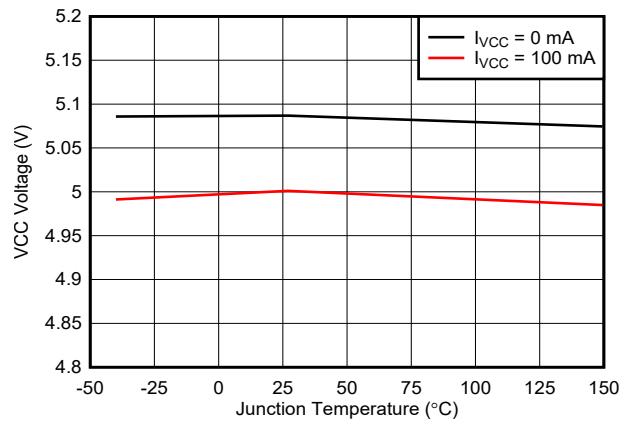
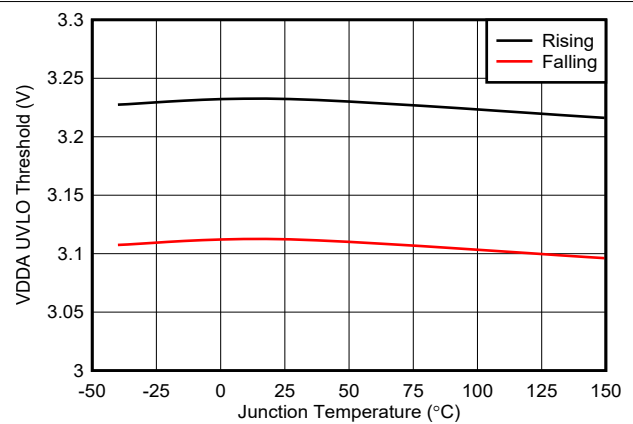図 7-12. VCC Regulation Voltage vs. Temperature

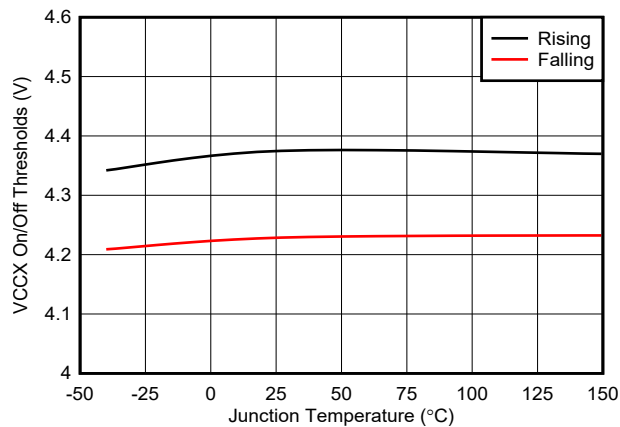**図 7-13. VCC UVLO Thresholds vs. Temperature**

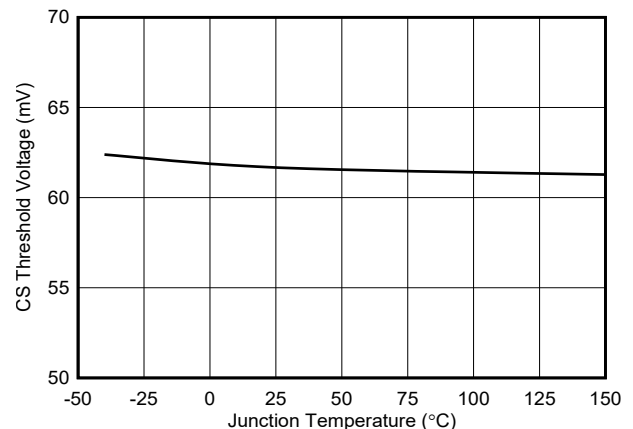**図 7-14. VCC Current Limit vs. Temperature**

図 7-15. VDDA Regulation Voltage vs. Temperature
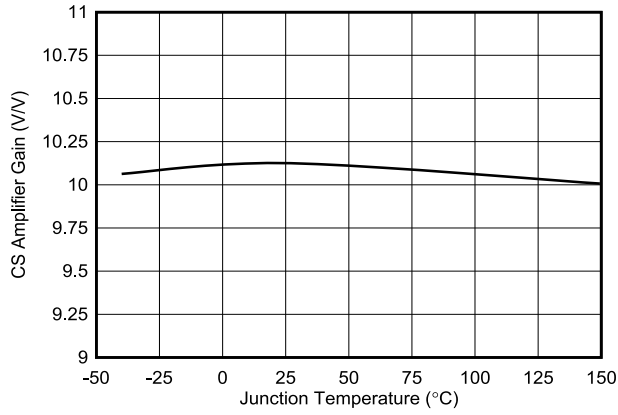

図 7-16. VDDA UVLO Thresholds vs. Temperature

図 7-17. VCCX On/Off Thresholds vs. Temperature

図 7-18. Current Sense (CS) Threshold vs. Temperature

Product Folder Links: *LM25149*
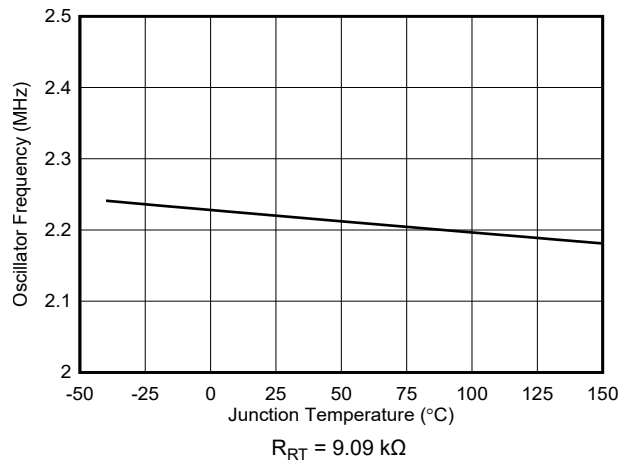
図 7-19. Current Sense (CS) Amplifier Gain vs. Temperature
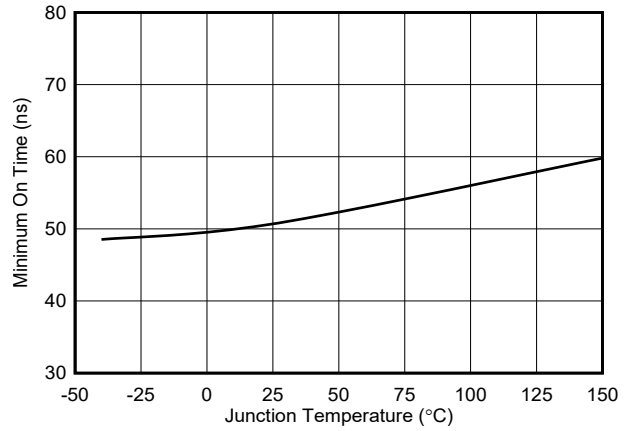
図 7-20. Minimum On Time (HO) vs. Temperature
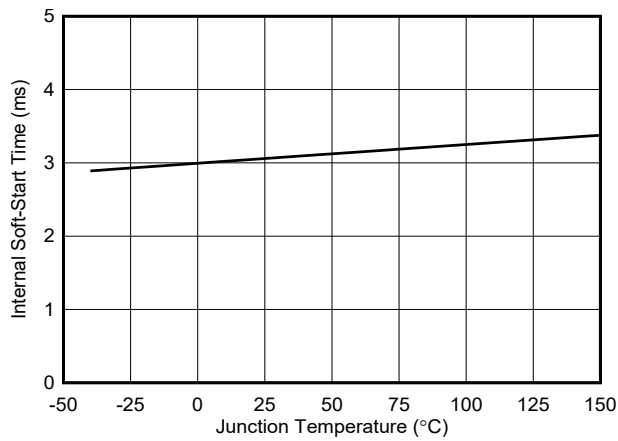
図 7-21. Soft-start Time vs. Temperature

R_{RT} = 9.09 kΩ

図 7-22. Switching Frequency vs. Temperature

8 Detailed Description

8.1 Overview

The LM25149 is a switching controller that features all of the functions necessary to implement a high-efficiency synchronous buck power supply operating over a wide input voltage range from 3.5 V to 42 V. The LM25149 is configured to provide a fixed 3.3-V, 5-V, or 12-V output, or an adjustable output between 0.8 V to 36 V. This easy-to-use controller integrates high-side and low-side MOSFET gate drivers capable of sourcing and sinking peak currents of 2.2 A and 3.2 A, respectively. Adaptive dead-time control is designed to minimize body diode conduction during switching transitions.

Current-mode control using a shunt resistor or inductor DCR current sensing provides inherent line feedforward, cycle-by-cycle peak current limiting, and easy loop compensation. It also supports a wide duty cycle range for high input voltage and low-dropout applications as well as application requiring a high step-down conversion ratio (for example, 10-to-1). The oscillator frequency is user-programmable between 100 kHz to 2.2 MHz, and the frequency can be synchronized as high as 2.5 MHz by applying an external clock to the PFM/SYNC pin.

An external bias supply can be connected to VCCX to maximize efficiency in high input voltage applications. A user-selectable diode emulation feature enables discontinuous conduction mode (DCM) operation to further improve efficiency and reduce power dissipation during light-load conditions. Fault protection features include current limiting, thermal shutdown, UVLO, and remote shutdown capability.

The LM25149 incorporates several features to simplify compliance with various EMI standards, for example, CISPR 11 and CISPR 32 Class B requirements. Active EMI filter and dual random spread spectrum (DRSS) techniques reduce the peak harmonic EMI signature.

The LM25149 is provided in a 24-pin VQFN package with an exposed pad to aid in thermal dissipation.

8.2 Functional Block Diagram
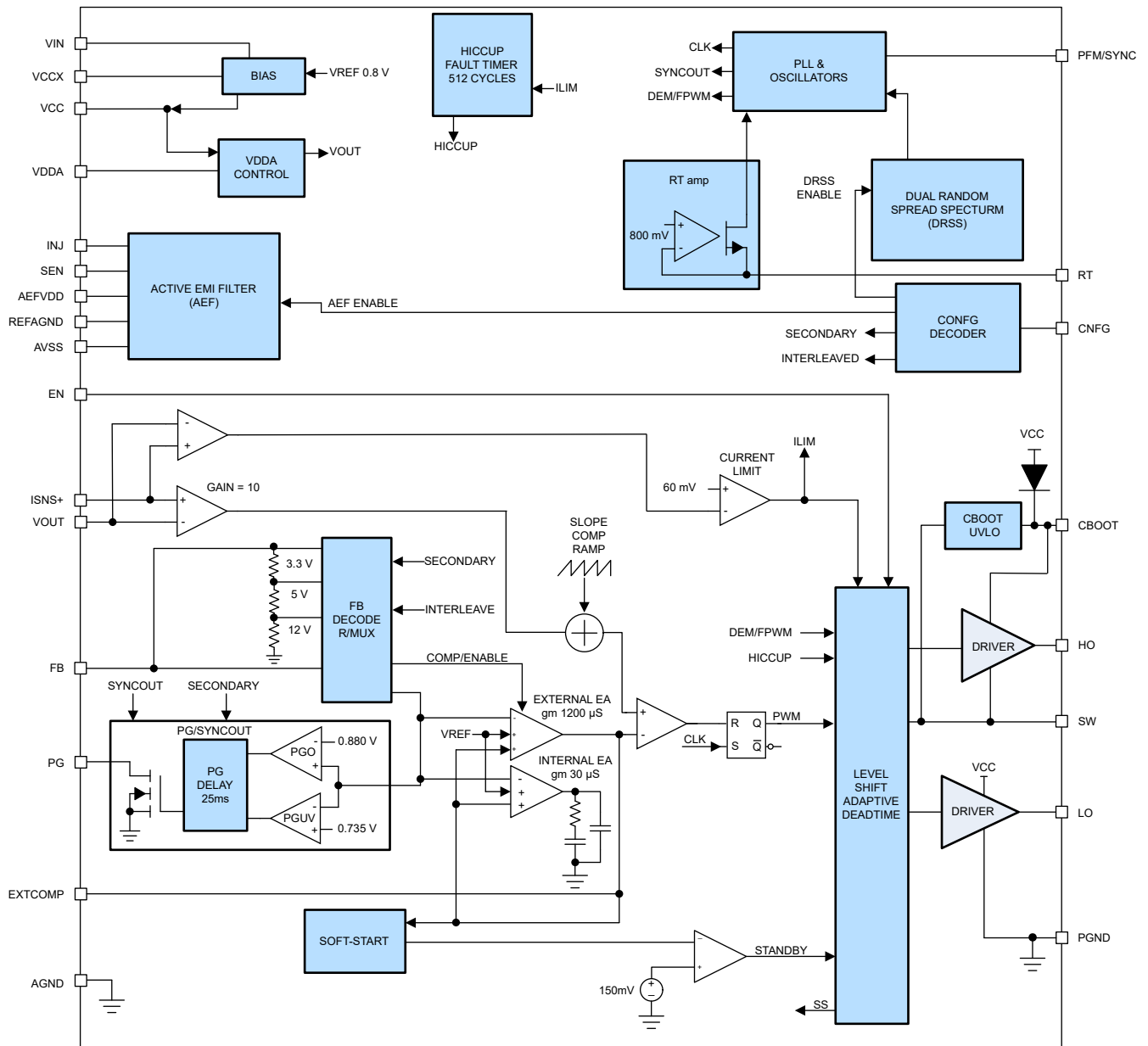
8.3 Feature Description

8.3.1 Input Voltage Range (V_{IN})

The LM25149 operational input voltage range is from 3.5 V to 42 V. The device is intended for step-down conversions from 12-V, 24-V, and 48-V supply rails. The application circuit in 図 9-5 shows all the necessary components to implement an LM25149 based wide-V_{IN}, single-output, step-down regulator using a single supply. The LM25149 uses an internal LDO to provide a 5-V VCC bias rail for the gate drive and control circuits (assuming the input voltage is higher than 5 V with additional voltage margin necessary for the subregulator dropout specification).

In high input voltage applications, take extra care to ensure that the VIN and SW pins do not exceed their absolute maximum voltage rating of 47 V during line or load transient events. Voltage excursions that exceed the applicable voltage specifications can damage the device.

Care should be taken in applications where there are fast transients at VIN that cause the voltage at VIN to suddenly drop more than 2 V below the VOUT setpoint. The LM25149 has an internal ESD diode from the VOUT to the VIN pins that can conduct under such conditions causing the output to discharge. To prevent damage to the internal ESD diode under the said conditions, TI recommends adding a Schottky diode in series with the VIN pin of the LM25149 to prevent reverse current flow from VOUT to VIN.

8.3.2 High-Voltage Bias Supply Regulator (VCC, VCCX, VDDA)

The LM25149 contains an internal high-voltage VCC bias regulator that provides the bias supply for the PWM controller and the gate drivers for the external MOSFETs. The input voltage pin (VIN) can be connected directly to an input voltage source up to 42 V. However, when the input voltage is below the VCC setpoint level, the VCC voltage tracks V_{IN} minus a small voltage drop.

The VCC regulator output current limit is 115 mA (minimum). At power up, the controller sources current into the capacitor connected at the VCC pin. When the VCC voltage exceeds 3.3 V and the EN pin is connected to a voltage greater than 1 V, the soft-start sequence begins. The output remains active unless the VCC voltage falls below the VCC UVLO falling threshold of 3.1 V (typical) or EN is switched to a low state. Connect a ceramic capacitor from VCC to PGND. The recommended range of the VCC capacitor is from 2.2 µF to 10 µF.

An internal 5-V linear regulator generates the VDDA bias supply. Bypass VDDA with a 100-nF ceramic capacitor or higher to achieve a low-noise internal bias rail. Normally, VDDA is 5 V. However, there is one condition where VDDA regulates at 3.3 V: this is in PFM mode with a light or no load on the output.

Minimize the internal power dissipation of the VCC regulator by connecting VCCX to a 5-V output or to an external 5-V supply. If the VCCX voltage is above 4.3 V, VCCX is internally connected to VCC and the internal VCC regulator is disabled. Tie VCCX to PGND if it is unused. Do not connect VCCX to a voltage greater than 6.5 V. If an external supply is connected to VCCX to power the LM25149, V_{IN} must be greater than the external bias voltage during all conditions to avoid damage to the controller.

8.3.3 Precision Enable (EN)

The EN pin can be connected to a voltage as high as 42 V. The LM25149 has a precision enable function. When the EN voltage is greater than 1 V, switching is enabled. If the EN pin is pulled below 0.5 V, the LM25149 is in shutdown with an I_Q of 2.3 µA (typical) current consumption from V_{IN}. When the EN voltage is between 0.5 V and 1 V, the LM25149 is in standby mode, the VCC regulator is active, and the controller is not switching. When the controller is in standby mode, the non-switching input quiescent current is 124 µA (typical). The LM25149 is enabled with a voltage greater than 1.0 V. However, many applications benefit from using a resistor divider R_{UV1} and R_{UV2}, as shown in 図 8-1, to establish a precision UVLO level. TI does not recommend leaving the EN pin floating.

When using precision enable and a VCCX supply, place a series diode with the cathode connected to the LM25149 VCCX pin.

Use 式 1 and 式 2 to calculate the UVLO resistors given the required input turn-on and turn-off voltages.

$$R_{UV1} = \frac{V_{IN(on)} - V_{IN(off)}}{I_{HYS}}$$

(1)

$$R_{UV2} = R_{UV1} \cdot \frac{V_{EN}}{V_{IN(on)} - V_{EN}}$$

(2)
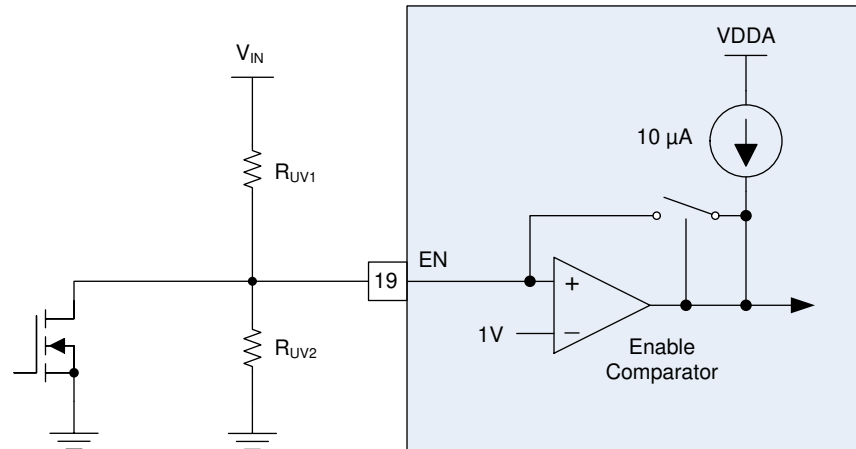
図 8-1. Programmable Input Voltage UVLO Turn-On

8.3.4 Power-Good Monitor (PG)

The LM25149 includes an output voltage monitoring signal for V_{OUT} to simplify sequencing and supervision. The power-good signal is used for start-up sequencing of downstream converters, fault protection, and output monitoring. The power-good output (PG) switches to a high impedance open-drain state when the output voltage is in regulation. The PG switches low when the output voltage drops below the lower power-good threshold (92% typical) or rises above the upper power-good threshold (110% typical). A 25-µs deglitch filter prevents false tripping of the power-good signal during transients. TI recommends a pullup resistor of 100 kΩ (typical) from PG to the relevant logic rail. PG is asserted low during soft start and when the buck regulator is disabled.

When the LM25149 is configured as a primary controller, the PG/SYNC pin becomes a synchronization clock output for the secondary controller. The synchronization signal is 180° out-of-phase with the primary HO driver output.

8.3.5 Switching Frequency (RT)

Program the LM25149 oscillator with a resistor from RT to AGND to set an oscillator frequency between 100 kHz and 2.2 MHz. Calculate the RT resistance for a given switching frequency using 式 3.

$$R_T(k\Omega) = \frac{\dfrac{10^6}{F_{SW}(kHz)} - 53}{45}$$

(3)

Under low V_{IN} conditions when the on time of the high-side MOSFET exceeds the programmed oscillator period, the LM25149 extends the switching period until the PWM latch is reset by the current sense ramp exceeding the controller compensation voltage.

The approximate input voltage level at which this occurs is given by 式 4.

$$V_{IN(min)} = V_{OUT} \cdot \frac{t_{SW}}{t_{SW} - t_{OFF(min)}}$$

(4)

where

- t_{SW} is the switching period.
- $t_{OFF(min)}$ is the minimum off time of 90 ns.

8.3.6 Active EMI Filter

Active EMI filter provides a higher level of EMI attenuation and a smaller solution size than a standard passive π-filter. Passive π-filters use large inductors and capacitors to attenuate the ripple and noise on the input DC bus. Passive filters are typically most effective at reducing the switching frequency harmonics to comply with EMI in the low-frequency range, less than 30 MHz.

Active EMI filter has a high gain, wide bandwidth amplifier, and a low output impedance that can source and sink current. It senses (at the SEN pin) any disturbance on the DC input bus and injects (at the INJ pin) a cancellation signal out of phase with the noise source to reduce the conducted emissions.

To maintain low I_Q at light loads, the LM25149 automatically enables active EMI filter when the load current is greater than 40% of the current limit value, and disables the active EMI filter when the load current is less then 30% of the current limit value. The active EMI filter is disabled by pulling the CNFG pin below 0.8 V after the LM25149 has been configured.
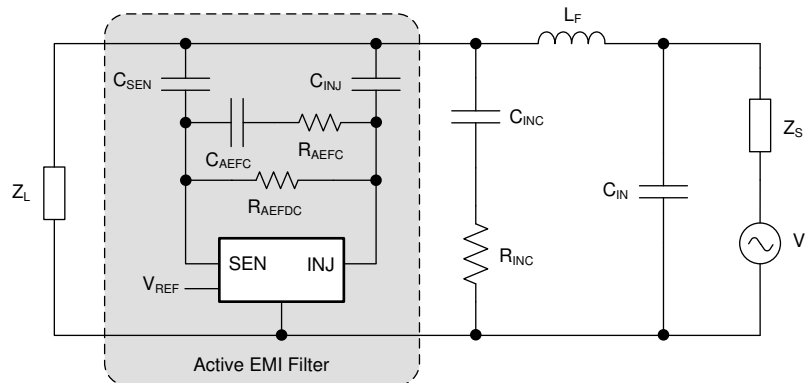

図 8-2. Active EMI Filter

8.3.7 Dual Random Spread Spectrum (DRSS)

The LM25149 provides a digital spread spectrum, which reduces the EMI of the power supply over a wide frequency range. DRSS combines a low-frequency triangular modulation profile with a high frequency cycle-by-cycle random modulation profile. The low-frequency triangular modulation improves performance in lower radio-frequency bands, while the high-frequency random modulation improves performance in higher radio frequency bands.

Spread spectrum works by converting a narrowband signal into a wideband signal that spreads the energy over multiple frequencies. Since industry standards require different EMI receiver resolution bandwidth (RBW) settings for different frequency bands, the RBW has an impact on the spread spectrum performance. DRSS is able to simultaneously improve the EMI performance in the low and high RBWs with its low-frequency triangular modulation profile and high frequency cycle-by-cycle random modulation, respectively. DRSS can reduce conducted emissions by 15 dBμV in the CISPR 25 low-frequency band (150 kHz to 30 MHz) and 5 dBμV in the high-frequency band (30 MHz to 108 MHz).

To enable DRSS, connect either a 41.2-kΩ or 71.5-kΩ resistor from CNFG to AGND. DRSS is disabled when an external clock is applied to the PFM/SYNC pin.

Product Folder Links: *LM25149*
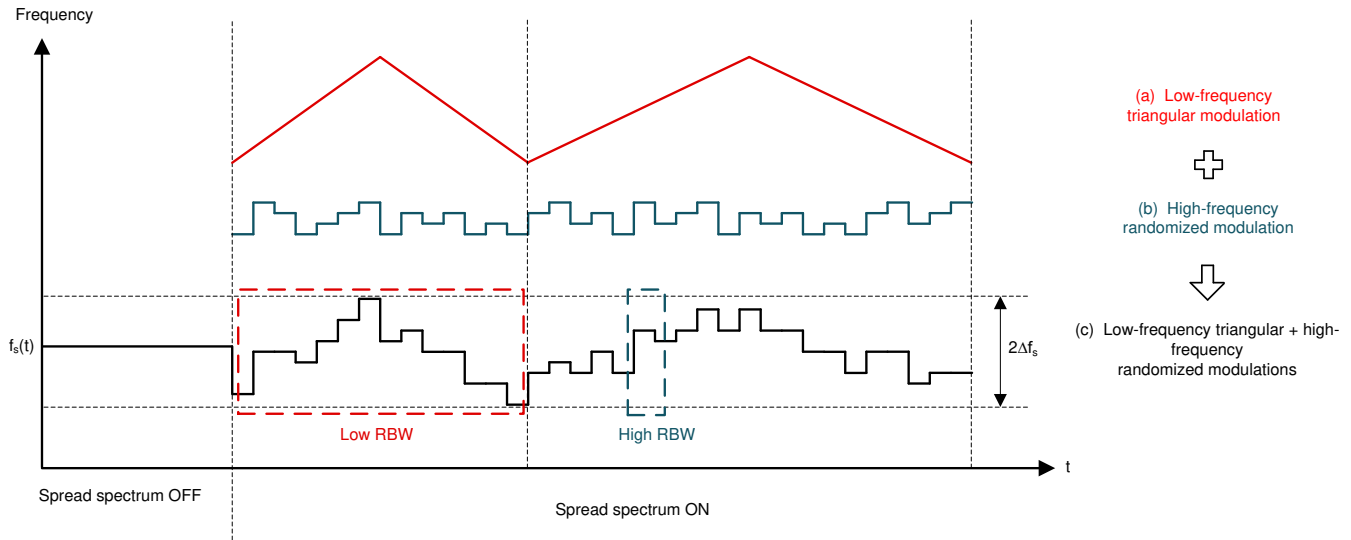
図 8-3. Dual Random Spread Spectrum Implementation

8.3.8 Soft Start

The LM25149 has an internal 3-ms soft-start timer (typical). The soft-start feature allows the regulator to gradually reach the steady-state operating point, thus reducing start-up stresses and surges.

8.3.9 Output Voltage Setpoint (FB)

The LM25149 output can be independently configured for one of three fixed output voltages without external feedback resistors, or adjusted to the desired voltage using an external resistor divider. Set the output to 3.3 V by connecting FB directly to VDDA. Alternatively, set the output to either 5 V or 12 V by installing a 24.9-kΩ or 49.9-kΩ resistor between FB and VDDA, respectively. See 表 8-1.

表 8-1. Feedback Configuration Resistors

PULLUP RESISTOR TO VDDA	V$_{OUT}$ SETPOINT
0 Ω	3.3 V
24.9 kΩ	5 V
49.9 kΩ	12 V
Not installed	External FB divider setting

The configuration settings are latched and cannot be changed until the LM25149 is powered down (with the VCC voltage decreasing below its falling UVLO threshold) and then powered up again (VCC rises above 3.4-V typical). Alternatively, set the output voltage with an external resistive divider from the output to AGND. The output voltage adjustment range is between 0.8 V and 36 V. The regulation voltage at FB is 0.8 V (V$_{REF}$). Use 式 5 to calculate the upper and lower feedback resistors, designated as R$_{FB1}$ and R$_{FB2}$, respectively.

$$R_{FB1} = \left(\frac{V_{OUT}}{V_{REF}} - 1 \right) \cdot R_{FB2}$$

(5)

The recommended starting value for R$_{FB2}$ is between 10 kΩ and 20 kΩ.

If low-I$_Q$ operation is required, take care when selecting the external feedback resistors. The current consumption of the external divider adds to the LM25149 sleep current (9.5-µA typical). The divider current reflected to V$_{IN}$ is scaled by the ratio of V$_{OUT}$/V$_{IN}$.

8.3.10 Minimum Controllable On Time

There are two limitations to the minimum output voltage adjustment range: the LM25149 voltage reference of 0.8 V and the minimum controllable switch-node pulse width, $t_{ON(min)}$.

$t_{ON(min)}$ effectively limits the voltage step-down conversion ratio V_{OUT} / V_{IN} at a given switching frequency. For fixed-frequency PWM operation, the voltage conversion ratio must satisfy 式 6.

$$\frac{V_{OUT}}{V_{IN}} > t_{ON(min)} \cdot F_{SW}$$

(6)

where

- $t_{ON(min)}$ is 50 ns (typical).
- F_{SW} is the switching frequency.

If the desired voltage conversion ratio does not meet the above condition, the LM25149 transitions from fixed switching frequency operation to a pulse-skipping mode to maintain output voltage regulation. For example, if the desired output voltage is 5 V with an input voltage of 24 V and switching frequency of 2.1 MHz, use 式 7 to verify that the conversion ratio.

$$\frac{5\,V}{24\,V} > 50\,ns \cdot 2.1\,MHz$$

$$0.208 > 0.105$$

(7)

For wide-V_{IN} applications and low output voltages, an alternative is to reduce the LM25149 switching frequency to meet the requirement of 式 6.

8.3.11 Error Amplifier and PWM Comparator (FB, EXTCOMP)

The LM25149 has a high-gain transconductance amplifier that generates an error current proportional to the difference between the feedback voltage and an internal precision reference (0.8 V). The control loop compensation is configured two ways. The first is using the internal compensation amplifier, which has a transconductance of 30 µS. Internal compensation is configured by connecting the EXTCOMP pin through a 100-kΩ resistance to VDDA. If a 100-kΩ resistor is not detected, the LM25149 defaults to the external loop compensation network. The transconductance of the amplifier for external compensation is 1200 µS. This is latched and cannot be reconfigured once programmed unless power to the device is recycled. Use an external compensation network if higher performance is required to meet a stringent transient response specification. To reconfigure the compensation (internal or external), remove power and allow VCC to drop below its VCC$_{UVLO}$ threshold, which is 3.3-V typical.

A type-II compensation network is generally recommended for peak current-mode control.

8.3.12 Slope Compensation

The LM25149 provides internal slope compensation for stable operation with peak current-mode control and a duty cycle greater than 50%. Calculate the buck inductance to provide a slope compensation contribution equal to one times the inductor downslope using 式 8.

$$L_{O\text{-}IDEAL}(\mu H) = \frac{V_{OUT}(V) \cdot R_S(m\Omega)}{24 \cdot F_{SW}(MHz)}$$

(8)

- A lower inductance value generally increases the peak-to-peak inductor current, which minimizes size and cost, and improves transient response at the cost of reduced light-load efficiency due to higher cores losses and peak currents.

- A higher inductance value generally decreases the peak-to-peak inductor current, reducing switch peak and RMS currents at the cost of requiring larger output capacitors to meet load-transient specifications.

8.3.13 Inductor Current Sense (ISNS+, VOUT)

There are two methods to sense the inductor current of the buck power stage. The first uses a current sense resistor (also known as a shunt) in series with the inductor, and the second avails of the DC resistance of the inductor (DCR current sensing).

8.3.13.1 Shunt Current Sensing

図 8-4 illustrates inductor current sensing using a shunt resistor. This configuration continuously monitors the inductor current to provide accurate overcurrent protection across the operating temperature range. For optimal current sense accuracy and overcurrent protection, use a *low inductance* ±1% tolerance shunt resistor between the inductor and the output, with a Kelvin connection to the LM25149 current sense amplifier.

If the peak voltage signal sensed from ISNS+ to VOUT exceeds the current limit threshold of 60 mV, the current limit comparator immediately terminates the HO output for cycle-by-cycle current limiting. Calculate the shunt resistance using 式 9.

$$R_S = \frac{V_{CS\text{-}TH}}{I_{OUT(CL)} + \frac{\Delta I_L}{2}}$$

(9)

where

- $V_{CS\text{-}TH}$ is current sense threshold of 60 mV.
- $I_{OUT(CL)}$ is the overcurrent setpoint that is set higher than the maximum load current to avoid tripping the overcurrent comparator during load transients.
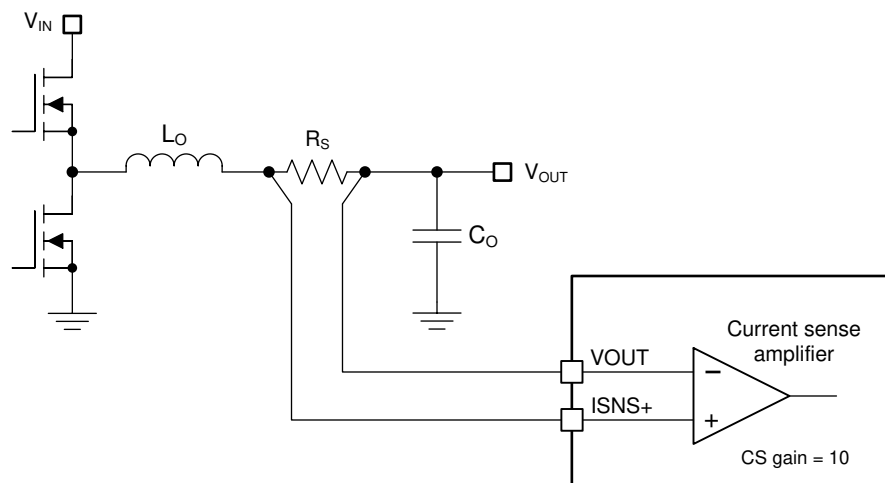- ΔI_L is the peak-to-peak inductor ripple current.

図 8-4. Shunt Current Sensing Implementation

The soft-start voltage is clamped 150 mV above FB during an overcurrent condition. Sixteen overcurrent events must occur before the SS clamp is enabled. This makes sure that SS can be pulled low during brief overcurrent events, preventing output voltage overshoot during recovery.

8.3.13.2 Inductor DCR Current Sensing

For high-power applications that do not require accurate current-limit protection, inductor DCR current sensing is preferable. This technique provides lossless and continuous monitoring of the inductor current using an RC sense network in parallel with the inductor. Select an inductor with a low DCR tolerance to achieve a typical

current limit accuracy within the range of 10% to 15% at room temperature. Components R_{CS} and C_{CS} in 図 8-5 create a low-pass filter across the inductor to enable differential sensing of the voltage across the inductor DCR.
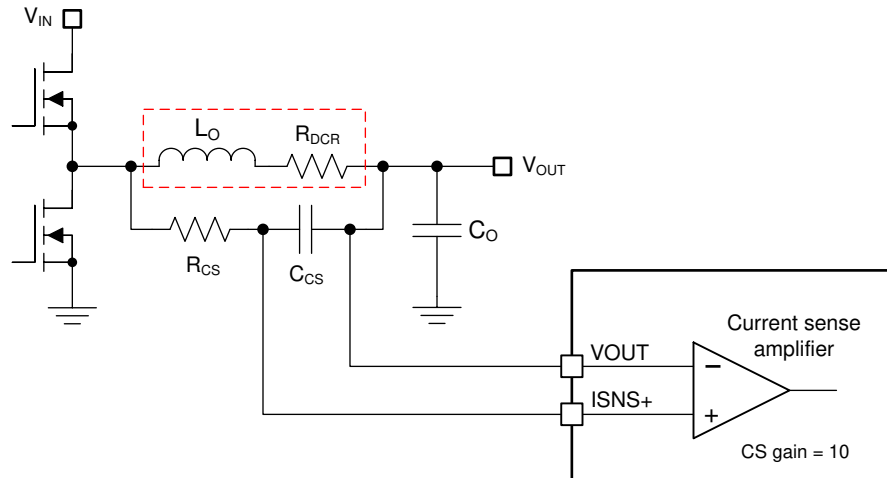

図 8-5. Inductor DCR Current Sensing Implementation

The voltage drop across the sense capacitor in the s-domain is given by 式 10. When the $R_{CS}C_{CS}$ time constant is equal to L_O/R_{DCR}, the voltage developed across the sense capacitor, C_{CS}, is a replica of the inductor DCR voltage and accurate current sensing is achieved. If the $R_{CS}C_{CS}$ time constant is not equal to the L_O/R_{DCR} time constant, there is a sensing error as follows:

- $R_{CS}C_{CS} > L_O/R_{DCR} \rightarrow$ the DC level is correct, but the AC amplitude is attenuated.
- $R_{CS}C_{CS} < L_O/R_{DCR} \rightarrow$ the DC level is correct, but the AC amplitude is amplified.
- $R_{CS}C_{CS} = L_O/R_{DCR} \rightarrow$ the DC level and AC amplitude are correct.

$$V_{CS}(s) = \frac{1 + s \cdot \dfrac{L_O}{R_{DCR}}}{1 + s \cdot R_{CS} \cdot C_{CS}} \cdot R_{DCR} \cdot \left(I_{OUT(CL)} + \frac{\Delta I_L}{2} \right)$$

(10)

Choose the C_{CS} capacitance greater than or equal to 0.1 µF to maintain a low-impedance sensing network, thus reducing the susceptibility of noise pickup from the switch node. Carefully observe セクション 11.1 to make sure that noise and DC errors do not corrupt the current sense signals applied between the ISNS+ and VOUT pins.

8.3.14 Hiccup Mode Current Limiting

The LM25149 includes an internal hiccup-mode protection function. After an overload is detected, 512 cycles of cycle-by-cycle current limiting occurs. The 512-cycle counter is reset if four consecutive switching cycles occur without exceeding the current limit threshold. Once the 512-cycle counter has expired, the internal soft start is pulled low, the HO and LO driver outputs are disabled, and the 16384 counter is enabled. After the counter reaches 16384, the internal soft start is enabled and the output restarts. The hiccup-mode current limit is disabled during soft start until the FB voltage exceeds 0.4 V.

8.3.15 High-Side and Low-Side Gate Drivers (HO, LO)

The LM25149 contains gate drivers and an associated high-side level shifter to drive the external N-channel power MOSFETs. The high-side gate driver works in conjunction with an internal bootstrap diode, D_{BOOT}, and bootstrap capacitor, C_{BOOT}. During the conduction interval of the low-side MOSFET, the SW voltage is approximately 0 V and C_{BOOT} charges from VCC through the internal D_{BOOT}. TI recommends a 0.1-µF ceramic capacitor connected with short traces between the CBOOT and SW pins.

The LO and HO outputs are controlled with an adaptive dead-time methodology so that both outputs (HO and LO) are never on at the same time, preventing cross conduction. Before the LO driver output is allowed to turn on, the adaptive dead-time logic first disables HO and waits for the HO-to-SW voltage to drop below 2-V typical.

LO is allow to turn on after a small delay (HO fall to LO rising delay). Similarly, the HO turn-on is delayed until the LO voltage has dropped below 2 V. This technique ensures adequate dead-time for any size N-channel power MOSFET implementations, including parallel MOSFET configurations.

Caution is advised when adding series gate resistors, as this can impact the effective dead-time. The selected high-side MOSFET determines the appropriate bootstrap capacitance value C_{BOOT} in accordance with 式 11.

$$C_{BOOT} = \frac{Q_G}{\Delta V_{CBOOT}}$$

(11)

where

- Q_G is the total gate charge of the high-side MOSFET at the applicable gate drive voltage.
- ΔV_{CBOOT} is the voltage variation of the high-side MOSFET driver after turn-on.

To determine C_{BOOT}, choose ΔV_{CBOOT} so that the available gate drive voltage is not significantly impacted. An acceptable range of ΔV_{CBOOT} is 100 mV to 300 mV. The bootstrap capacitor must be a low-ESR ceramic capacitor, typically 0.1 µF. Use high-side and low-side MOSFETs with logic-level gate threshold voltages.

8.3.16 Output Configurations (CNFG)

The LM25149 can be configured as a primary controller (interleaved mode) or as a secondary controller for paralleling the outputs for high-current applications with a resistor R_{CNFG}. This resistor also configures if spread spectrum is enabled or disabled. See 表 8-2. Once the VCC voltage is above 3.3 V (typical), the CNFG pin is monitored and latched. The configuration cannot be changed on the fly – the LM25149 must be powered down, and VCC must drop below 3.3 V. 図 8-6 shows the configuration timing diagram.

When the LM25149 is configured as a primary controller with spread spectrum enabled (R_{CNFG} of 41.2 kΩ or 71.5 kΩ), the LM25149 cannot be synchronized to an external clock.

表 8-2. Configuration Modes

R_{CNFG}	PRIMARY/SECONDARY	SPREAD SPECTRUM	DUAL PHASE
29.9 kΩ	Primary	OFF	Disabled
41.2 kΩ	Primary	ON	Disabled
54.9 kΩ	Primary	OFF	Enabled
71.5 kΩ	Primary	ON	Enabled
90.9 kΩ	Secondary	N/A	Enabled
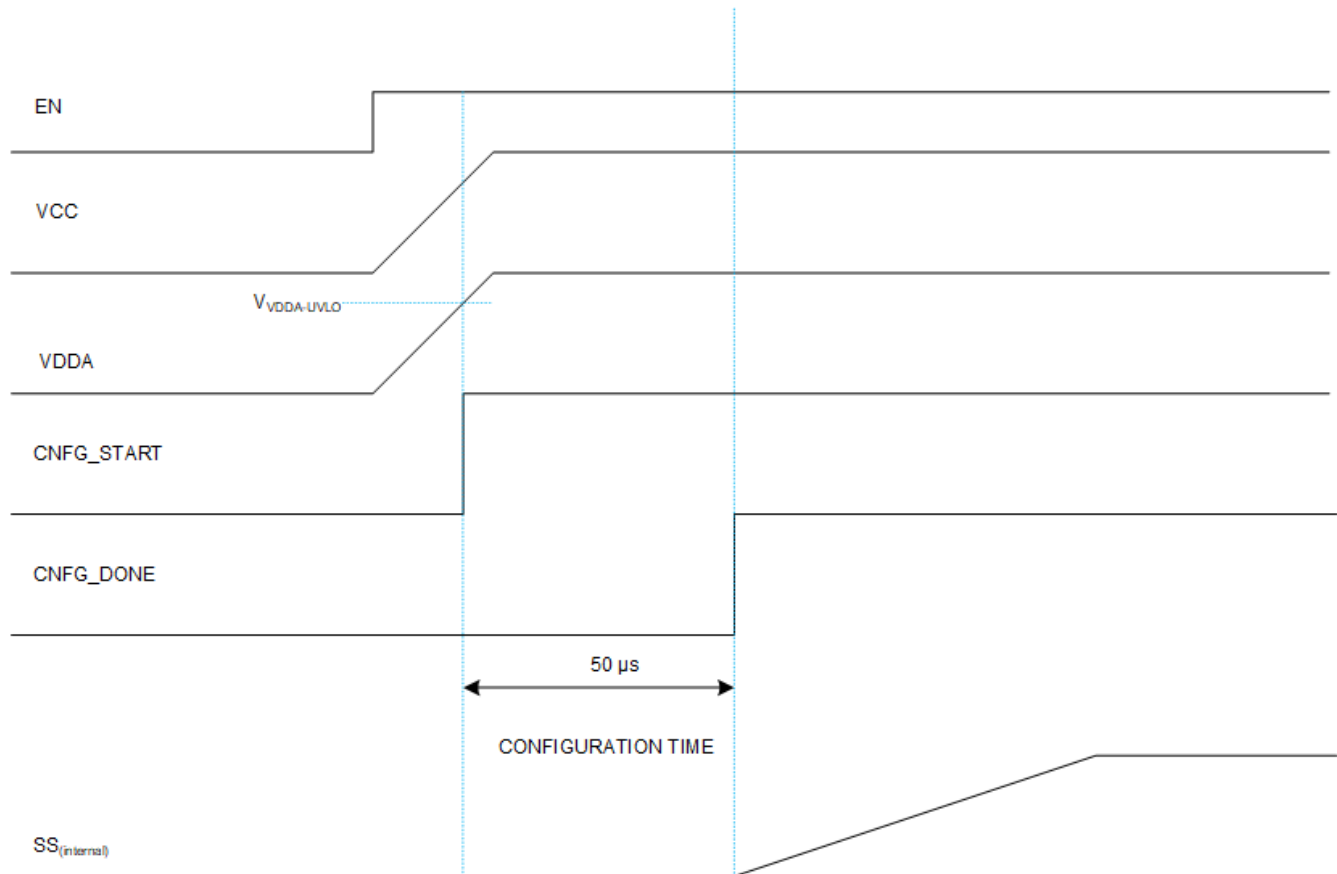
図 8-6. Configuration Timing

After the configuration has been latched, the CNFG pin become an enable input for the active EMI filter, where a logic high (> 2 V) enables the active EMI filter and a logic low (< 0.8 V) disables AEF.
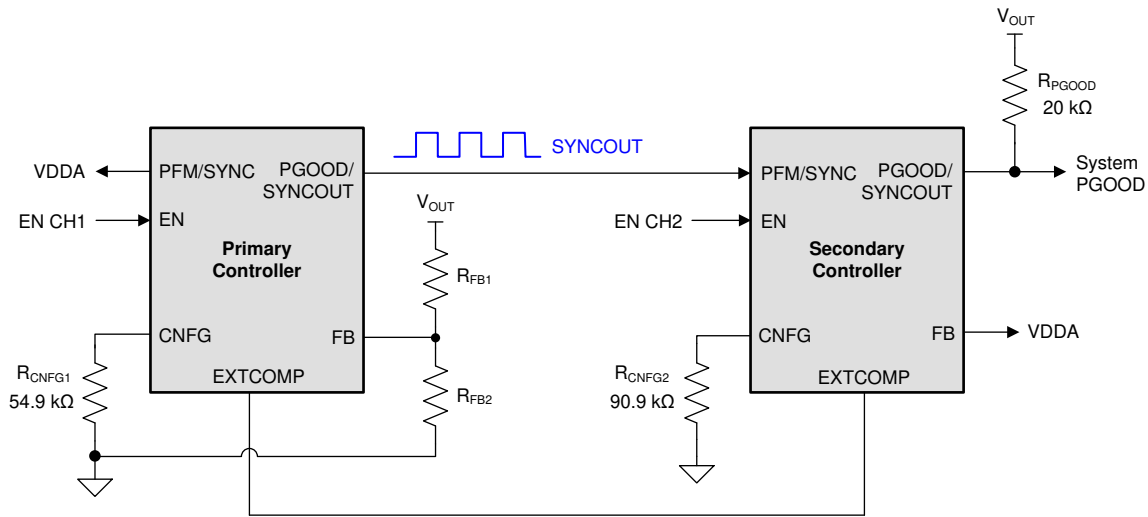
8.3.17 Single-Output Dual-Phase Operation

To configure for dual-phase operation, two controllers are required. The LM25149 can only be configured in a single or dual-phase configuration where both outputs are tied together. Additional phases cannot be added. Refer to 図 8-7. Configure the first controller (CNTRL1) as a primary controller and the second controller (CNTRL2) as a secondary. To configure CNTRL1 as a primary controller, install a 54-kΩ or a 71.5-kΩ resistor from CNFG to AGND. To configure the CNTRL2 as a secondary controller, install a 90.9-kΩ resistor from CNFG to AGND. This disables the error amplifier of CNTRL2, placing it into a high-impedance state. Connect the EXTCOMP pins of the primary and secondary controllers together. The internal compensation amplifier feature is not supported when the controller is in dual-phase mode.

In dual-phase mode, the PG/SYNC pin of the primary controller becomes a SYNCOUT. Refer to the *Electrical Characteristics* for voltage levels. Connect PG of the primary to PFM/SYNC (SYNCIN) of the secondary controller. The PG/SYNCOUT signal of the primary controller is 180° out-of-phase and facilitates interleaved operation. RT is not used for the oscillator when the LM25149 is in secondary controller mode, but instead is used for slope compensation. Therefore, select the RT resistance to be the same as that of the primary controller. The oscillator is derived from the primary controller. When in primary/secondary mode, enable both controllers simultaneously for start-up. After the regulator has started, pull the secondary EN pin low (< 0.8 V) for phase shedding if needed at light load to increase the efficiency.

Configure PFM mode by connecting the PFM/SYNC of the primary to VDDA and the FB of the secondary to VDDA as shown in 図 8-7. Configure FPWM mode by connecting PFM/SYNC of the primary and FB of the secondary both to AGND. An external synchronization signal can be applied to the primary PFM/SYNC (SYNCIN), and the secondary FB must be configured for FPWM. If an external SYNCIN signal is applied after

Product Folder Links: *LM25149*

start-up while in primary/secondary mode, there is a two-clock cycle delay before the LM25149 locks on to the external synchronization signal.

図 8-7. Schematic Configured for Single-Output Dual-Phase Operation

PFM pulse skipping is used to reduce the I_Q current and the light-load efficiency. When this occurs, the primary controller disables its synchronization clock output, so phase shedding is not supported. Phase shedding is supported in FPWM only. In FPWM, enable or disable the secondary controller as needed to support higher load current or better light-load efficiency, respectively. When the secondary is disabled and then re-enabled, its internal soft-start is pulled low and the LM25149 goes through a normal soft-start sequence.

When the LM25149 is configured for a single-output dual-phase operation using the internal 3.3-V feedback resistor divider, the internal bootstrap UV circuit can source current out of the SW pin, charging up the output capacitors approximately to 3.6 V. If this behavior is undesirable, the user can add a 100-kΩ resistor from VOUT to GND to bleed off the charge on the output capacitors.

For more information, see *Benefits of a Multiphase Buck Converter* technical brief and *Multiphase Buck Design From Start to Finish* application report.

Product Folder Links: *LM25149*

8.4 Device Functional Modes

8.4.1 Sleep Mode

The LM25149 operates with peak current-mode control such that the compensation voltage is proportional to the peak inductor current. During no-load or light-load conditions, the output capacitor discharges very slowly. As a result, the compensation voltage does not demand the driver output pulses on a cycle-by-cycle basis. When the LM25149 controller detects 16 missed switching cycles, it enters sleep mode and switches to a low I_Q state to reduce the current drawn from the input. For the LM25149 to go into sleep mode, the controller must be programmed for diode emulation (tie PFM/SYNC to VDDA).

The typical controller I_Q in sleep mode is 9.5 µA with a 3.3-V output.

8.4.2 Pulse Frequency Modulation and Synchronization (PFM/SYNC)

A synchronous buck regulator implemented with a low-side synchronous MOSFET rather than a diode has the capability to sink negative current from the output during conditions of, light-load, output overvoltage, and pre-bias start-up conditions. The LM25149 provides a diode emulation feature that can be enabled to prevent reverse (drain-to-source) current flow in the low-side MOSFET. When configured for diode emulation mode, the low-side MOSFET is switched off when reverse current flow is detected by sensing the SW voltage using a zero-cross comparator. The benefit of this configuration is lower power loss during light-load conditions; the disadvantage of diode emulation mode is slower light-load transient response.

Diode emulation is configured with the PFM/SYNC pin. To enable diode emulation and thus achieve low-I_Q current at light loads, connect PFM/SYNC to VDDA. If FPWM with continuous conduction mode (CCM) operation is desired, tie PFM/SYNC to AGND. Note that diode emulation is automatically engaged to prevent reverse current flow during a prebias start-up. A gradual change from DCM to CCM operation provides monotonic start-up performance.

To synchronize the LM25149 to an external source, apply a logic-level clock to the PFM/SYNC pin. The LM25149 can be synchronized to ±20% of the programmed frequency up to a maximum of 2.5 MHz. If there is an RT resistor and a synchronization signal, the LM25149 ignores the RT resistor and synchronizes to the external clock. Under low-V_{IN} conditions when the minimum off time is reached, the synchronization signal is ignored, allowing the switching frequency to be reduce to maintain output voltage regulation.

8.4.3 Thermal Shutdown

The LM25149 includes an internal junction temperature monitor. If the temperature exceeds 175°C (typical), thermal shutdown occurs. When entering thermal shutdown, the device:
1. Turns off the high-side and low-side MOSFETs.
2. PG/SYNCOUT switches low.
3. Turns off the VCC regulator.
4. Initiates a soft-start sequence when the die temperature decreases by the thermal shutdown hysteresis of 15°C (typical).

This is a non-latching protection and as such, the device cycles into and out of thermal shutdown if the fault persists.

9 Application and Implementation

Note

以下のアプリケーション情報は、TI の製品仕様に含まれるものではなく、TI ではその正確性または完全性を保証いたしません。個々の目的に対する製品の適合性については、お客様の責任で判断していただくことになります。お客様は自身の設計実装を検証しテストすることで、システムの機能を確認する必要があります。

9.1 Application Information

9.1.1 Power Train Components

A comprehensive understanding of the buck regulator power train components is critical to successfully completing a synchronous buck regulator design. The following sections discuss the output inductor, input and output capacitors, power MOSFETs, and EMI input filter.

9.1.1.1 Buck Inductor

For most applications, choose a buck inductance such that the inductor ripple current, ΔI_L, is between 30% to 50% of the maximum DC output current at nominal input voltage. Choose the inductance using 式 12 based on a peak inductor current given by 式 13.

$$L_O = \frac{V_{OUT}}{\Delta I_L \cdot F_{SW}} \cdot \left(1 - \frac{V_{OUT}}{V_{IN}}\right)$$

(12)

$$I_{L(peak)} = I_{OUT} + \frac{\Delta I_L}{2}$$

(13)

Check the inductor data sheet to make sure that the saturation current of the inductor is well above the peak inductor current of a particular design. Ferrite designs have very low core loss and are preferred at high switching frequencies, so design goals can then concentrate on copper loss and preventing saturation. Low inductor core loss is evidenced by reduced no-load input current and higher light-load efficiency. However, ferrite core materials exhibit a hard saturation characteristic and the inductance collapses abruptly when the saturation current is exceeded. This results in an abrupt increase in inductor ripple current and higher output voltage ripple, not to mention reduced efficiency and compromised reliability. Note that the saturation current of an inductor generally decreases as its core temperature increases. Of course, accurate overcurrent protection is key to avoiding inductor saturation.

9.1.1.2 Output Capacitors

Ordinarily, the output capacitor energy storage of the regulator combined with the control loop response are prescribed to maintain the integrity of the output voltage within the dynamic (transient) tolerance specifications. The usual boundaries restricting the output capacitor in power management applications are driven by finite available PCB area, component footprint and profile, and cost. The capacitor parasitics—equivalent series resistance (ESR) and equivalent series inductance (ESL)—take greater precedence in shaping the load transient response of the regulator as the load step amplitude and slew rate increase.

The output capacitor, C_{OUT}, filters the inductor ripple current and provides a reservoir of charge for step-load transient events. Typically, ceramic capacitors provide extremely low ESR to reduce the output voltage ripple and noise spikes, while tantalum and electrolytic capacitors provide a large bulk capacitance in a relatively compact footprint for transient loading events.

Based on the static specification of peak-to-peak output voltage ripple denoted by ΔV_{OUT}, choose an output capacitance that is larger than that given by 式 14.

$$C_{OUT} \geq \frac{\Delta I_L}{8 \cdot F_{SW} \sqrt{\Delta V_{OUT}^2 - \left(R_{ESR} \cdot \Delta I_L \right)^2}}$$

(14)

図 9-1 conceptually illustrates the relevant current waveforms during both load step-up and step-down transitions. As shown, the large-signal slew rate of the inductor current is limited as the inductor current ramps to match the new load-current level following a load transient. This slew-rate limiting exacerbates the deficit of charge in the output capacitor, which must be replenished as fast as possible during and after the load step-up transient. Similarly, during and after a load step-down transient, the slew rate limiting of the inductor current adds to the surplus of charge in the output capacitor that must be depleted as quickly as possible.
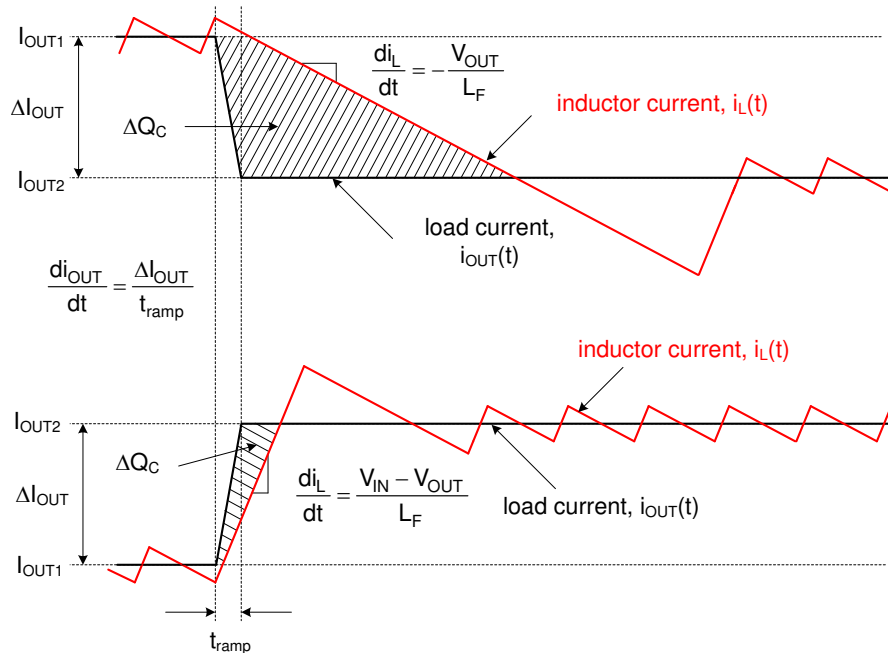

図 9-1. Load Transient Response Representation Showing C_{OUT} Charge Surplus or Deficit

In a typical regulator application of 12-V input to low output voltage (for example, 3.3 V), the load-off transient represents the worst case in terms of output voltage transient deviation. In that conversion ratio application, the steady-state duty cycle is approximately 28% and the large-signal inductor current slew rate when the duty cycle collapses to zero is approximately $-V_{OUT} / L$. Compared to a load-on transient, the inductor current takes much longer to transition to the required level. The surplus of charge in the output capacitor causes the output voltage to significantly overshoot. In fact, to deplete this excess charge from the output capacitor as quickly as possible, the inductor current must ramp below its nominal level following the load step. In this scenario, a large output capacitance can be advantageously employed to absorb the excess charge and minimize the voltage overshoot.

To meet the dynamic specification of output voltage overshoot during such a load-off transient (denoted as $\Delta V_{OVERSHOOT}$ with step reduction in output current given by ΔI_{OUT}), the output capacitance should be larger than:

$$C_{OUT} \geq \frac{L_O \cdot \Delta I_{OUT}^2}{\left(V_{OUT} + \Delta V_{OVERSHOOT} \right)^2 - V_{OUT}^2}$$

(15)

The ESR of a capacitor is provided in the manufacturer's data sheet either explicitly as a specification or implicitly in the impedance versus frequency curve. Depending on type, size, and construction, electrolytic capacitors have significant ESR, 5 mΩ and above, and relatively large ESL, 5 nH to 20 nH. PCB traces contribute some parasitic resistance and inductance as well. Ceramic output capacitors, on the other hand, have

low ESR and ESL contributions at the switching frequency, and the capacitive impedance component dominates. However, depending on package and voltage rating of the ceramic capacitor, the effective capacitance can drop quite significantly with applied DC voltage and operating temperature.

Ignoring the ESR term in 式 14 gives a quick estimation of the minimum ceramic capacitance necessary to meet the output ripple specification. Two to four 47-µF, 10-V, X7R capacitors in 1206 or 1210 footprint is a common choice for a 5-V output. Use 式 15 to determine if additional capacitance is necessary to meet the load-off transient overshoot specification.

A composite implementation of ceramic and electrolytic capacitors highlights the rationale for paralleling capacitors of dissimilar chemistries yet complementary performance. The frequency response of each capacitor is accretive in that each capacitor provides desirable performance over a certain portion of the frequency range. While the ceramic provides excellent mid- and high-frequency decoupling characteristics with its low ESR and ESL to minimize the switching frequency output ripple, the electrolytic device with its large bulk capacitance provides low-frequency energy storage to cope with load transient demands.

9.1.1.3 Input Capacitors

Input capacitors are necessary to limit the input ripple voltage to the buck power stage due to switching-frequency AC currents. TI recommends using X7S or X7R dielectric ceramic capacitors to provide low impedance and high RMS current rating over a wide temperature range. To minimize the parasitic inductance in the switching loop, position the input capacitors as close as possible to the drain of the high-side MOSFET and the source of the low-side MOSFET. The input capacitor RMS current for a single-channel buck regulator is given by 式 16.

$$I_{CIN,rms} = \sqrt{D \cdot \left(I_{OUT}^2 \cdot (1-D) + \frac{\Delta I_L^2}{12} \right)}$$

(16)

The highest input capacitor RMS current occurs at D = 0.5, at which point the RMS current rating of the input capacitors should be greater than half the output current.

Ideally, the DC component of input current is provided by the input voltage source and the AC component by the input filter capacitors. Neglecting inductor ripple current, the input capacitors source current of amplitude (I_{OUT} − I_{IN}) during the D interval and sinks I_{IN} during the 1−D interval. Thus, the input capacitors conduct a square-wave current of peak-to-peak amplitude equal to the output current. It follows that the resultant capacitive component of AC ripple voltage is a triangular waveform. Together with the ESR-related ripple component, the peak-to-peak ripple voltage amplitude is given by 式 17.

$$\Delta V_{IN} = \frac{I_{OUT} \cdot D \cdot (1-D)}{F_{SW} \cdot C_{IN}} + I_{OUT} \cdot R_{ESR}$$

(17)

The input capacitance required for a particular load current, based on an input voltage ripple specification of ΔV_{IN}, is given by 式 18.

$$C_{IN} \geq \frac{D \cdot (1-D) \cdot I_{OUT}}{F_{SW} \cdot (\Delta V_{IN} - R_{ESR} \cdot I_{OUT})}$$

(18)

Low-ESR ceramic capacitors can be placed in parallel with higher valued bulk capacitance to provide optimized input filtering for the regulator and damping to mitigate the effects of input parasitic inductance resonating with high-Q ceramics. One bulk capacitor of sufficiently high current rating and four 10-µF 50-V X7R ceramic decoupling capacitors are usually sufficient for 12-V battery automotive applications. Select the input bulk capacitor based on its ripple current rating and operating temperature range.

Of course, a two-channel buck regulator with 180° out-of-phase interleaved switching provides input ripple current cancellation and reduced input capacitor current stress. The above equations represent valid calculations when one output is disabled and the other output is fully loaded.

9.1.1.4 Power MOSFETs

The choice of power MOSFETs has significant impact on DC/DC regulator performance. A MOSFET with low on-state resistance, $R_{DS(on)}$, reduces conduction loss, whereas low parasitic capacitances enable faster transition times and reduced switching loss. Normally, the lower the $R_{DS(on)}$ of a MOSFET, the higher the gate charge and output charge (Q_G and Q_{OSS}, respectively), and vice versa. As a result, the product of $R_{DS(on)}$ and Q_G is commonly specified as a MOSFET figure-of-merit. Low thermal resistance of a given package ensures that the MOSFET power dissipation does not result in excessive MOSFET die temperature.

The main parameters affecting power MOSFET selection in a LM25149 application are as follows:

- $R_{DS(on)}$ at $V_{GS} = 5$ V
- Drain-source voltage rating, BV_{DSS}, typically 40 V, 60 V, depending on the maximum input voltage
- Gate charge parameters at $V_{GS} = 5$ V
- Output charge, Q_{OSS}, at the relevant input voltage
- Body diode reverse recovery charge, Q_{RR}
- Gate threshold voltage, $V_{GS(th)}$, derived from the Miller plateau evident in the Q_G versus V_{GS} plot in the MOSFET data sheet. With a Miller plateau voltage typically in the range of 2 V to 3 V, the 5-V gate drive amplitude of the LM25149 provides an adequately enhanced MOSFET when on and a margin against Cdv/dt shootthrough when off.

The MOSFET-related power losses for one channel are summarized by the equations presented in 表 9-1, where suffixes one and two represent high-side and low-side MOSFET parameters, respectively. While the influence of inductor ripple current is considered, second-order loss modes, such as those related to parasitic inductances and SW node ringing, are not included. Consult the LM25149 *Quickstart Calculator*.

表 9-1. MOSFET Power Losses

POWER LOSS MODE	HIGH-SIDE MOSFET	LOW-SIDE MOSFET
MOSFET conduction[2] [3]	$P_{cond1} = D \cdot \left(I_{OUT}^2 + \dfrac{\Delta I_L^2}{12} \right) \cdot R_{DS(on)1}$	$P_{cond2} = D' \cdot \left(I_{OUT}^2 + \dfrac{\Delta I_L^2}{12} \right) \cdot R_{DS(on)2}$
MOSFET switching	$P_{sw1} = \dfrac{V_{IN} \cdot F_{SW}}{2} \left[\left(I_{OUT} - \dfrac{\Delta I_L}{2} \right) \cdot t_R + \left(I_{OUT} + \dfrac{\Delta I_L}{2} \right) \cdot t_F \right]$	Negligible
MOSFET gate drive[1]	$P_{Gate1} = V_{CC} \cdot F_{SW} \cdot Q_{G1}$	$P_{Gate2} = V_{CC} \cdot F_{SW} \cdot Q_{G2}$
MOSFET output charge[4]	$P_{Coss} = F_{SW} \cdot \left(V_{IN} \cdot Q_{oss2} + E_{oss1} - E_{oss2} \right)$	
Body diode conduction	N/A	$P_{cond_{BD}} = V_F \cdot F_{SW} \left[\left(I_{OUT} + \dfrac{\Delta I_L}{2} \right) \cdot t_{dt1} + \left(I_{OUT} - \dfrac{\Delta I_L}{2} \right) \cdot t_{dt2} \right]$
Body diode reverse recovery[5]	$P_{RR} = V_{IN} \cdot F_{SW} \cdot Q_{RR2}$	

(1) Gate drive loss is apportioned based on the internal gate resistance of the MOSFET, externally added series gate resistance and the relevant driver resistance of the LM25149.

(2) MOSFET $R_{DS(on)}$ has a positive temperature coefficient of approximately 4500 ppm/°C. The MOSFET junction temperature, T_J, and its rise over ambient temperature is dependent upon the device total power dissipation and its thermal impedance. When operating at or near minimum input voltage, make sure that the MOSFET $R_{DS(on)}$ is rated for the available gate drive voltage.

(3) D' = 1–D is the duty cycle complement.

(4) MOSFET output capacitances, C_{oss1} and C_{oss2}, are highly non-linear with voltage. These capacitances are charged losslessly by the inductor current at high-side MOSFET turnoff. During turn-on, however, a current flows from the input to charge the output capacitance of the low-side MOSFET. E_{oss1}, the energy of C_{oss1}, is dissipated at turn-on, but this is offset by the stored energy E_{oss2} on C_{oss2}.

(5) MOSFET body diode reverse recovery charge, Q_{RR}, depends on many parameters, particularly forward current, current transition speed and temperature.

The high-side (control) MOSFET carries the inductor current during the PWM on time (or D interval) and typically incurs most of the switching losses. It is, therefore, imperative to choose a high-side MOSFET that balances conduction and switching loss contributions. The total power dissipation in the high-side MOSFET is the sum of the losses due to conduction, switching (voltage-current overlap), output charge, and typically two-thirds of the net loss attributed to body diode reverse recovery.

The low-side (synchronous) MOSFET carries the inductor current when the high-side MOSFET is off (or during the 1–D interval). The low-side MOSFET switching loss is negligible as it is switched at zero voltage – current just commutates from the channel to the body diode or vice versa during the transition deadtimes. LM25149, with its adaptive gate drive timing, minimizes body diode conduction losses when both MOSFETs are off. Such losses scale directly with switching frequency.

In high step-down ratio applications, the low-side MOSFET carries the current for a large portion of the switching period. Therefore, to attain high efficiency, it is critical to optimize the low-side MOSFET for low $R_{DS(on)}$. In cases where the conduction loss is too high or the target $R_{DS(on)}$ is lower than available in a single MOSFET, connect two low-side MOSFETs in parallel. The total power dissipation of the low-side MOSFET is the sum of the losses due to channel conduction, body diode conduction, and typically one-third of the net loss attributed to body diode reverse recovery. The LM25149 is well suited to drive TI's portfolio of NexFET™ power MOSFETs.
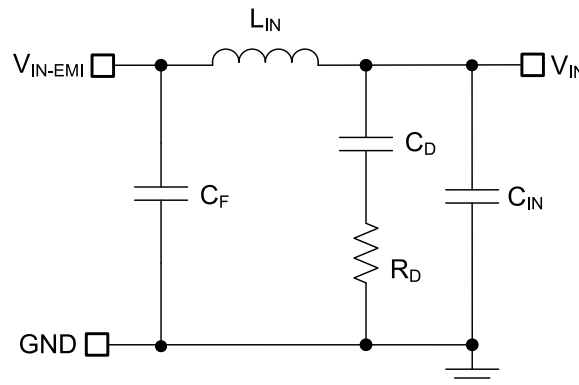
9.1.1.5 EMI Filter

Switching regulators exhibit negative input impedance, which is lowest at the minimum input voltage. An underdamped LC filter exhibits a high output impedance at the resonant frequency of the filter. For stability, the filter output impedance must be less than the absolute value of the converter input impedance.

$$Z_{IN} = \left| -\frac{V_{IN(min)}^2}{P_{IN}} \right|$$

(19)

The passive EMI filter design steps are as follows:
- Calculate the required attenuation of the EMI filter at the switching frequency, where C_{IN} represents the existing capacitance at the input of the switching converter.
- Input filter inductor L_{IN} is usually selected between 1 μH and 10 μH, but it can be lower to reduce losses in a high-current design.
- Calculate input filter capacitor C_F.

図 9-2. Passive π-Stage EMI Filter for Buck Regulator

By calculating the first harmonic current from the Fourier series of the input current waveform and multiplying it by the input impedance (the impedance is defined by the existing input capacitor C_{IN}), a formula is derived to obtain the required attenuation as shown by 式 20.

$$Attn = 20\log\left(\frac{I_{L(PEAK)}}{\pi^2 \cdot F_{SW} \cdot C_{IN}} \cdot \sin(\pi \cdot D_{MAX}) \cdot \frac{1}{1\,\mu V} \right) - V_{MAX}$$

(20)

where

- V_{MAX} is the allowed dBμV noise level for the applicable conducted EMI specification, for example CISPR 32 Class B.

- C_{IN} is the existing input capacitance of the buck regulator.
- D_{MAX} is the maximum duty cycle.
- I_{PEAK} is the peak inductor current.

For filter design purposes, the current at the input can be modeled as a square-wave. Determine the passive EMI filter capacitance C_F from 式 21.

$$C_F = \frac{1}{L_{IN}} \left(\frac{10^{\frac{|Attn|}{40}}}{2\pi \cdot F_{SW}} \right)^2$$

(21)

Adding an input filter to a switching regulator modifies the control-to-output transfer function. The output impedance of the filter must be sufficiently small so that the input filter does not significantly affect the loop gain of the buck converter. The impedance peaks at the filter resonant frequency. The resonant frequency of the passive filter is given by 式 22.

$$f_{res} = \frac{1}{2\pi \cdot \sqrt{L_{IN} \cdot C_F}}$$

(22)

The purpose of R_D is to reduce the peak output impedance of the filter at the resonant frequency. Capacitor C_D blocks the DC component of the input voltage to avoid excessive power dissipation in R_D. Capacitor C_D should have lower impedance than R_D at the resonant frequency with a capacitance value greater than that of the input capacitor C_{IN}. This prevents C_{IN} from interfering with the cutoff frequency of the main filter. Added input damping is needed when the output impedance of the filter is high at the resonant frequency (Q of filter formed by L_{IN} and C_{IN} is too high). An electrolytic capacitor C_D can be used for input damping with a value given by 式 23.

$$C_D \geq 4 \cdot C_{IN}$$

(23)

Select the input damping resistor R_D using 式 24.

$$R_D = \sqrt{\frac{L_{IN}}{C_{IN}}}$$

(24)

9.1.1.6 Active EMI Filter

Active EMI filtering uses a capacitive multiplier to reduce the magnitude of the LC filtering components. Extra compensation components are needed, but the reduction in LC size outweigh the required network. The active EMI filter design steps are as follows:

- Calculate the required attenuation of the EMI filter at the switching frequency, similar to the passive EMI filter.
- Select input filter inductor L_{IN} between 0.47 µH and 4.7 µH, lower than the passive EMI inductor.
- Use recommended values for sensing and compensation components C_{SEN}, C_{AEFC}, R_{AEFC}, C_{INC}, and R_{INC}.
- Calculate active EMI injection capacitor C_{INJ}.
- Calculate active EMI damping resistor R_{DAMP}.
- For low-frequency designs (F_{SW} < 1 MHz), calculate the active EMI damping capacitance C_{DAMP}.
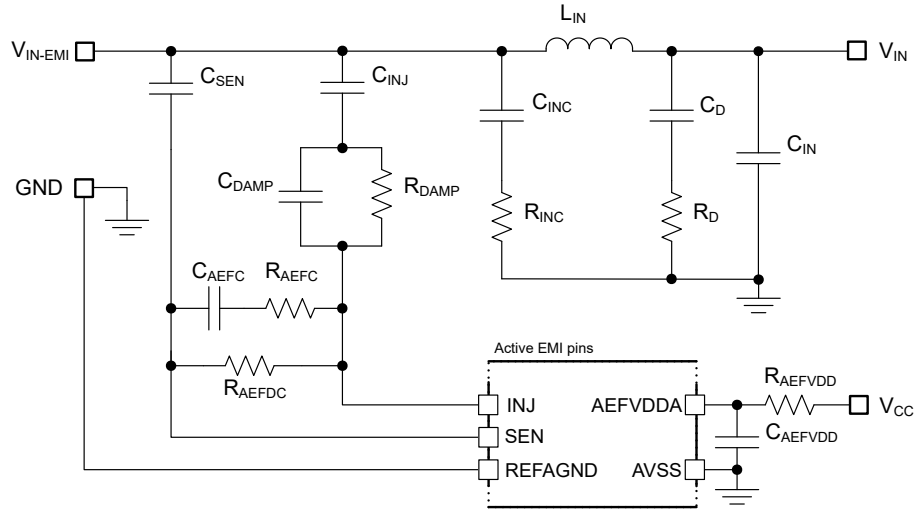
図 9-3. Active EMI Filter for a Buck Regulator

Use 式 20 to determine the attenuation required. 表 9-2 lists the recommended compensation and sensing component values. Use low F_{SW} component values if $F_{SW} \leq 1$ MHz and high F_{SW} component values if $F_{SW} > 1$MHz.

表 9-2. Recommended Active EMI Compensation Component Values

AEF COMPONENT	LOW F_{SW}	HIGH F_{SW}	DESCRIPTION
C_{SEN}	0.1 µF	0.1 µF	Sensing capacitor
R_{AEFC}	1 kΩ	200 Ω	Compensation
C_{AEFC}	1 nF	5 nF	Compensation
R_{INC}	0.47 Ω	0.47 Ω	Compensation
C_{INC}	0.1 µF	0.1 µF	Compensation
R_{AEFVDD}	3 Ω	3 Ω	Decoupling
C_{AEFVDD}	2.2 µF	2.2 µF	Decoupling

Select the desired L_{IN}. Determine the Active EMI filter capacitance C_{INJ} from 式 25.

$$C_{INJ} = \frac{1}{\frac{C_{SEN}}{C_{AEFC}} \cdot L_{IN}} \left(\frac{10^{\frac{|Attn|}{40}}}{2\pi \cdot F_{SW}} \right)^2$$

(25)

Determine the Active EMI damping resistor R_{DAMP} from 式 26.

$$R_{DAMP} = \sqrt{\frac{C_{SEN}}{C_{AEFC}} \cdot \frac{L_{IN}}{C_{INJ}}}$$

(26)

Determine the Active EMI damping capacitance C_{DAMP} from 式 27. C_{DAMP} is not needed for $F_{SW} > 1$ MHz.

$$C_{DAMP} = \frac{1}{2} \cdot C_{INJ}$$

(27)

9.1.2 Error Amplifier and Compensation

図 9-4 shows a type-II compensator using a transconductance error amplifier (EA). The dominant pole of the EA open-loop gain is set by the EA output resistance, $R_{O\text{-}EA}$, and effective bandwidth-limiting capacitance, C_{BW}, as shown by 式 28.

$$G_{EA(open\,loop)}(s) = -\frac{g_m \cdot R_{O\text{-}EA}}{1 + s \cdot R_{O\text{-}EA} \cdot C_{BW}}$$

(28)

The EA high-frequency pole is neglected in the above expression. 式 29 calculates the compensator transfer function from output voltage to COMP node, including the gain contribution from the (internal or external) feedback resistor network.

$$G_c(s) = \frac{\hat{v}_c(s)}{\hat{v}_{out}(s)} = -\frac{V_{REF}}{V_{OUT}} \cdot \frac{g_m \cdot R_{O\text{-}EA} \cdot \left(1 + \dfrac{s}{\omega_{z1}}\right)}{\left(1 + \dfrac{s}{\omega_{p1}}\right) \cdot \left(1 + \dfrac{s}{\omega_{p2}}\right)}$$

(29)

where

- V_{REF} is the feedback voltage reference of 0.8 V.
- g_m is the EA gain transconductance of 1200 µS.
- $R_{O\text{-}EA}$ is the error amplifier output impedance of 64 MΩ.

$$\omega_{Z1} = \frac{1}{R_{COMP} \cdot C_{COMP}}$$

(30)

$$\omega_{p1} = \frac{1}{R_{O\text{-}EA} \cdot \left(C_{COMP} + C_{HF} + C_{BW}\right)} \cong \frac{1}{R_{O\text{-}EA} \cdot C_{COMP}}$$

(31)

$$\omega_{p2} = \frac{1}{R_{COMP} \cdot \left(C_{COMP} \| \left(C_{HF} + C_{BW}\right)\right)} \cong \frac{1}{R_{COMP} \cdot C_{HF}}$$

(32)

The EA compensation components create a pole close to the origin, a zero, and a high-frequency pole. Typically, $R_{COMP} \ll R_{O\text{-}EA}$ and $C_{COMP} \gg C_{BW}$ and C_{HF}, so the approximations are valid.
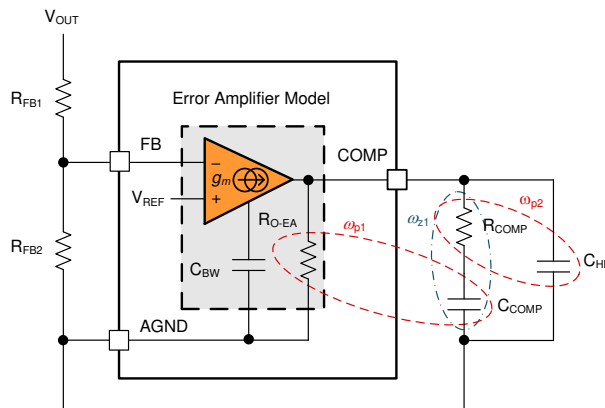

図 9-4. Error Amplifier and Compensation Network

9.2 Typical Applications

9.2.1 Design 1 – High Efficiency 2.1-MHz Synchronous Buck Regulator

図 9-5 shows the schematic diagram of a single-output synchronous buck regulator with an output voltage of 5 V and a rated load current of 8 A. In this example, the target half-load and full-load efficiencies are 93.5% and 92.5%, respectively, based on a nominal input voltage of 12 V that ranges from 5.5 V to 36 V. The switching frequency is set at 2.1 MHz by resistor R_{RT}. The 5-V output is connected to VCCX to reduce IC bias power dissipation and improve efficiency. An output voltage of 3.3 V is also feasible simply by connecting FB to VDDA (tie VCCX to GND in this case).
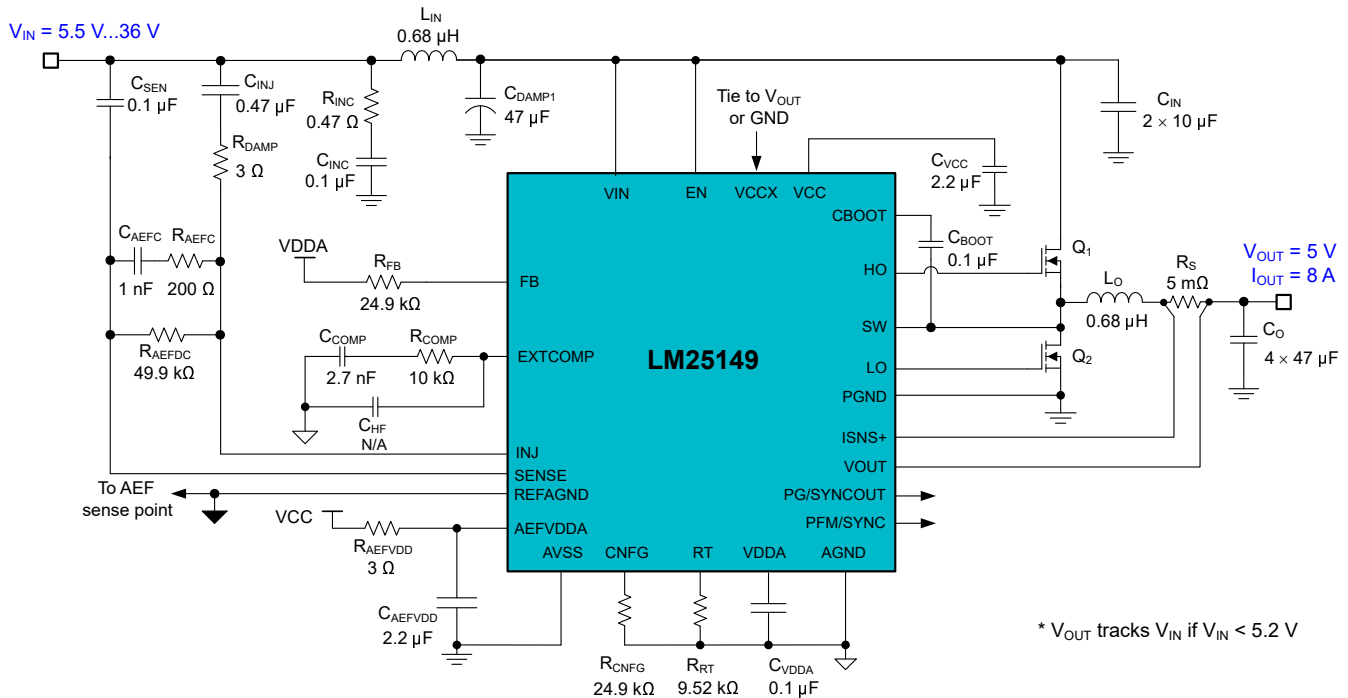
図 9-5. Application Circuit 1 With LM25149 Buck Regulator at 2.1 MHz

---

Note

This and subsequent design examples are provided herein to showcase the LM25149 controller in several different applications. Depending on the source impedance of the input supply bus, an electrolytic capacitor can be required at the input to ensure stability, particularly at low input voltage and high output current operating conditions. See セクション 10 for more detail.

9.2.1.1 Design Requirements

表 9-3 shows the intended input, output, and performance parameters for this design example. Reference the LM25149-Q1EVM-2100 evaluation module.

表 9-3. Design Parameters

DESIGN PARAMETER	VALUE
Input voltage range (steady-state)	8 V to 18 V
Min transient input voltage	5.5 V
Max transient input voltage	36 V
Output voltage	5 V
Output current	8 A
Switching frequency	2.1 MHz
Output voltage regulation	±1%
Standby current, no-load	12 µA
Shutdown current	2.3 µA
Soft-start time	3 ms

The switching frequency is set at 2.1 MHz by resistor R_{RT}. In terms of control loop performance, the target loop crossover frequency is 60 kHz with a phase margin greater than 50°.

The selected buck regulator powertrain components are cited in 表 9-4, and many of the components are available from multiple vendors. The MOSFETs in particular are chosen for both lowest conduction and switching power loss, as discussed in detail in セクション 9.1.1.4. This design uses a low-DCR metal-powder composite inductor and ceramic output capacitor implementation.

表 9-4. List of Materials for Application Circuit 1

REFERENCE DESIGNATOR	QTY	SPECIFICATION	MANUFACTURER	PART NUMBER
C_{IN}	2	10 µF, 50 V, X7S, 1210, ceramic	Taiyo Yuden	UMJ325KB7106KMHT
			Murata	GCM32EC71H106KA03
			TDK	CGA6P3X7S1H106K250AB
C_O	4	47 µF, 6.3 V, X7R, 1210, ceramic	Murata	GCM32ER70J476KE19L
			Taiyo Yuden	JMK325B7476KMHTR
		47 µF, 10 V, X7S, 1210, ceramic	TDK	CGA6P1X7S1A476M250AC
L_O	1	0.68 µH, 2.9 mΩ, 15.3 A, 6.7 × 6.5 × 3.1 mm	Coilcraft	XGL6030-681MEB
		0.56 µH, 3.6 mΩ, 13 A, 6.6 × 6.6 × 4.8 mm	Würth Electronik	744373490056
		0.68 µH, 4.5 mΩ, 22 A, 6.95 × 6.6 × 2.8 mm	Cyntec	VCMV063T-R68MN2T
Q_1	1	40 V, 4.7 mΩ, 12 nC, SON 5 × 6	Texas Instruments	CSD18503Q5A
Q_2	1	40 V, 2.7 mΩ, 35 nC, SON 5 × 6	Texas Instruments	CSD18511Q5A
R_S	1	Shunt, 5 mΩ, 0508, 1 W	Susumu	KRL2012E-M-R005-F-T5
U_1	1	LM25149 42-V synchronous buck controller with AEF	Texas Instruments	LM25149RGYR

Product Folder Links: LM25149

9.2.1.2 Detailed Design Procedure

9.2.1.2.1 Custom Design With WEBENCH® Tools

Click here to create a custom design using the LM25149 device with the WEBENCH® Power Designer.

1. Start by entering the input voltage (V_{IN}), output voltage (V_{OUT}), and output current (I_{OUT}) requirements.
2. Optimize the design for key parameters such as efficiency, footprint, and cost using the optimizer dial.
3. Compare the generated design with other possible solutions from Texas Instruments.

The WEBENCH Power Designer provides a customized schematic along with a list of materials with real-time pricing and component availability.

In most cases, these actions are available:
- Run electrical simulations to see important waveforms and circuit performance
- Run thermal simulations to understand board thermal performance
- Export customized schematic and layout into popular CAD formats
- Print PDF reports for the design, and share the design with colleagues

Get more information about WEBENCH tools at www.ti.com/WEBENCH.

9.2.1.2.2 Custom Design With Excel Quickstart Tool

Select components based on the regulator specifications using the LM25149 *Quickstart Calculator* available for download from the LM25149 product folder.

9.2.1.2.3 Buck Inductor

1. Use 式 33 to calculate the required buck inductance based on a 30% inductor ripple current at nominal input voltages.

$$L_O = \frac{V_{OUT}}{\Delta I_{LO} \cdot F_{SW}} \cdot \left(1 - \frac{V_{OUT}}{V_{IN(nom)}}\right) = \frac{5\,V}{2.4\,A \cdot 2.1\,MHz} \cdot \left(1 - \frac{5\,V}{12\,V}\right) = 0.58\,\mu H$$

(33)

2. Select a standard inductor value of 0.56 µH or use a 0.68 µH to account for effective inductance derating with current of molded inductors. Use 式 34 to calculate the peak inductor current at maximum steady-state input voltage. Subharmonic oscillation occurs with a duty cycle greater than 50% for peak current-mode control. For design simplification, the LM25149 has an internal slope compensation ramp proportional to the switching frequency that is added to the current sense signal to damp any tendency toward subharmonic oscillation.

$$I_{LO(PK)} = I_{OUT} + \frac{\Delta I_{LO}}{2} = I_{OUT} + \frac{V_{OUT}}{2 \cdot L_O \cdot F_{SW}} \cdot \left(1 - \frac{V_{OUT}}{V_{IN(max)}}\right) = 8\,A + \frac{5\,V}{0.56\,\mu H \cdot 2.1\,MHz} \cdot \left(1 - \frac{5\,V}{18\,V}\right) = 9.53\,A$$

(34)

3. Based on 式 8, use 式 35 to cross-check the inductance to set a slope compensation close to the ideal one times the inductor current downslope.

$$L_{O(sc)} = \frac{V_{OUT} \cdot R_S}{24 \cdot F_{SW}} = \frac{5\,V \cdot 5\,m\Omega}{24 \cdot 2.1\,MHz} = 0.5\,\mu H$$

(35)

9.2.1.2.4 Current-Sense Resistance

1. Calculate the current-sense resistance based on a maximum peak current capability of at least 25% higher than the peak inductor current at full load to provide sufficient margin during start-up and load-on transients. Calculate the current sense resistances using 式 36.

$$R_S = \frac{V_{CS-TH}}{1.25 \cdot I_{LO(PK)}} = \frac{60\,mV}{1.25 \cdot 9.53\,A} = 5.04\,m\Omega$$

(36)

where

- V_{CS-TH} is the 60-mV current limit threshold.

2. Select a standard resistance value of 5 mΩ for the shunt. An 0508 footprint component with wide aspect ratio termination design provides 1-W power rating, low parasitic series inductance, and compact PCB layout. Carefully adhere to the layout guidelines in セクション 11.1 to make sure that noise and DC errors do not corrupt the differential current-sense voltages measured at the ISNS+ and VOUT pins.
3. Place the shunt resistor close to the inductor.
4. Use Kelvin-sense connections, and route the sense lines differentially from the shunt to the LM25149.
5. The CS-to-output propagation delay (related to the current limit comparator, internal logic, and power MOSFET gate drivers) causes the peak current to increase above the calculated current limit threshold. For a total propagation delay $t_{DELAY-ISNS+}$ of 40 ns, use 式 37 to calculate the worst-case peak inductor current with the output shorted.

$$I_{LO-PK(SC)} = \frac{V_{CS-TH}}{R_S} + \frac{V_{IN(max)} \cdot t_{DELAY-ISNS+}}{L_O} = \frac{60\,mV}{5\,m\Omega} + \frac{18\,V \cdot 45\,ns}{0.56\,\mu H} = 13.5\,A$$

(37)

6. Based on this result, select an inductor with saturation current greater than 16 A across the full operating temperature range.

9.2.1.2.5 Output Capacitors

1. Use 式 38 to estimate the output capacitance required to manage the output voltage overshoot during a load-off transient (from full load to no load) assuming a load transient deviation specification of 1.5% (75 mV for a 5-V output).

$$C_{OUT} \geq \frac{L_O \cdot \Delta I_{OUT}^2}{(V_{OUT} + \Delta V_{OVERSHOOT})^2 - V_{OUT}^2} = \frac{0.56\,\mu H \cdot (8\,A)^2}{(5\,V + 75\,mV)^2 - (5\,V)^2} = 47.4\,\mu F$$

(38)

2. Noting the voltage coefficient of ceramic capacitors where the effective capacitance decreases significantly with applied voltage, select four 47-µF, 10-V, X7R, 1210 ceramic output capacitors. Generally, when sufficient capacitance is used to satisfy the load-off transient response requirement, the voltage undershoot during a no-load to full-load transient is also satisfactory.
3. Use 式 39 to estimate the peak-peak output voltage ripple at nominal input voltage.

$$\Delta V_{OUT} = \sqrt{\left(\frac{\Delta I_{LO}}{8 \cdot F_{SW} \cdot C_{OUT}}\right)^2 + (R_{ESR} \cdot \Delta I_{LO})^2} = \sqrt{\left(\frac{2.54\,A}{8 \cdot 2.1\,MHz \cdot 44\,\mu F}\right)^2 + (1\,m\Omega \cdot 2.54\,A)^2} = 4.3\,mV$$

(39)

where

- R_{ESR} is the effective equivalent series resistance (ESR) of the output capacitors.
- 44 µF is the total effective (derated) ceramic output capacitance at 5 V.

4. Use 式 40 to calculate the output capacitor RMS ripple current using and verify that the ripple current is within the capacitor ripple current rating.

$$I_{CO(RMS)} = \frac{\Delta I_{LO}}{\sqrt{12}} = \frac{2.54\,A}{\sqrt{12}} = 0.73\,A$$

(40)

9.2.1.2.6 Input Capacitors

A power supply input typically has a relatively high source impedance at the switching frequency. Good-quality input capacitors are necessary to limit the input ripple voltage. In general, the ripple current splits between the input capacitors based on the relative impedance of the capacitors at the switching frequency.

1. Select the input capacitors with sufficient voltage and RMS ripple current ratings.

2. Use 式 41 to calculate the input capacitor RMS ripple current assuming a worst-case duty-cycle operating point of 50%.

$$I_{CIN(RMS)} = I_{OUT} \cdot \sqrt{D \cdot (1-D)} = 8A \cdot \sqrt{0.5 \cdot (1-0.5)} = 4\,A \tag{41}$$

3. Use 式 42 to find the required input capacitance.

$$C_{IN} \geq \frac{D \cdot (1-D) \cdot I_{OUT}}{F_{SW} \cdot (\Delta V_{IN} - R_{ESR} \cdot I_{OUT})} = \frac{0.5 \cdot (1-0.5) \cdot 8\,A}{2.1MHz \cdot (120mV - 2m\Omega \cdot 8\,A)} = 9.2\ \mu F \tag{42}$$

where

- ΔV_{IN} is the input peak-to-peak ripple voltage specification.
- R_{ESR} is the input capacitor ESR.

4. Recognizing the voltage coefficient of ceramic capacitors, select two 10-µF, 50-V, X7R, 1210 ceramic input capacitors. Place these capacitors adjacent to the power MOSFETs. See セクション 11.1.1 for more detail.

5. Use four 10-nF, 50-V, X7R, 0603 ceramic capacitors near the high-side MOSFET to supply the high di/dt current during MOSFET switching transitions. Such capacitors offer high self-resonant frequency (SRF) and low effective impedance above 100 MHz. The result is lower power loop parasitic inductance, thus minimizing switch-node voltage overshoot and ringing for lower conducted and radiated EMI signature. Refer to セクション 11.1 for more detail.

9.2.1.2.7 Frequency Set Resistor

Calculate the RT resistance for a switching frequency of 2.1 MHz using 式 43. Choose a standard E96 value of 9.53 kΩ.

$$R_T(k\Omega) = \frac{\dfrac{10^6}{F_{SW}(kHz)} - 53}{45} = \frac{\dfrac{10^6}{2100kHz} - 53}{45} = 9.4\,k\Omega \tag{43}$$

9.2.1.2.8 Feedback Resistors

If an output voltage setpoint other than 3.3 V or 5 V is required (or to measure a bode plot when using either of the fixed output voltage options), determine the feedback resistances using 式 44.

$$R_{FB1} = R_{FB2} \cdot \left(\frac{V_{OUT}}{V_{REF}} - 1\right) = 15k\Omega \cdot \left(\frac{5\,V}{0.8\,V} - 1\right) = 78.7\,k\Omega \tag{44}$$

9.2.1.2.9 Compensation Components

Choose compensation components for a stable control loop using the procedure outlined as follows:

1. Based on a specified loop gain crossover frequency, f_C, of 60 kHz, use 式 45 to calculate R_{COMP}, assuming an effective output capacitance of 100 µF. Choose a standard value for R_{COMP} of 10 kΩ.

$$R_{COMP} = 2\pi \cdot f_C \cdot \frac{V_{OUT}}{V_{REF}} \cdot \frac{R_S \cdot G_{CS}}{g_m} \cdot C_{OUT} = 2\pi \cdot 60kHz \cdot \frac{5\,V}{0.8\,V} \cdot \frac{5m\Omega \cdot 10}{1200\mu S} \cdot 100\mu F = 9.82k\Omega \tag{45}$$

2. To provide adequate phase boost at crossover while also allowing a fast settling time during a load or line transient, select C_{COMP} to place a zero at the higher of (1) one tenth of the crossover frequency, or (2) the load pole. Choose a standard value for C_{COMP} of 2.7 nF.

$$C_{COMP} = \frac{10}{2\pi \cdot f_C \cdot R_{COMP}} = \frac{10}{2\pi \cdot 60\,kHz \cdot 10\,k\Omega} = 2.65\ nF$$

(46)

Such a low capacitance value also helps to avoid output voltage overshoot when recovering from dropout (when the input voltage is less than the output voltage setpoint and V_{COMP} is railed high).

3. Calculate C_{HF} to create a pole at the ESR zero and to attenuate high-frequency noise at COMP. C_{BW} is the bandwidth-limiting capacitance of the error amplifier. C_{HF} may not be significant enough to be necessary in some designs, like this one. C_{HF} can be unpopulated, or used with a small 22 pF for more noise filtering.

$$C_{HF} = \frac{1}{2\pi \cdot f_{ESR} \cdot R_{COMP}} - C_{BW} = \frac{1}{2\pi \cdot 500\,kHz \cdot 10\,k\Omega} - 31\,pF = 0.8\ pF$$

(47)

Note

Set a fast loop with high R_{COMP} and low C_{COMP} values to improve the response when recovering from operation in dropout.

For technical solutions, industry trends, and insights for designing and managing power supplies, please refer to TI's technical articles.

9.2.1.2.10 Active EMI Components

Choose active EMI filter components for sufficient attenuation using the following procedure.

1. Refer to *Active EMI Filter* for sensing and compensation components.
2. Based on a selected L_{IN} of 0.68 μH and a required attenuation of 60 dB, use 式 48 to calculate C_{INJ}. Choose a standard value for C_{INJ} of 0.47 μF.

$$C_{INJ} = \frac{1}{\dfrac{C_{SEN}}{C_{AEFC}} \cdot L_{IN}}\left(\frac{10^{\frac{|Attn|}{40}}}{2\pi \cdot F_{SW}}\right)^2 = \frac{1}{\dfrac{100\ nF}{5\ nF} \cdot 0.68\ \mu H}\left(\frac{10^{\frac{|60|}{40}}}{2\pi \cdot 2.1\ MHz}\right)^2 = 0.42\ \mu F$$
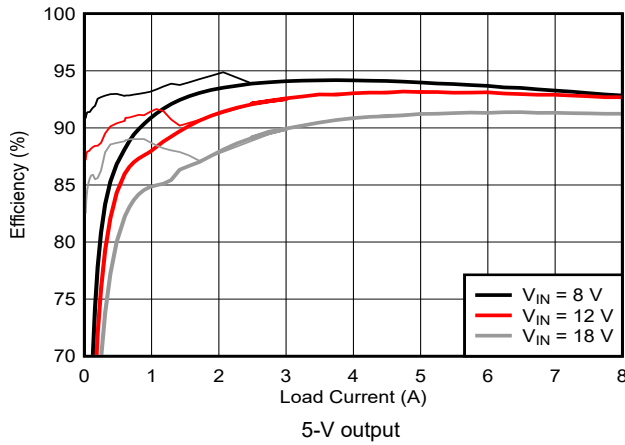
(48)

3. To prevent the active EMI filter from undamped resonance with the L_{IN} inductor, use 式 49 to select an adequate R_{DAMP}. Choose a standard value for R_{DAMP} of 5.01 Ω.

$$R_{DAMP} = \sqrt{\frac{C_{SEN}}{C_{AEFC}} \cdot \frac{L_{IN}}{C_{INJ}}} = \sqrt{\frac{100\ nF}{5\ nF} \cdot \frac{0.68\ \mu H}{0.47\ \mu F}} = 5.4\ \Omega$$

(49)

Note
For 2.1-MHz designs C_{DAMP} is not required.

9.2.1.3 Application Curves

5-V output

図 9-6. Efficiency vs. I_OUT

5-V output

図 9-7. Efficiency vs. I_OUT, Log Scale

8-A resistive load

図 9-8. Full load Switching

No load

図 9-9. PFM Switching

V_IN ramps from 12 to 36 V   5-A load
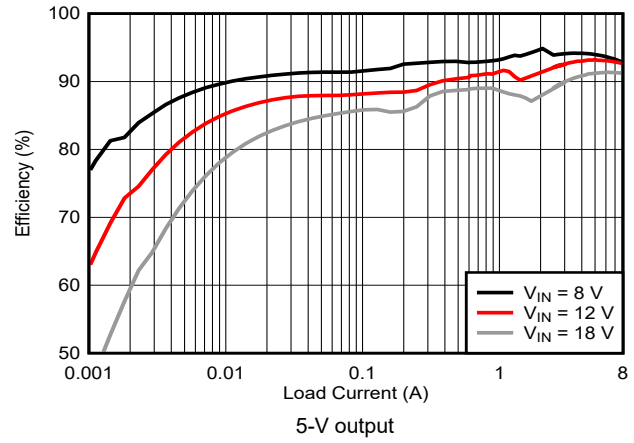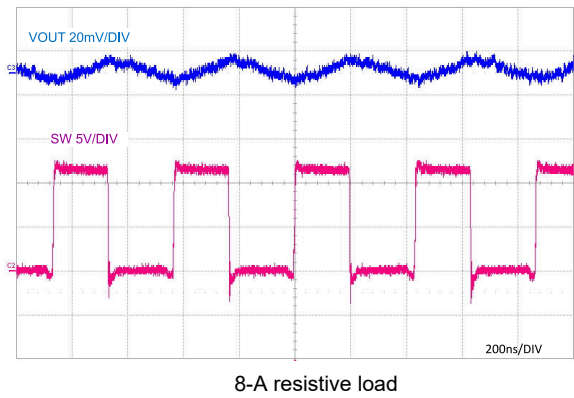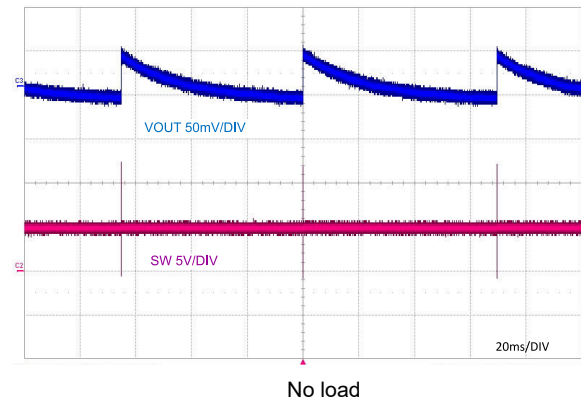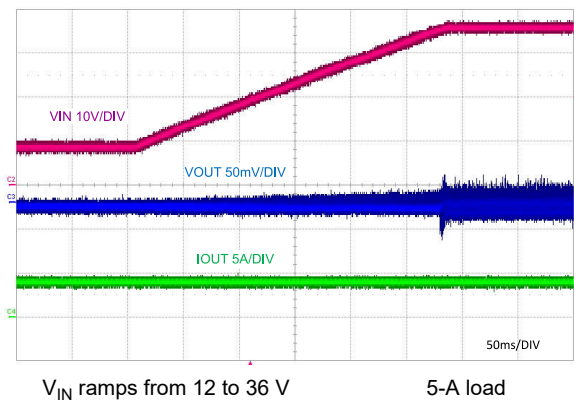
図 9-10. Line Transient Response to V_IN = 36 V

V_IN falls to 4 V   5-A load
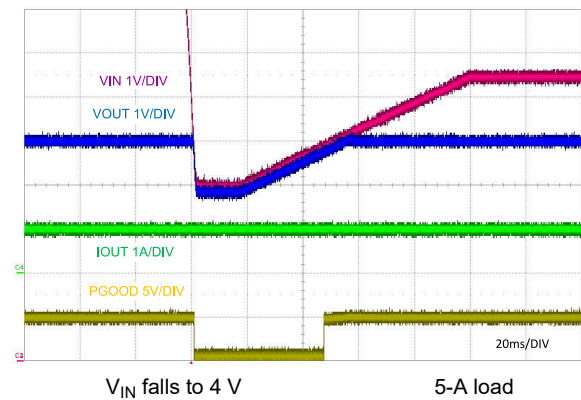
図 9-11. Line Transient Response to V_IN = 4 V

Product Folder Links: *LM25149*
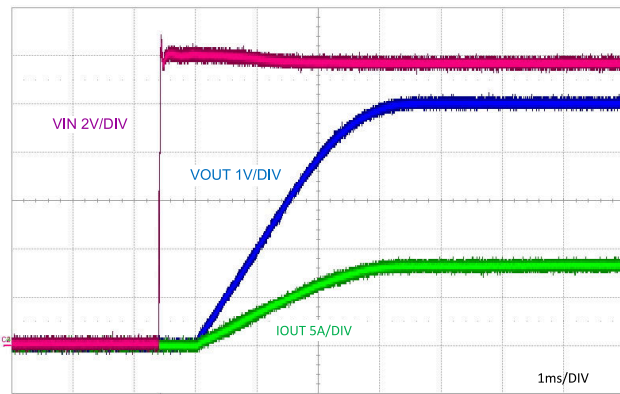
V_IN step to 12 V   8-A resistive load

図 9-12. Start-Up Characteristic
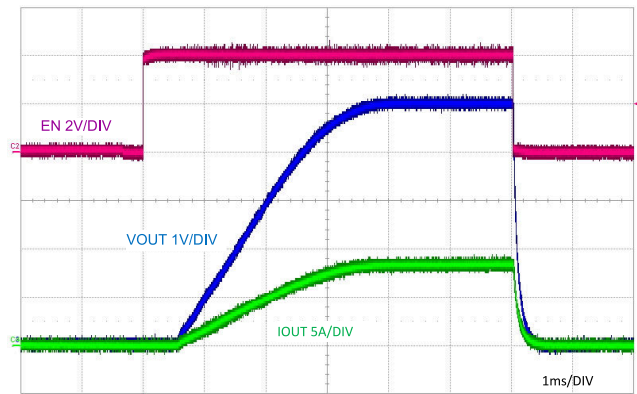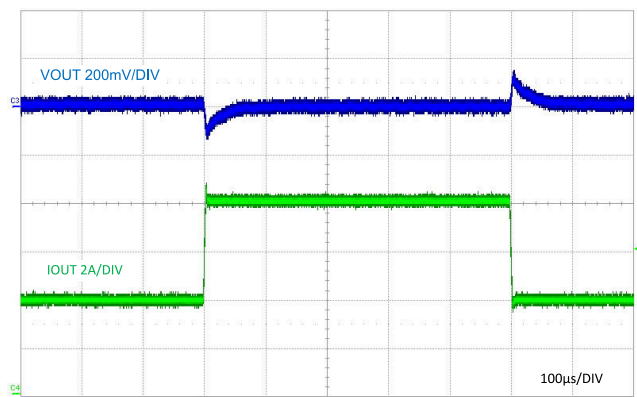
V_IN = 12 V   8-A resistive load
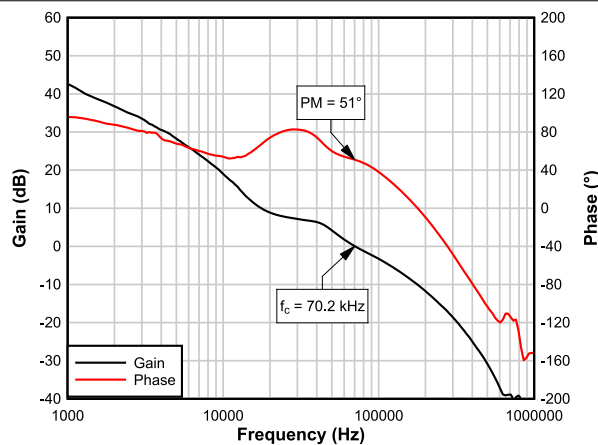
図 9-13. ENABLE ON and OFF Characteristic
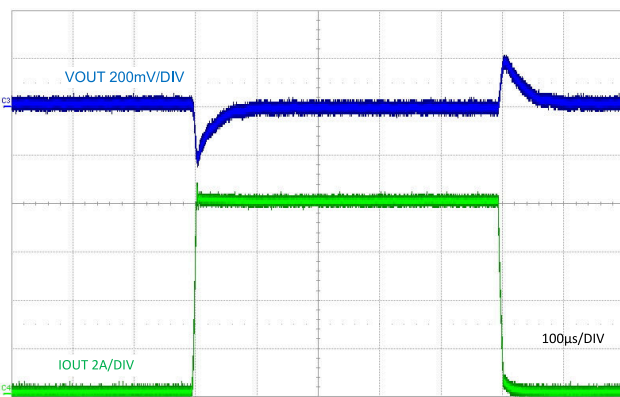
V_IN = 12 V   FPWM

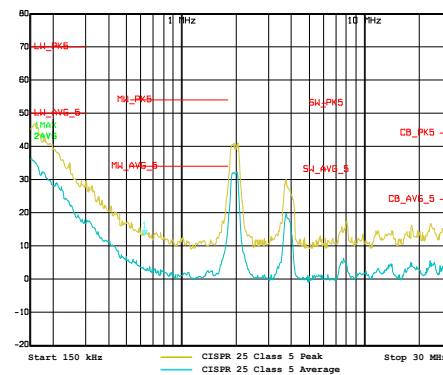**図 9-14. Load Transient, 0 A to 8 A**

V_IN = 12 V   FPWM

図 9-15. Load Transient, 4 A to 8 A

V_IN = 12 V   8-A resistive load

図 9-16. Bode Plot, 5-V Output

V_IN = 13.8 V   150 kHz to 30 MHz   7-A resistive load

図 9-17. CISPR 25 Class 5 Conducted EMI

9.2.2 Design 2 – High Efficiency 440-kHz Synchronous Buck Regulator

図 9-18 shows the schematic diagram of a single-output synchronous buck regulator with an output voltage of 5 V and a rated load current of 10 A. In this example, the target half-load and full-load efficiencies are 97% and 95%, respectively, based on a nominal input voltage of 12 V that ranges from 5.5 V to 36 V. The switching frequency is set at 440 kHz by resistor R_{RT}. The 5-V output is connected to VCCX to reduce IC bias power dissipation and improve efficiency. An output voltage of 3.3 V is also feasible simply by connecting FB to VDDA (tie VCCX to GND in this case).
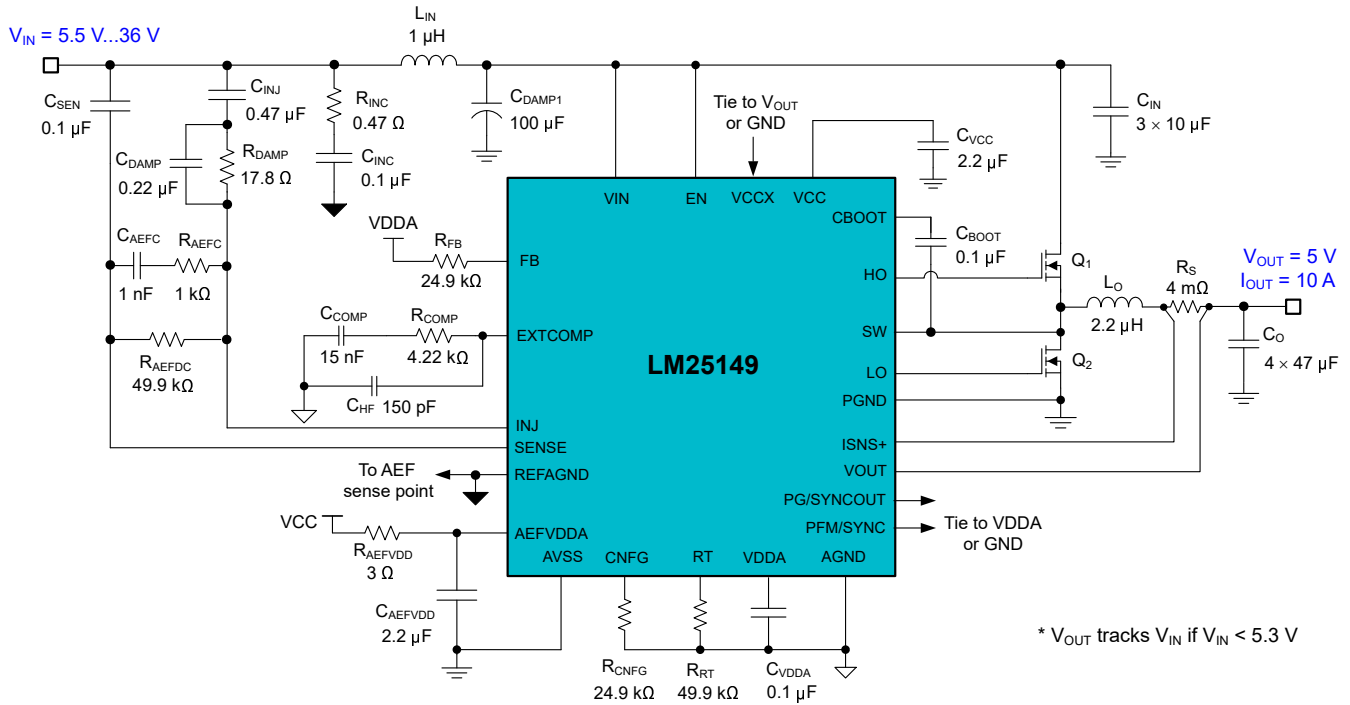

図 9-18. Application Circuit 2 With LM25149 Buck Regulator at 440 kHz

Product Folder Links: LM25149

9.2.2.1 Design Requirements

表 9-5 shows the intended input, output, and performance parameters for this design example.

表 9-5. Design Parameters

DESIGN PARAMETER	VALUE
Input voltage range (steady-state)	8 V to 36 V
Min transient input voltage	5.5 V
Max transient input voltage	40 V
Output voltage	5 V
Output current	10 A
Switching frequency	440 kHz
Output voltage regulation	±1%
Standby current, no-load	12 µA
Shutdown current	2.3 µA
Soft-start time	3 ms

The switching frequency is set at 440 kHz by resistor R_{RT}. The selected buck regulator powertrain components are cited in 表 9-6, and many of the components are available from multiple vendors. The MOSFETs in particular are chosen for both lowest conduction and switching power loss, as discussed in detail in セクション 9.1.1.4.

表 9-6. List of Materials for Application Circuit 2

| REFERENCE DESIGNATOR	QTY	SPECIFICATION	MANUFACTURER	PART NUMBER
C_{IN}	2	10 µF, 50 V, X7R, 1210, ceramic	AVX	12105C106K4Z2A
			TDK	C3225X7R1H106K250AC
			Murata	GRM32ER71H106KA12L
C_O	4	47 µF, 6.3 V, X7R, 1210, ceramic	Murata	GCM32ER70J476KE19L
			Taiyo Yuden	JMK325B7476KMHTR
		47 µF, 10 V, X7S, 1210, ceramic	TDK	CGA6P1X7S1A476M250AC
L_O	1	2.2 µH, 4.3 mΩ, 12.5 A, 6.7 × 6.5 × 6.1 mm	Coilcraft	XGL6060-222MEC
		2.2 µH, 6.5 mΩ, 10 A, 10 × 11 × 3.8 mm	Würth Electronik	74437368022
Q_1	1	40 V, 4.7 mΩ, 12 nC, SON 5 × 6	Texas Instruments	CSD18503Q5A
Q_2	1	40 V, 2.7 mΩ, 35 nC, SON 5 × 6	Texas Instruments	CSD18511Q5A
R_S	1	Shunt, 4 mΩ, 0508, 1 W	Susumu	KRL2012E-M-R004-F-T5
U_1	1	LM25149 42-V synchronous buck controller with AEF	Texas Instruments	LM25149RGYR

9.2.2.2 Detailed Design Procedure

See セクション 9.2.1.2.

9.2.2.3 Application Curves
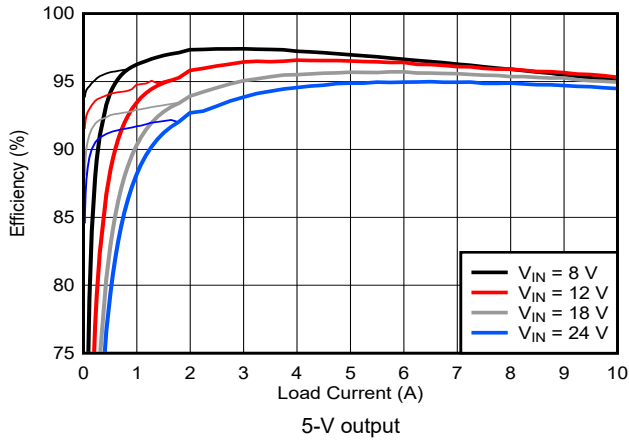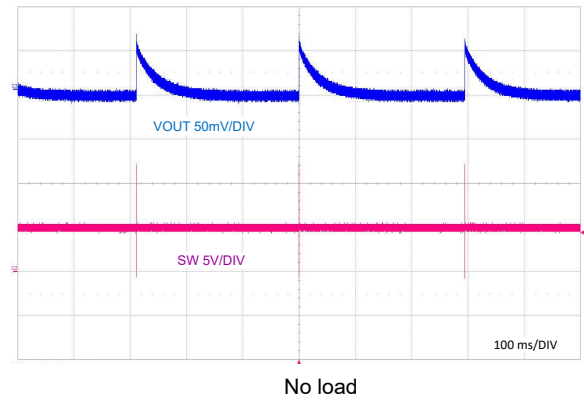

図 9-19. Efficiency vs. I_{OUT}
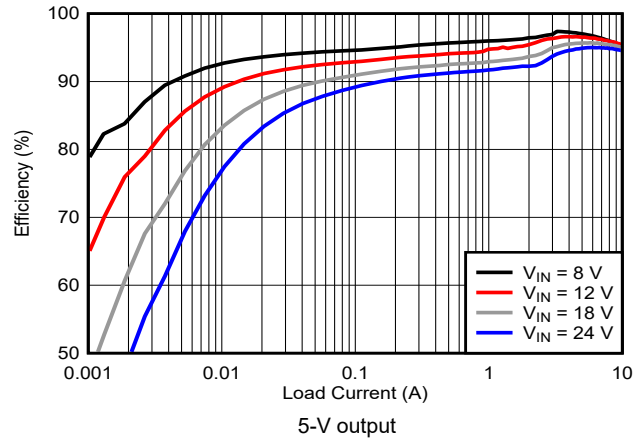
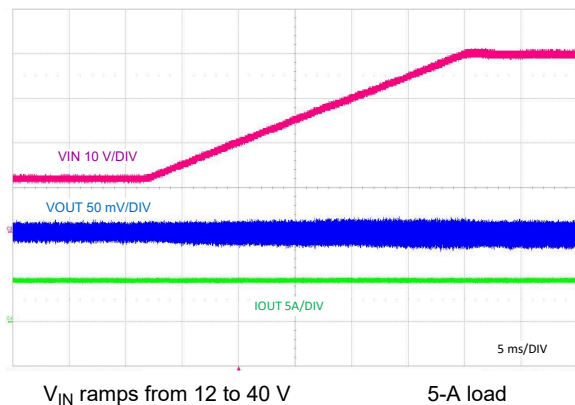**図 9-20. Efficiency vs. I_{OUT}, Log Scale**
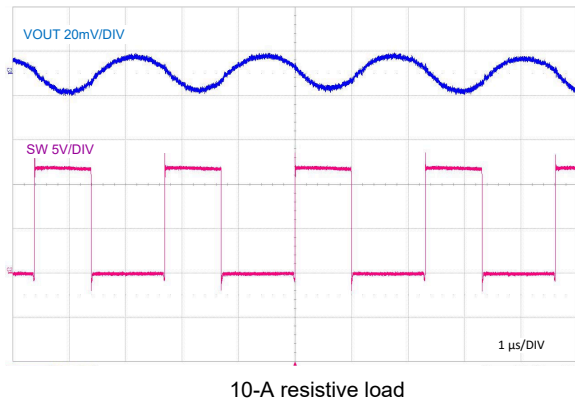
図 9-21. Full load Switching

図 9-22. PFM Switching
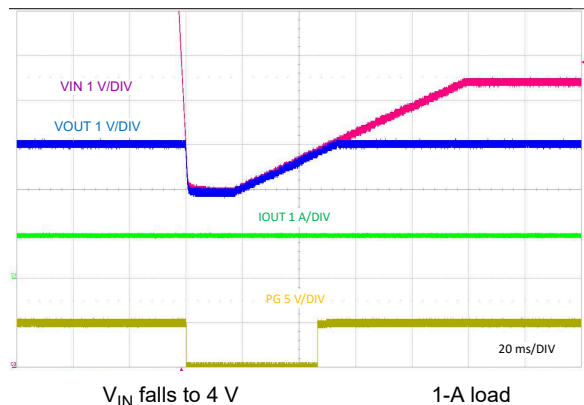
図 9-23. Line Transient Response to V_{IN} = 40 V

図 9-24. Line Transient Response to V_{IN} = 4 V

Product Folder Links: *LM25149*

VIN 2V/DIV

VOUT 1V/DIV

IOUT 5A/DIV

1 ms/DIV
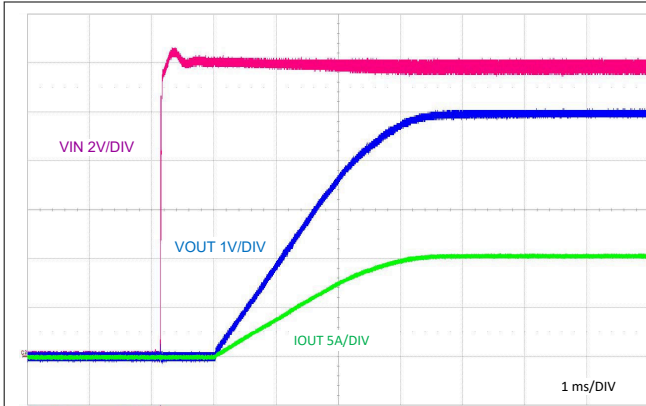
V$_{IN}$ step to 12 V   10-A resistive load

図 9-25. Start-Up Characteristic

EN 2V/DIV

VOUT 1V/DIV

IOUT 5A/DIV

1 ms/DIV
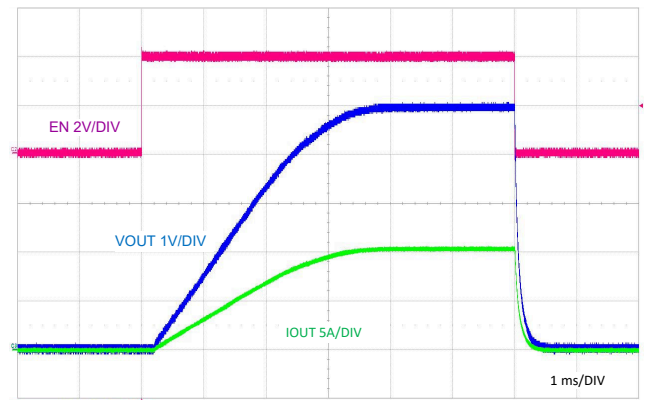
V$_{IN}$ = 12 V   10-A resistive load

図 9-26. ENABLE ON and OFF Characteristic

VOUT 500 mV/DIV

IOUT 5 A/DIV

100 µs/DIV
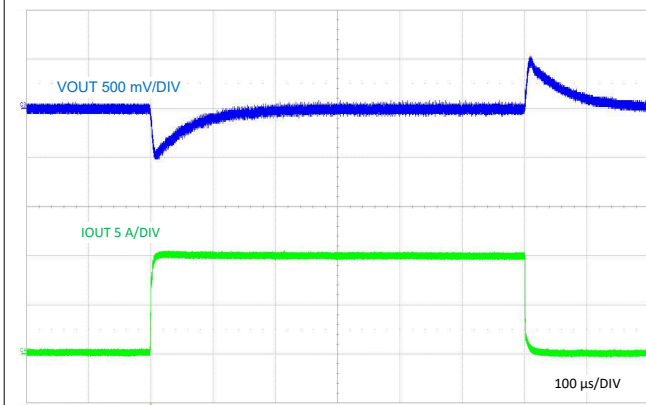
V$_{IN}$ = 12 V   FPWM

図 9-27. Load Transient, 0 A to 10 A

VOUT 500 mV/DIV

IOUT 5 A/DIV

100 µs/DIV
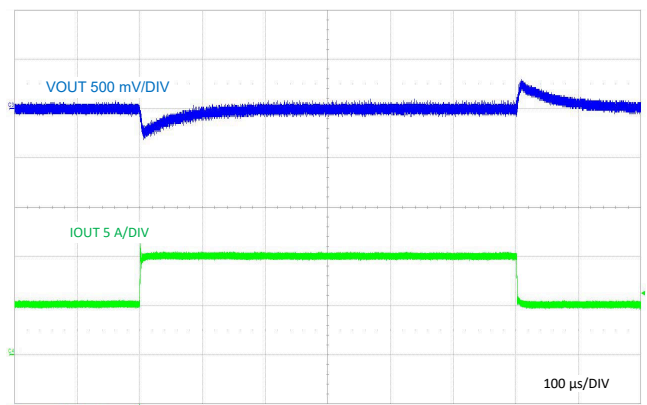
V$_{IN}$ = 12 V   FPWM

図 9-28. Load Transient, 5 A to 10 A

Product Folder Links: *LM25149*

9.2.3 Design 3 – Dual-Phase 400-kHz 20-A Synchronous Buck Regulator

図 9-29 shows the schematic diagram of a dual-phase synchronous buck regulator with an output voltage of 3.3 V and a rated load current of 20 A. In this example, the target half-load and full-load efficiencies are 95% and 92%, respectively, based on a nominal input voltage of 12 V that ranges from 4 V to 36 V. The switching frequency is set at 400 kHz by resistors R_{RT1} and R_{RT2}.
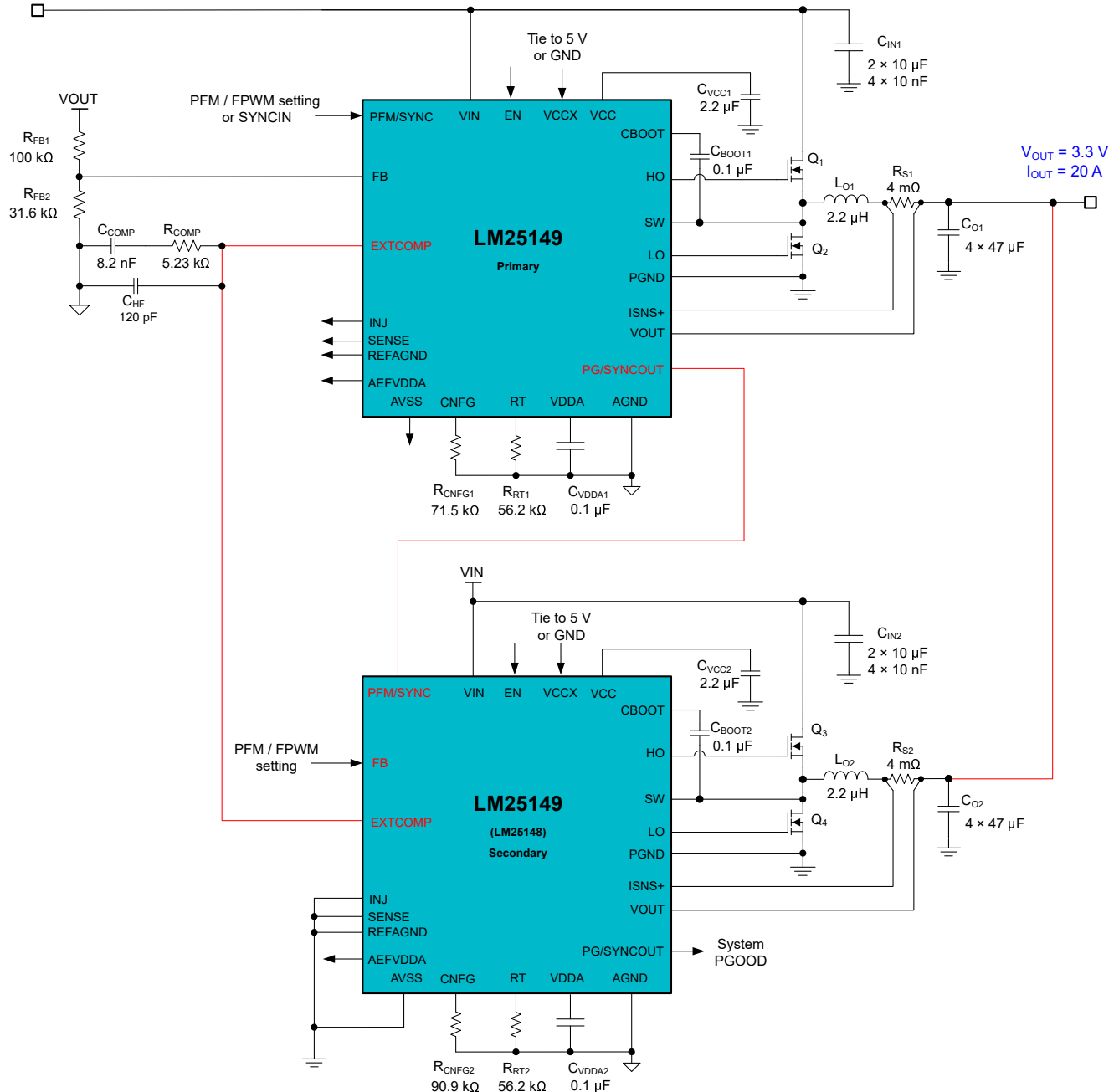
図 9-29. Application Circuit 3 With Two LM25149 Buck Controllers at 400 kHz

9.2.3.1 Design Requirements

表 9-7 shows the intended input, output, and performance parameters for this design example.

表 9-7. Design Parameters

DESIGN PARAMETER	VALUE
Input voltage range (steady-state)	8 V to 36 V
Min transient input voltage	4 V
Max transient input voltage	40 V
Output voltage	3.3 V
Output current	20 A
Switching frequency	400 kHz
Output voltage regulation	±1%
Standby current, no-load	44 µA
Shutdown current	4.6 µA
Soft-start time	3 ms

The switching frequency is set at 400 kHz by resistors R_{RT1} and R_{RT2}. The selected buck regulator powertrain components are cited in 表 9-6, and many of the components are available from multiple vendors. The MOSFETs in particular are chosen for both lowest conduction and switching power loss, as discussed in detail in セクション 9.1.1.4.

表 9-8. List of Materials for Application Circuit 3

REFERENCE DESIGNATOR	QTY	SPECIFICATION	MANUFACTURER	PART NUMBER
C_{IN}	4	10 µF, 50 V, X7R, 1210, ceramic	AVX	12105C106K4Z2A
			TDK	C3225X7R1H106K250AC
			Murata	GRM32ER71H106KA12L
C_O	8	47 µF, 6.3 V, X7R, 1210, ceramic	Murata	GCM32ER70J476KE19L
		47 µF, 10 V, X7S, 1210, ceramic	TDK	CGA6P1X7S1A476M250AC
	4	100 µF, 6.3 V, X7S, 1210, ceramic	Murata	GRT32EC70J107ME13
L_{O1}, L_{O2}	2	2.2 µH, 4.5 mΩ, 32 A, 11.3 × 10 × 6 mm	Coilcraft	XKL1060-222MEC
		2.2 µH, 4.3 mΩ, 12.5 A, 6.7 × 6.5 × 6.1 mm	Coilcraft	XGL6060-222MEC
		2.2 µH, 6.5 mΩ, 10 A, 10 × 11 × 3.8 mm	Würth Electronik	74437368022
Q_1, Q_3	2	40 V, 4.7 mΩ, 12 nC, SON 5 × 6	Texas Instruments	CSD18503Q5A
Q_2, Q_4	2	40 V, 2.7 mΩ, 35 nC, SON 5 × 6	Texas Instruments	CSD18511Q5A
R_{S1}, R_{S2}	2	Shunt, 4 mΩ, 0508, 1 W	Susumu	KRL2012E-M-R004-F-T5
U_1, U_2	2	LM25149 42-V synchronous buck controller with AEF	Texas Instruments	LM25149RGYR
		LM25148 42-V synchronous buck controller	Texas Instruments	LM25148RGYR

9.2.3.2 Detailed Design Procedure

See セクション 9.2.1.2.

9.2.3.3 Application Curves

図 9-30. Efficiency vs. I_OUT

3.3-V output

図 9-31. Efficiency vs. I_OUT, Log Scale

3.3-V output

V_IN step to 12 V   20-A load
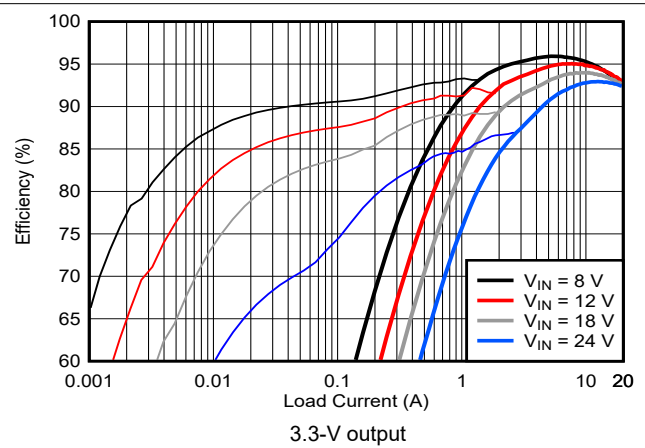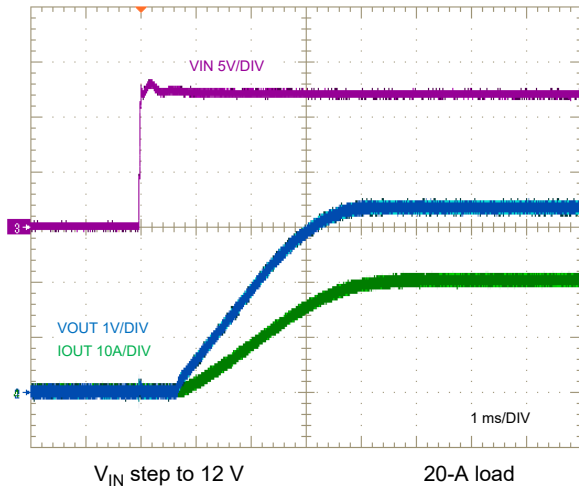
図 9-32. VIN Start-Up Characteristic

V_IN = 12 V   20-A load
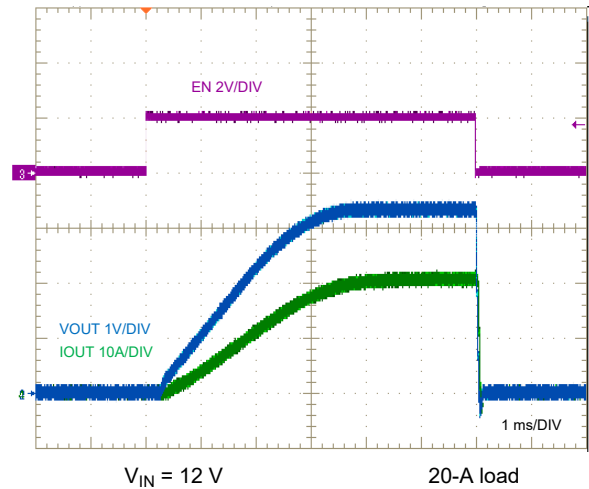
図 9-33. ENABLE ON and OFF Characteristic

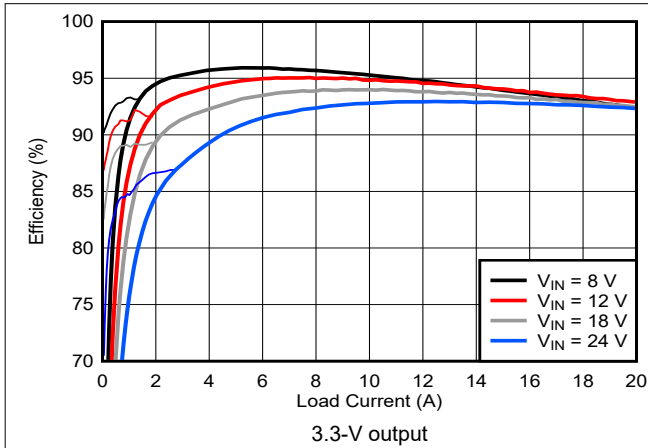V_IN = 12 V   FPWM
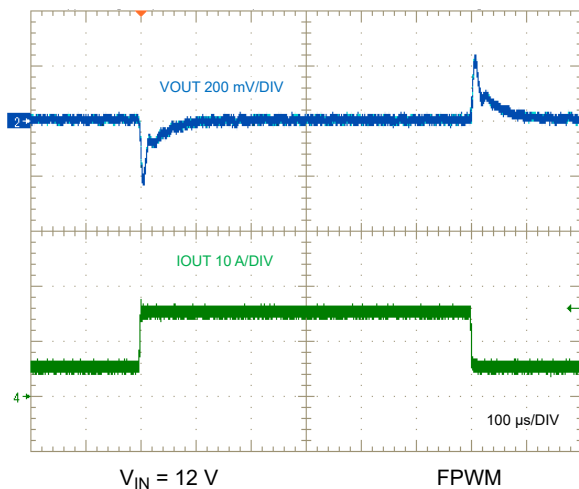
図 9-34. Load Transient, 5 A to 15 A

V_IN = 12 V   FPWM
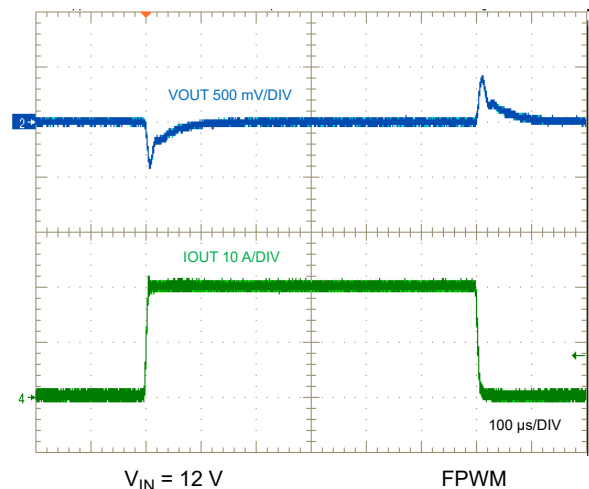
図 9-35. Load Transient, 0 A to 20 A

Product Folder Links: *LM25149*

10 Power Supply Recommendations

The LM25149 buck controller is designed to operate from a wide input voltage range of 3.5 V to 42 V. The characteristics of the input supply must be compatible with the *Absolute Maximum Ratings* and *Recommended Operating Conditions*. In addition, the input supply must be capable of delivering the required input current to the fully loaded regulator. Estimate the average input current with 式 50.

$$I_{IN} = \frac{P_{OUT}}{V_{IN} \cdot \eta}$$

(50)

where

- η is the efficiency.

If the regulator is connected to an input supply through long wires or PCB traces with a large impedance, take special care to achieve stable performance. The parasitic inductance and resistance of the input cables can have an adverse affect on converter operation. The parasitic inductance in combination with the low-ESR ceramic input capacitors form an underdamped resonant circuit. This circuit can cause overvoltage transients at VIN each time the input supply is cycled ON and OFF. The parasitic resistance causes the input voltage to dip during a load transient. The best way to solve such issues is to reduce the distance from the input supply to the regulator and use an aluminum or polymer input capacitor in parallel with the ceramics. The moderate ESR of the electrolytic capacitors helps damp the input resonant circuit and reduce any voltage overshoots. A capacitance in the range of 10 µF to 47 µF is usually sufficient to provide parallel input damping and helps to hold the input voltage steady during large load transients.

An EMI input filter is often used in front of the regulator that, unless carefully designed, can lead to instability as well as some of the effects mentioned above. The *Simple Success with Conducted EMI for DC-DC Converters* application report provides helpful suggestions when designing an input filter for any switching regulator.

11 Layout

11.1 Layout Guidelines

Proper PCB design and layout is important in a high-current, fast-switching circuit (with high current and voltage slew rates) to achieve a robust and reliable design. As expected, certain issues must be considered before designing a PCB layout using the LM25149. The high-frequency power loop of a buck regulator power stage is denoted by loop 1 in the shaded area of 図 11-1. The topological architecture of a buck regulator means that particularly high di/dt current flows in the components of loop 1, and it becomes mandatory to reduce the parasitic inductance of this loop by minimizing its effective loop area. Also important are the gate drive loops of the high-side and low-side MOSFETs, denoted by 2 and 3, respectively, in 図 11-1.
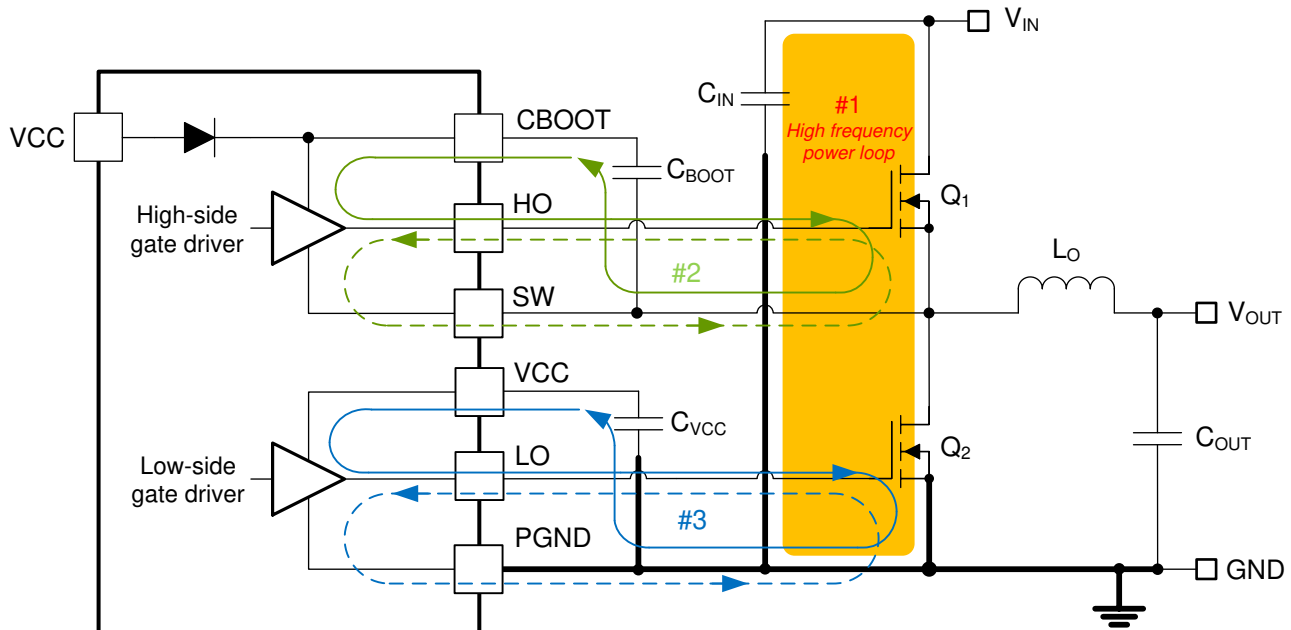

図 11-1. DC/DC Regulator Ground System With Power Stage and Gate Drive Circuit Switching Loops

11.1.1 Power Stage Layout

1. Input capacitors, output capacitors, and MOSFETs are the constituent components of the power stage of a buck regulator and are typically placed on the top side of the PCB (solder side). The benefits of convective heat transfer are maximized because of leveraging any system-level airflow. In a two-sided PCB layout, small-signal components are typically placed on the bottom side (component side). Insert at least one inner plane, connected to ground, to shield and isolate the small-signal traces from noisy power traces and lines.
2. The DC/DC regulator has several high-current loops. Minimize the area of these loops in order to suppress generated switching noise and optimize switching performance.
   - Loop 1: The most important loop area to minimize is the path from the input capacitor or capacitors through the high- and low-side MOSFETs, and back to the capacitor or capacitors through the ground connection. Connect the input capacitor or capacitors negative terminal close to the source of the low-side MOSFET (at ground). Similarly, connect the input capacitor or capacitors positive terminal close to the drain of the high-side MOSFET (at VIN). Refer to loop 1 of 図 11-1.
   - Another loop, not as critical as loop 1, is the path from the low-side MOSFET through the inductor and output capacitor or capacitors, and back to source of the low-side MOSFET through ground. Connect the source of the low-side MOSFET and negative terminal of the output capacitor or capacitors at ground as close as possible.

3. The PCB trace defined as SW node, which connects to the source of the high-side (control) MOSFET, the drain of the low-side (synchronous) MOSFET and the high-voltage side of the inductor, must be short and wide. However, the SW connection is a source of injected EMI and thus must not be too large.

4. Follow any layout considerations of the MOSFETs as recommended by the MOSFET manufacturer, including pad geometry and solder paste stencil design.

5. The SW pin connects to the switch node of the power conversion stage and acts as the return path for the high-side gate driver. The parasitic inductance inherent to loop 1 in 図 11-1 and the output capacitance (C_{OSS}) of both power MOSFETs form a resonant circuit that induces high frequency (greater than 50 MHz) ringing at the SW node. The voltage peak of this ringing, if not controlled, can be significantly higher than the input voltage. Make sure that the peak ringing amplitude does not exceed the absolute maximum rating limit for the SW pin. In many cases, a series resistor and capacitor snubber network connected from the SW node to GND damps the ringing and decreases the peak amplitude. Provide provisions for snubber network components in the PCB layout. If testing reveals that the ringing amplitude at the SW pin is excessive, then include snubber components as needed.

11.1.2 Gate-Drive Layout

The LM25149 high-side and low-side gate drivers incorporate short propagation delays, adaptive deadtime control, and low-impedance output stages capable of delivering large peak currents with very fast rise and fall times to facilitate rapid turn-on and turnoff transitions of the power MOSFETs. Very high di/dt can cause unacceptable ringing if the trace lengths and impedances are not well controlled.

Minimization of stray or parasitic gate loop inductance is key to optimizing gate drive switching performance, whether it be series gate inductance that resonates with MOSFET gate capacitance or common source inductance (common to gate and power loops) that provides a negative feedback component opposing the gate drive command, thereby increasing MOSFET switching times. The following loops are important:

*   Loop 2: high-side MOSFET, Q_1. During the high-side MOSFET turn-on, high current flows from the bootstrap (boot) capacitor through the gate driver and high-side MOSFET, and back to the negative terminal of the boot capacitor through the SW connection. Conversely, to turn off the high-side MOSFET, high current flows from the gate of the high-side MOSFET through the gate driver and SW, and back to the source of the high-side MOSFET through the SW trace. Refer to loop 2 of 図 11-1.
*   Loop 3: low-side MOSFET, Q_2. During the low-side MOSFET turn-on, high current flows from the VCC decoupling capacitor through the gate driver and low-side MOSFET, and back to the negative terminal of the capacitor through ground. Conversely, to turn off the low-side MOSFET, high current flows from the gate of the low-side MOSFET through the gate driver and GND, and back to the source of the low-side MOSFET through ground. Refer to loop 3 of 図 11-1.

TI strongly recommends following circuit layout guidelines when designing with high-speed MOSFET gate drive circuits.

*   Connections from gate driver outputs, HO and LO, to the respective gates of the high-side or low-side MOSFETs must be as short as possible to reduce series parasitic inductance. Be aware that peak gate drive currents can be as high as 3.3 A. Use 0.65 mm (25 mils) or wider traces. Use via or vias, if necessary, of at least 0.5 mm (20 mils) diameter along these traces. Route HO and SW gate traces as a differential pair from the LM25149 to the high-side MOSFET, taking advantage of flux cancellation.
*   Minimize the current loop path from the VCC and HB pins through their respective capacitors as these provide the high instantaneous current, up to 3.3 A, to charge the MOSFET gate capacitances. Specifically, locate the bootstrap capacitor, C_{BST}, close to the CBOOT and SW pins of the LM25149 to minimize the area of loop 2 associated with the high-side driver. Similarly, locate the VCC capacitor, C_{VCC}, close to the VCC and PGND pins of the LM25149 to minimize the area of loop 3 associated with the low-side driver.

11.1.3 PWM Controller Layout

With the provison to locate the controller as close as possible to the power MOSFETs to minimize gate driver trace runs, the components related to the analog and feedback signals as well as current sensing are considered in the following:

*   Separate power and signal traces, and use a ground plane to provide noise shielding.

- Place all sensitive analog traces and components related to COMP, FB, ISNS+, and RT away from high-voltage switching nodes such as SW, HO, LO, or CBOOT to avoid mutual coupling. Use internal layer or layers as ground plane or planes. Pay particular attention to shielding the feedback (FB) and current sense (ISNS+ and VOUT) traces from power traces and components.
- Locate the upper and lower feedback resistors (if required) close to the FB pin, keeping the FB trace as short as possible. Route the trace from the upper feedback resistor to the required output voltage sense point at the load.
- Route the ISNS+ and VOUT sense traces as differential pairs to minimize noise pickup and use Kelvin connections to the applicable shunt resistor (if shunt current sensing is used) or to the sense capacitor (if inductor DCR current sensing is used).
- Minimize the loop area from the VCC and VIN pins through their respective decoupling capacitors to the PGND pin. Locate these capacitors as close as possible to the LM25149.

11.1.4 Active EMI Layout

Active EMI layout is critical for enhanced EMI performance. Layout considerations are as follows:

- Connect AVSS to a quiet GND connection, further from IC if possible. Keep decoupling capacitor $C_{AEFVDDA}$ close to the AEFVDDA pin and AVSS GND connection. See capacitor C23 in 図 11-2.
- Route the SEN and INJ traces differentially as close together as possible on an internal quiet layer. Avoid noisy layer or layers carrying high-voltage traces.
- Place the active EMI compensation components C_{AEFC}, R_{AEFC}, and R_{AEFDC} close together and near the V_{IN-EMI} node to the input filter inductor.
- C_{SEN} and C_{INJ} components should be placed directly outside of the compensation loop.
- Place input compensation components R_{AEFC} and C_{AEFC} nearby the other Active EMI components. Ensure the GND connection is far away from any noise sources. Do not connect the input compensation GND near the power stage.
- Route REFAGND directly to the GND of the input power connector. Do not tie to the GND plane connection. The REFAGND trace can partially shield the SEN and INJ differential pair on the way to the input power connector.

11.1.5 Thermal Design and Layout

The useful operating temperature range of a PWM controller with integrated gate drivers and bias supply LDO regulator is greatly affected by the following:

- Average gate drive current requirements of the power MOSFETs
- Switching frequency
- Operating input voltage (affecting bias regulator LDO voltage drop and hence its power dissipation)
- Thermal characteristics of the package and operating environment

For a PWM controller to be useful over a particular temperature range, the package must allow for the efficient removal of the heat produced while keeping the junction temperature within rated limits. The LM25149 controller is available in a small 4-mm × 4-mm 24-pin VQFN PowerPAD package to cover a range of application requirements. セクション 11.1.5 summarizes the thermal metrics of this package.

The 24-pin VQFN package offers a means of removing heat from the semiconductor die through the exposed thermal pad at the base of the package. While the exposed pad of the package is not directly connected to any leads of the package, it is thermally connected to the substrate of the LM25149 device (ground). This allows a significant improvement in heat sinking, and it becomes imperative that the PCB is designed with thermal lands, thermal vias, and a ground plane to complete the heat removal subsystem. The exposed pad of the LM25149 is soldered to the ground-connected copper land on the PCB directly underneath the device package, reducing the thermal resistance to a very low value.

Numerous vias with a 0.3-mm diameter connected from the thermal land to the internal and solder-side ground plane or planes are vital to help dissipation. In a multi-layer PCB design, a solid ground plane is typically placed on the PCB layer below the power components. Not only does this provide a plane for the power stage currents to flow but it also represents a thermally conductive path away from the heat generating devices.

The thermal characteristics of the MOSFETs also are significant. The drain pads of the high-side MOSFETs are normally connected to a VIN plane for heat sinking. The drain pads of the low-side MOSFETs are tied to the SW plane, but the SW plane area is purposely kept as small as possible to mitigate EMI concerns.

11.1.6 Ground Plane Design

As mentioned previously, TI recommends using one or more of the inner PCB layers as a solid ground plane. A ground plane offers shielding for sensitive circuits and traces and also provides a quiet reference potential for the control circuitry. In particular, a full ground plane on the layer directly underneath the power stage components is essential. Connect the source terminal of the low-side MOSFET and return terminals of the input and output capacitors to this ground plane. Connect the PGND and AGND pins of the controller at the DAP and then connect to the system ground plane using an array of vias under the DAP. The PGND nets contain noise at the switching frequency and can bounce because of load current variations. The power traces for PGND, VIN, and SW can be restricted to one side of the ground plane, for example on the top layer. The other side of the ground plane contains much less noise and is ideal for sensitive analog trace routes.

11.2 Layout Example

図 11-2 shows a single-sided layout of a synchronous buck regulator with discrete power MOSFETs, Q1 and Q2, in SON 5-mm × 6-mm case size. The power stage is surrounded by a GND pad geometry to connect an EMI shield if needed. The design uses layer 2 of the PCB as a power-loop return path directly underneath the top layer to create a low-area switching power loop of approximately 2 mm². This loop area, and hence parasitic inductance, must be as small as possible to minimize EMI as well as switch-node voltage overshoot and ringing.

The high-frequency power loop current flows through MOSFETs Q1 and Q2, through the power ground plane on layer 2, and back to VIN through the 0402 ceramic capacitors C17 through C22. The currents flowing in opposing directions in the vertical loop configuration provide field self-cancellation, reducing parasitic inductance. 図 11-4 shows a side view to illustrate the concept of creating a low-profile, self-canceling loop in a multilayer PCB structure. The layer-2 GND plane layer, shown in 図 11-3, provides a tightly-coupled current return path directly under the MOSFETs to the source terminals of Q2.

Six 10-nF input capacitors with small 0402 or 0603 case size are placed in parallel very close to the drain of Q1. The low equivalent series inductance (ESL) and high self-resonant frequency (SRF) of the small footprint capacitors yield excellent high-frequency performance. The negative terminals of these capacitors are connected to the layer-2 GND plane with multiple 12-mil (0.3-mm) diameter vias, further minimizing parasitic loop inductance.
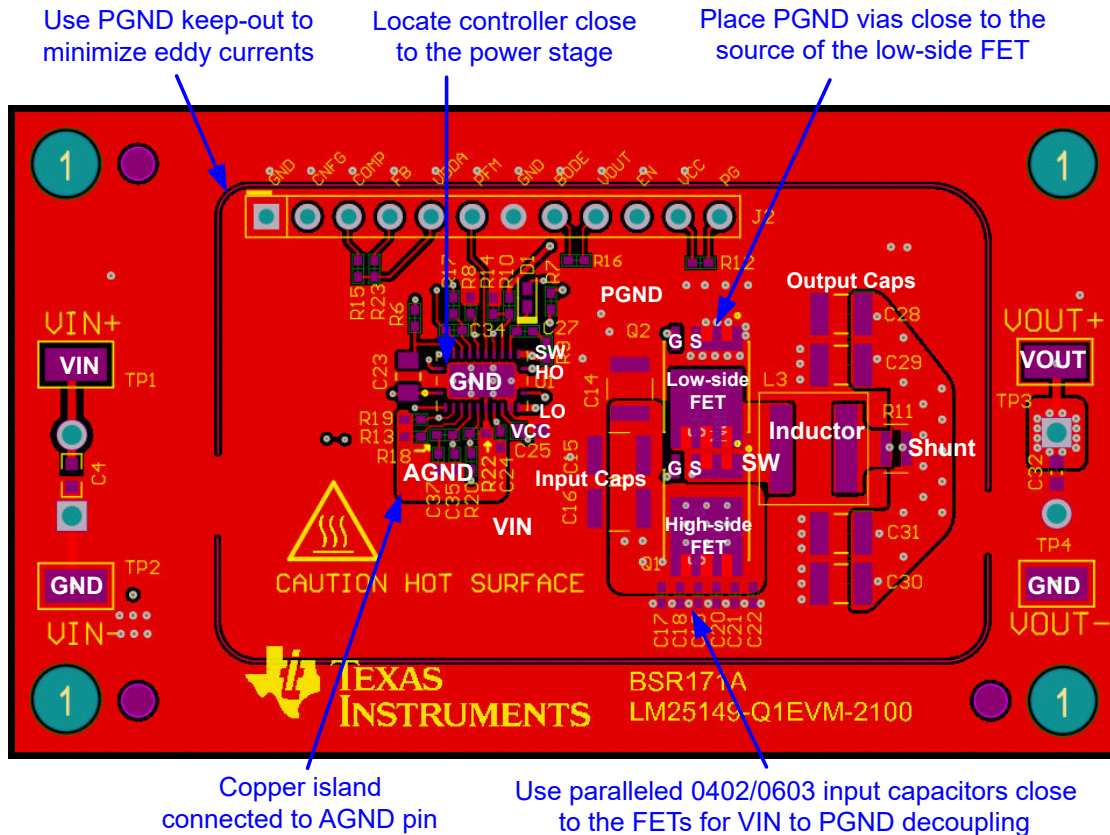
図 11-2. PCB Top Layer – High Density, Single-sided Design

Additional guidelines to improve noise immunity and reduce EMI are as follows:

- Make the ground connections to the LM25149 controller as shown in 図 11-2. Create a power ground directly connected to all high-power components and an analog ground plane for sensitive analog components. The analog ground plane for AGND and power ground plane for PGND must be connected at a single point directly under the IC – at the die attach pad (DAP).
- Connect the MOSFETs (switch node) directly to the inductor terminal with short copper connections (without vias) as this net has high dv/dt and contributes to radiated EMI. The single-layer routing of the switch-node connection means that switch-node vias with high dv/dt do not appear on the bottom side of the PCB. This avoids e-field coupling to the reference ground plane during the EMI test. VIN and PGND plane copper pours shield the polygon connecting the MOSFETs to the inductor terminal, further reducing the radiated EMI signature.
- Place the *EMI filter* components on the bottom side of the PCB so that they are shielded from the power stage components on the top side.
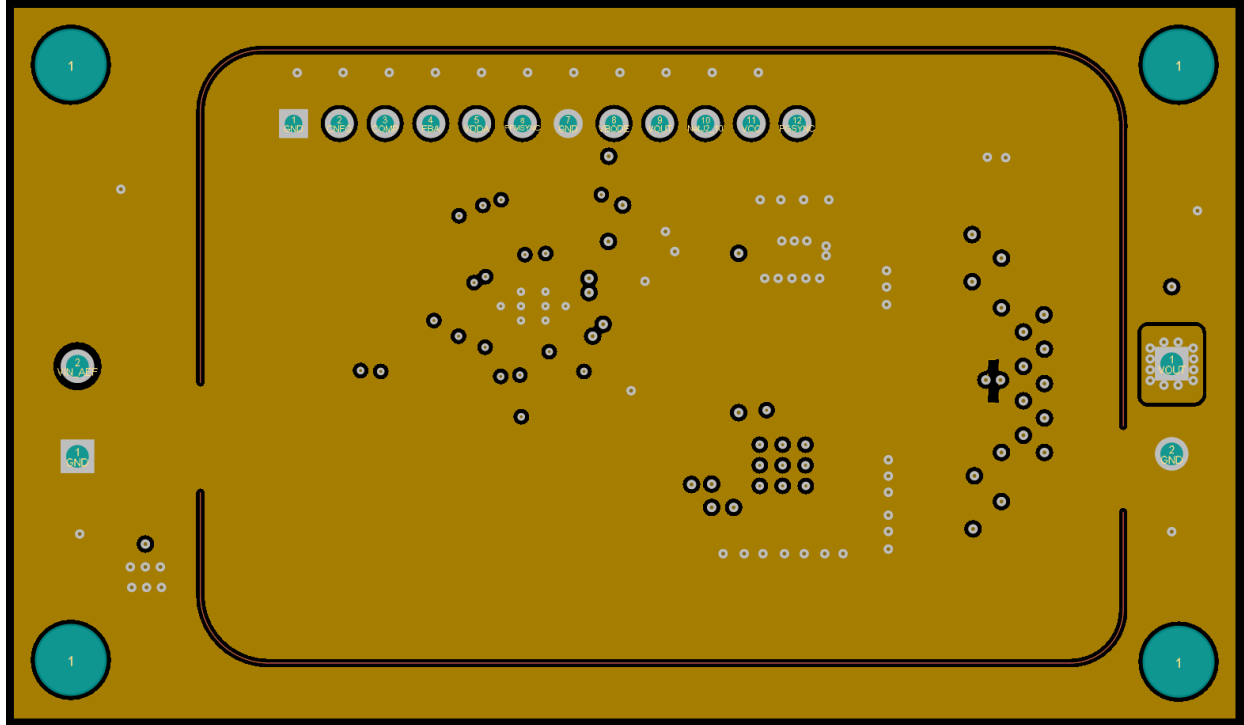
図 11-3. Layer 2 Full Ground Plane Directly Under the Power Components
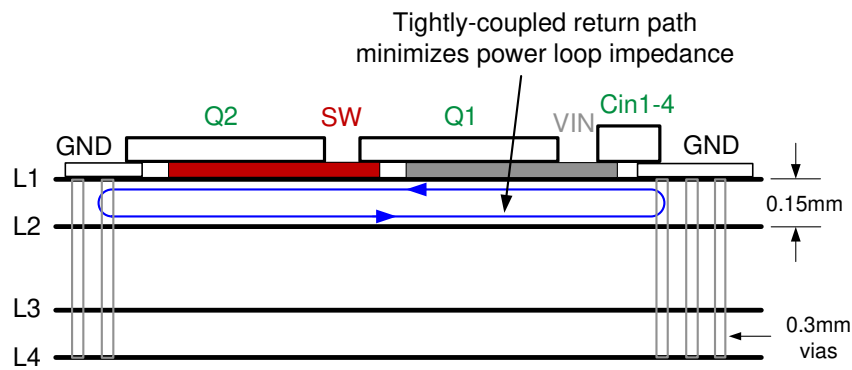
図 11-4. PCB Stack-up Diagram With Low L1-L2 Intra-layer Spacing [1]

---

[1] See *Improve High-current DC/DC Regulator Performance for Free with Optimized Power Stage Layout* for more detail.

12 Device and Documentation Support

12.1 Device Support

12.1.1 Development Support

With an input operating voltage as low as 3.5 V and up to 100 V as specified in 表 12-1, the LM(2)514x family of synchronous buck controllers from TI provides flexibility, scalability and optimized solution size for a range of applications. These controllers enable DC/DC solutions with high density, low EMI and increased flexibility. Available EMI mitigation features include dual-random spread spectrum (DRSS) or triangular spread spectrum (TRSS), split gate driver outputs for slew rate (SR) control, and integrated active EMI filtering (AEF). All controllers are rated for a maximum operating junction temperature of 150°C and have AEC-Q100 grade 1 qualification.

表 12-1. Synchronous Buck DC/DC Controller Family

DC/DC CONTROLLER	SINGLE or DUAL	V_{IN} RANGE	CONTROL METHOD	GATE DRIVE VOLTAGE	SYNC OUTPUT	EMI MITIGATION
LM25141	Single	3.8 V to 42 V	Peak current mode	5 V	N/A	SR control, TRSS
LM25143	Dual	3.5 V to 42 V	Peak current mode	5 V	90° phase shift	SR control, TRSS
LM25145	Single	6 V to 42 V	Voltage mode	7.5 V	180° phase shift	N/A
LM25148	Single	3.5 V to 42 V	Peak current mode	5 V	180° phase shift	DRSS
LM25149	Single	3.5 V to 42 V	Peak current mode	5 V	180° phase shift	AEF, DRSS
LM5141	Single	3.8 V to 42 V	Peak current mode	5 V	N/A	SR control, TRSS
LM5143	Dual	3.5 V to 65 V	Peak current mode	5 V	90° phase shift	SR control, TRSS
LM5145	Single	6 V to 75 V	Voltage mode	7.5 V	180° phase shift	N/A
LM5146	Single	5.5 V to 100 V	Voltage mode	7.5 V	180° phase shift	N/A
LM5148	Single	3.5 V to 80 V	Peak current mode	5 V	180° phase shift	DRSS
LM5149	Single	3.5 V to 80 V	Peak current mode	5 V	180° phase shift	AEF, DRSS

For development support see the following:

- LM25149 Quickstart Calculator
- LM25149 Simulation Models
- For TI's reference design library, visit TI Designs
- For TI's WEBENCH Design Environment, visit the WEBENCH® Design Center
- TI Designs:
  - *ADAS 8-Channel Sensor Fusion Hub Reference Design with Two 4-Gbps Quad Deserializers*
  - *Automotive EMI and Thermally Optimized Synchronous Buck Converter Reference Design*
  - *Automotive High Current, Wide V_{IN} Synchronous Buck Controller Reference Design Featuring LM5141-Q1*
  - *25W Automotive Start-Stop Reference Design Operating at 2.2 MHz*
  - *Synchronous Buck Converter for Automotive Cluster Reference Design*
  - *137W Holdup Converter for Storage Server Reference Design*
  - *Automotive Synchronous Buck With 3.3V @ 12.0A Reference Design*
  - *Automotive Synchronous Buck Reference Design*
  - *Wide Input Synchronous Buck Converter Reference Design With Frequency Spread Spectrum*
  - *Automotive Wide V_{IN} Front-end Reference Design for Digital Cockpit Processing Units*
- Technical Articles:
  - *High-Density PCB Layout of DC/DC Converters*
  - *Synchronous Buck Controller Solutions Support Wide V_{IN} Performance and Flexibility*
  - *How to Use Slew Rate for EMI Control*
- To view a related device of this product, see the LM5141

12.1.2 Custom Design With WEBENCH® Tools

Click here to create a custom design using the LM25149 device with the WEBENCH® Power Designer.

1. Start by entering the input voltage (V_{IN}), output voltage (V_{OUT}), and output current (I_{OUT}) requirements.
2. Optimize the design for key parameters such as efficiency, footprint, and cost using the optimizer dial.
3. Compare the generated design with other possible solutions from Texas Instruments.

The WEBENCH Power Designer gives a customized schematic along with a list of materials with real-time pricing and component availability.

In most cases, these actions are available:
- Run electrical simulations to see important waveforms and circuit performance
- Run thermal simulations to understand board thermal performance
- Export customized schematic and layout into popular CAD formats
- Print PDF reports for the design, and share the design with colleagues

Get more information about WEBENCH tools at www.ti.com/WEBENCH.

12.2 Documentation Support

12.2.1 Related Documentation

For related documentation see the following:

- User's Guides:
  - *LM25149-Q1 Synchronous Buck Controller High Density EVM*
  - *LM5141-Q1 Synchronous Buck Controller EVM*
  - *LM5143-Q1 Synchronous Buck Controller EVM*
  - *LM5146-Q1 EVM User's Guide*
  - *LM5145 EVM User's Guide*
- Application Reports:
  - *Improve High-current DC/DC Regulator Performance for Free with Optimized Power Stage Layout Application Report*
  - *AN-2162 Simple Success with Conducted EMI from DC-DC Converters*
  - *Maintaining Output Voltage Regulation During Automotive Cold-Crank with LM5140-Q1 Dual Synchronous Buck Controller*
- Technical Briefs:
  - *Reduce Buck Converter EMI and Voltage Stress by Minimizing Inductive Parasitics*
- White Papers:
  - *An Overview of Conducted EMI Specifications for Power Supplies*
  - *An Overview of Radiated EMI Specifications for Power Supplies*
  - *Valuing Wide V_{IN}, Low EMI Synchronous Buck Circuits for Cost-driven, Demanding Applications*

12.2.1.1 PCB Layout Resources

- Application Reports:
  - *Improve High-current DC/DC Regulator Performance for Free with Optimized Power Stage Layout*
  - *AN-1149 Layout Guidelines for Switching Power Supplies*
  - *AN-1229 Simple Switcher PCB Layout Guidelines*
  - *Low Radiated EMI Layout Made SIMPLE with LM4360x and LM4600x*
- Seminars:
  - *Constructing Your Power Supply – Layout Considerations*

12.2.1.2 Thermal Design Resources

- Application Reports:
  - *AN-2020 Thermal Design by Insight, Not Hindsight*
  - *AN-1520 A Guide to Board Layout for Best Thermal Resistance for Exposed Pad Packages*
  - *Semiconductor and IC Package Thermal Metrics*
  - *Thermal Design Made Simple with LM43603 and LM43602*
  - *PowerPAD™Thermally Enhanced Package*
  - *PowerPAD Made Easy*
  - *Using New Thermal Metrics*

12.3 Receiving Notification of Documentation Updates

To receive notification of documentation updates, navigate to the device product folder on ti.com. Click on *Subscribe to updates* to register and receive a weekly digest of any product information that has changed. For change details, review the revision history included in any revised document.

12.4 サポート・リソース

TI E2E™ サポート・フォーラムは、エンジニアが検証済みの回答と設計に関するヒントをエキスパートから迅速かつ直接得ることができる場所です。既存の回答を検索したり、独自の質問をしたりすることで、設計で必要な支援を迅速に得ることができます。

リンクされているコンテンツは、該当する貢献者により、現状のまま提供されるものです。これらは TI の仕様を構成するものではなく、必ずしも TI の見解を反映したものではありません。TI の使用条件を参照してください。

12.5 Trademarks

NexFET™ and TI E2E™ are trademarks of Texas Instruments.
PowerPAD™ is a trademark of Texas Instruments.
WEBENCH® is a registered trademark of Texas Instruments.
is a registered trademark of TI.
すべての商標は、それぞれの所有者に帰属します。

12.6 Electrostatic Discharge Caution

This integrated circuit can be damaged by ESD. Texas Instruments recommends that all integrated circuits be handled with appropriate precautions. Failure to observe proper handling and installation procedures can cause damage.

ESD damage can range from subtle performance degradation to complete device failure. Precision integrated circuits may be more susceptible to damage because very small parametric changes could cause the device not to meet its published specifications.

12.7 Glossary

TI Glossary   This glossary lists and explains terms, acronyms, and definitions.

13 Mechanical, Packaging, and Orderable Information

The following pages show mechanical, packaging, and orderable information. This information is the most current data available for the designated devices. This data is subject to change without notice and revision of this document. For browser-based versions of this data sheet, refer to the left-hand navigation.

PACKAGING INFORMATION

Orderable Device	Status (1)	Package Type	Package Drawing	Pins	Package Qty	Eco Plan (2)	Lead finish/ Ball material (6)	MSL Peak Temp (3)	Op Temp (°C)	Device Marking (4/5)	Samples
LM25149RGYR	ACTIVE	VQFN	RGY	24	3000	RoHS & Green	NIPDAU	Level-2-260C-1 YEAR	-40 to 150	LM25149	Samples

(1) The marketing status values are defined as follows:
ACTIVE: Product device recommended for new designs.
LIFEBUY: TI has announced that the device will be discontinued, and a lifetime-buy period is in effect.
NRND: Not recommended for new designs. Device is in production to support existing customers, but TI does not recommend using this part in a new design.
PREVIEW: Device has been announced but is not in production. Samples may or may not be available.
OBSOLETE: TI has discontinued the production of the device.

(2) **RoHS:** TI defines "RoHS" to mean semiconductor products that are compliant with the current EU RoHS requirements for all 10 RoHS substances, including the requirement that RoHS substance do not exceed 0.1% by weight in homogeneous materials. Where designed to be soldered at high temperatures, "RoHS" products are suitable for use in specified lead-free processes. TI may reference these types of products as "Pb-Free".
RoHS Exempt: TI defines "RoHS Exempt" to mean products that contain lead but are compliant with EU RoHS pursuant to a specific EU RoHS exemption.
Green: TI defines "Green" to mean the content of Chlorine (Cl) and Bromine (Br) based flame retardants meet JS709B low halogen requirements of <=1000ppm threshold. Antimony trioxide based flame retardants must also meet the <=1000ppm threshold requirement.

(3) MSL, Peak Temp. - The Moisture Sensitivity Level rating according to the JEDEC industry standard classifications, and peak solder temperature.

(4) There may be additional marking, which relates to the logo, the lot trace code information, or the environmental category on the device.

(5) Multiple Device Markings will be inside parentheses. Only one Device Marking contained in parentheses and separated by a "~" will appear on a device. If a line is indented then it is a continuation of the previous line and the two combined represent the entire Device Marking for that device.

(6) Lead finish/Ball material - Orderable Devices may have multiple material finish options. Finish options are separated by a vertical ruled line. Lead finish/Ball material values may wrap to two lines if the finish value exceeds the maximum column width.

Important Information and Disclaimer: The information provided on this page represents TI's knowledge and belief as of the date that it is provided. TI bases its knowledge and belief on information provided by third parties, and makes no representation or warranty as to the accuracy of such information. Efforts are underway to better integrate information from third parties. TI has taken and continues to take reasonable steps to provide representative and accurate information but may not have conducted destructive testing or chemical analysis on incoming materials and chemicals. TI and TI suppliers consider certain information to be proprietary, and thus CAS numbers and other limited information may not be available for release.

In no event shall TI's liability arising out of such information exceed the total purchase price of the TI part(s) at issue in this document sold by TI to Customer on an annual basis.

OTHER QUALIFIED VERSIONS OF LM25149 :

PACKAGE OPTION ADDENDUM

● Automotive : LM25149-Q1

NOTE: Qualified Version Definitions:

    ● Automotive - Q100 devices qualified for high-reliability automotive applications targeting zero defects

TAPE AND REEL INFORMATION

REEL DIMENSIONS

TAPE DIMENSIONS

A0	Dimension designed to accommodate the component width
B0	Dimension designed to accommodate the component length
K0	Dimension designed to accommodate the component thickness
W	Overall width of the carrier tape
P1	Pitch between successive cavity centers

QUADRANT ASSIGNMENTS FOR PIN 1 ORIENTATION IN TAPE

*All dimensions are nominal

Device	Package Type	Package Drawing	Pins	SPQ	Reel Diameter (mm)	Reel Width W1 (mm)	A0 (mm)	B0 (mm)	K0 (mm)	P1 (mm)	W (mm)	Pin1 Quadrant
LM25149RGYR	VQFN	RGY	24	3000	330.0	12.4	3.8	5.8	1.2	8.0	12.0	Q1

PACKAGE MATERIALS INFORMATION

TAPE AND REEL BOX DIMENSIONS

*All dimensions are nominal

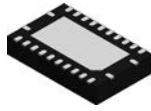| Device	Package Type	Package Drawing	Pins	SPQ	Length (mm)	Width (mm)	Height (mm)
LM25149RGYR	VQFN	RGY	24	3000	367.0	367.0	35.0

RGY 24

VQFN - 1 mm max height

5.5 x 3.5 mm, 0.5 mm pitch
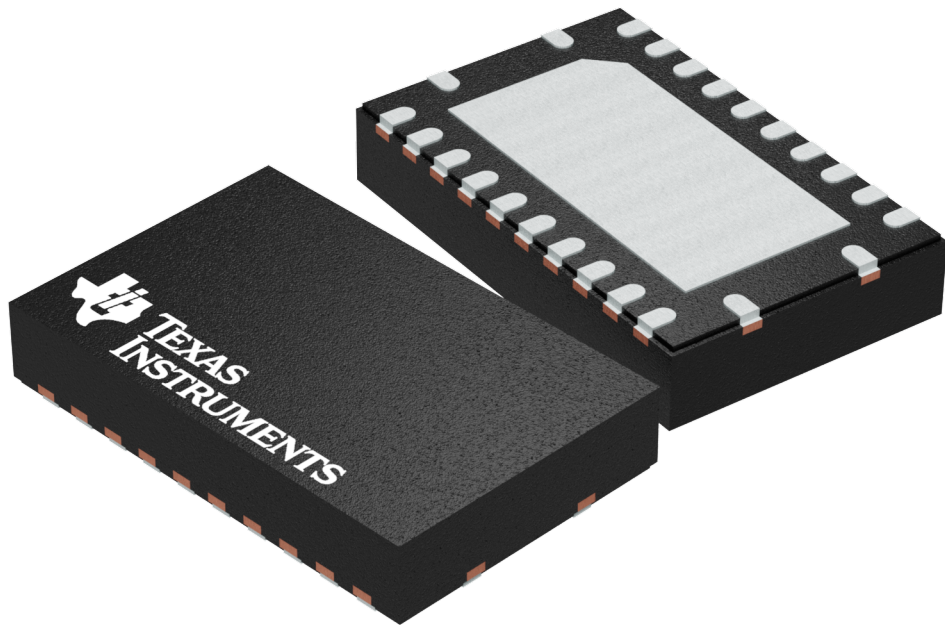
Images above are just a representation of the package family, actual package may vary.
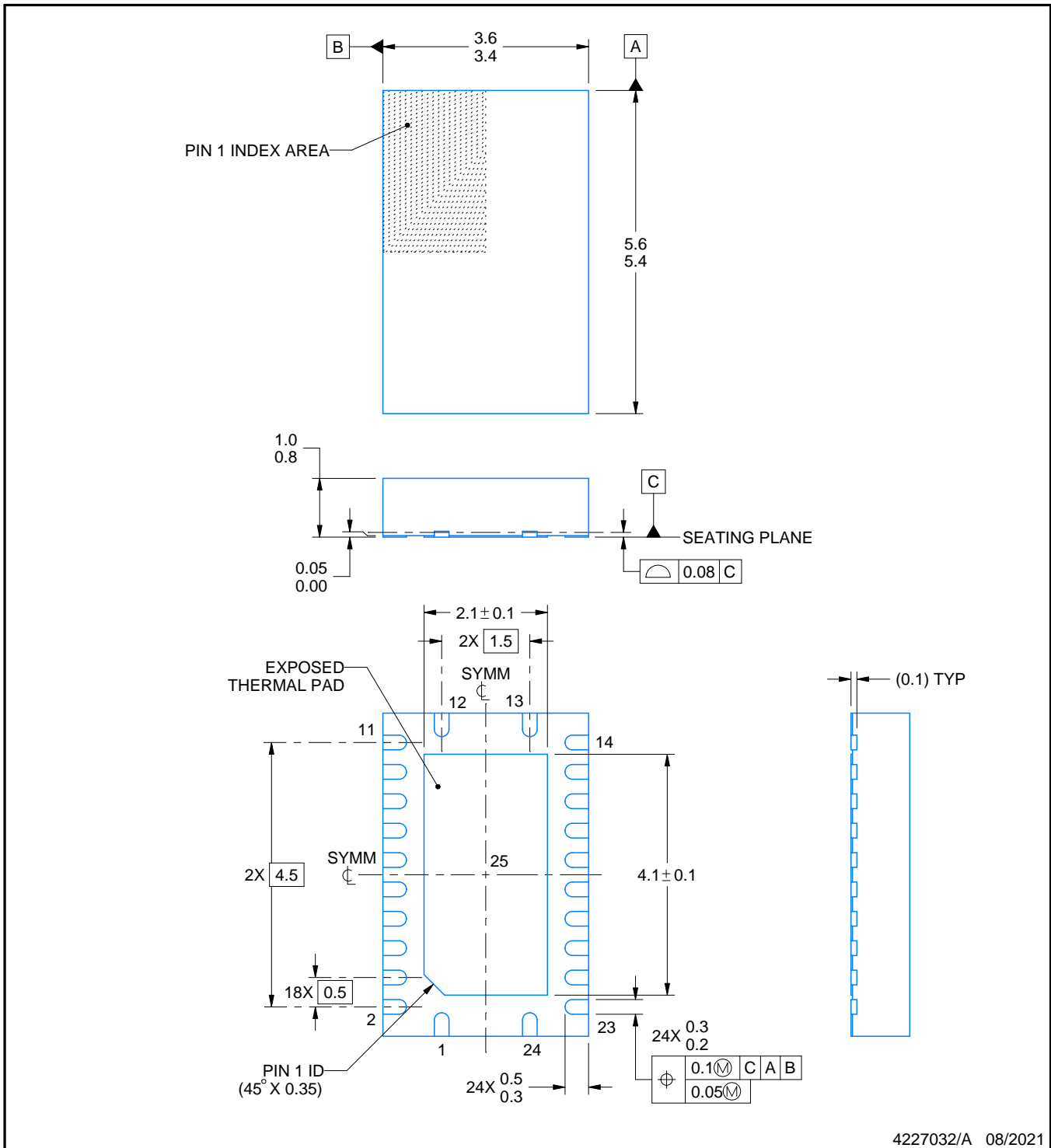Refer to the product data sheet for package details.

4203539-5/J

TEXAS
INSTRUMENTS

B $\frac{3.6}{3.4}$ A

PIN 1 INDEX AREA

$\frac{5.6}{5.4}$

$\frac{1.0}{0.8}$

C

SEATING PLANE

$\frac{0.05}{0.00}$

0.08 C

2.1 ± 0.1

2X 1.5

SYMM

EXPOSED THERMAL PAD

12 13

11

14

(0.1) TYP

SYMM

25

2X 4.5

4.1 ± 0.1

18X 0.5

2

23

24X $\frac{0.3}{0.2}$

PIN 1 ID
(45° X 0.35)

1   24

0.1 Ⓜ C A B
0.05 Ⓜ

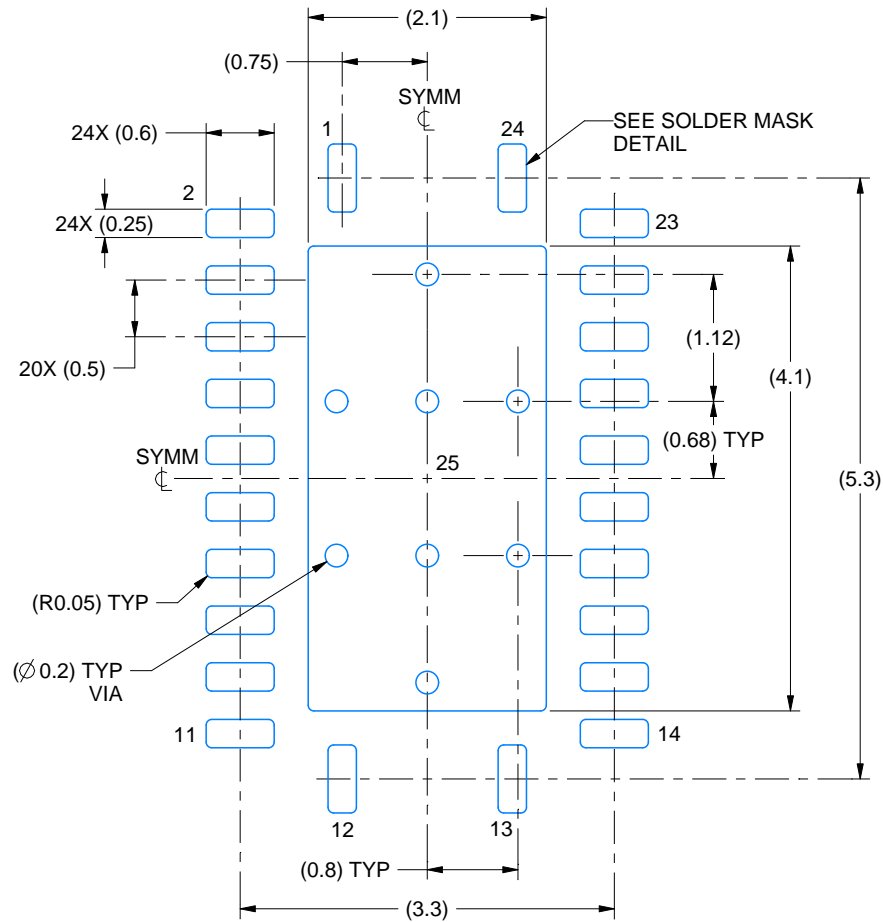24X $\frac{0.5}{0.3}$

4227032/A   08/2021

NOTES:

1. All linear dimensions are in millimeters. Any dimensions in parenthesis are for reference only. Dimensioning and tolerancing per ASME Y14.5M.
2. This drawing is subject to change without notice.
3. The package thermal pad must be soldered to the printed circuit board for thermal and mechanical performance.
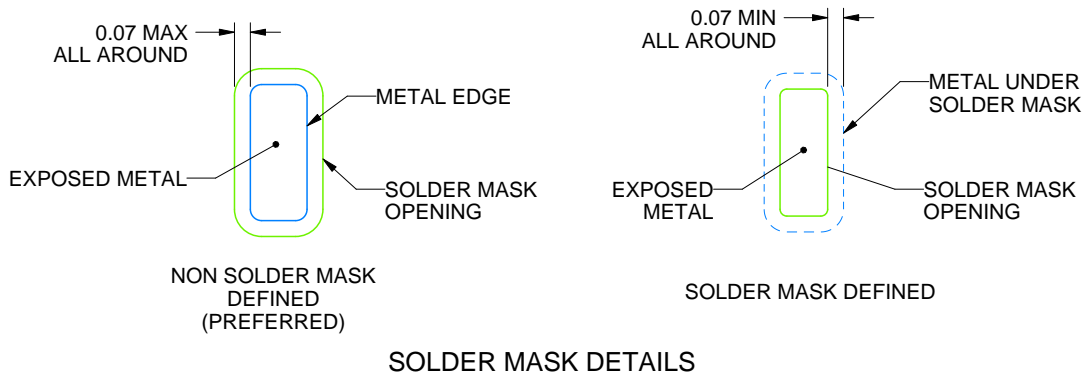
LAND PATTERN EXAMPLE
EXPOSED METAL SHOWN
SCALE: 15X

(2.1)

(0.75)

SYMM

24X (0.6)

2

24X (0.25)

20X (0.5)

SYMM

(R0.05) TYP

(⌀ 0.2) TYP
VIA

1

24

SEE SOLDER MASK
DETAIL

23

(1.12)

(4.1)

(0.68) TYP

(5.3)

25

11

12   13

14

(0.8) TYP

(3.3)

SOLDER MASK DETAILS

0.07 MAX
ALL AROUND

METAL EDGE

EXPOSED METAL

SOLDER MASK
OPENING

NON SOLDER MASK
DEFINED
(PREFERRED)

0.07 MIN
ALL AROUND

METAL UNDER
SOLDER MASK

EXPOSED
METAL

SOLDER MASK
OPENING

SOLDER MASK DEFINED

4227032/A   08/2021

NOTES: (continued)

4. This package is designed to be soldered to a thermal pad on the board. For more information, see Texas Instruments literature number SLUA271 (www.ti.com/lit/slua271).
5. Vias are optional depending on application, refer to device data sheet. If any vias are implemented, refer to their locations shown on this view. It is recommended that vias under paste be filled, plugged or tented.
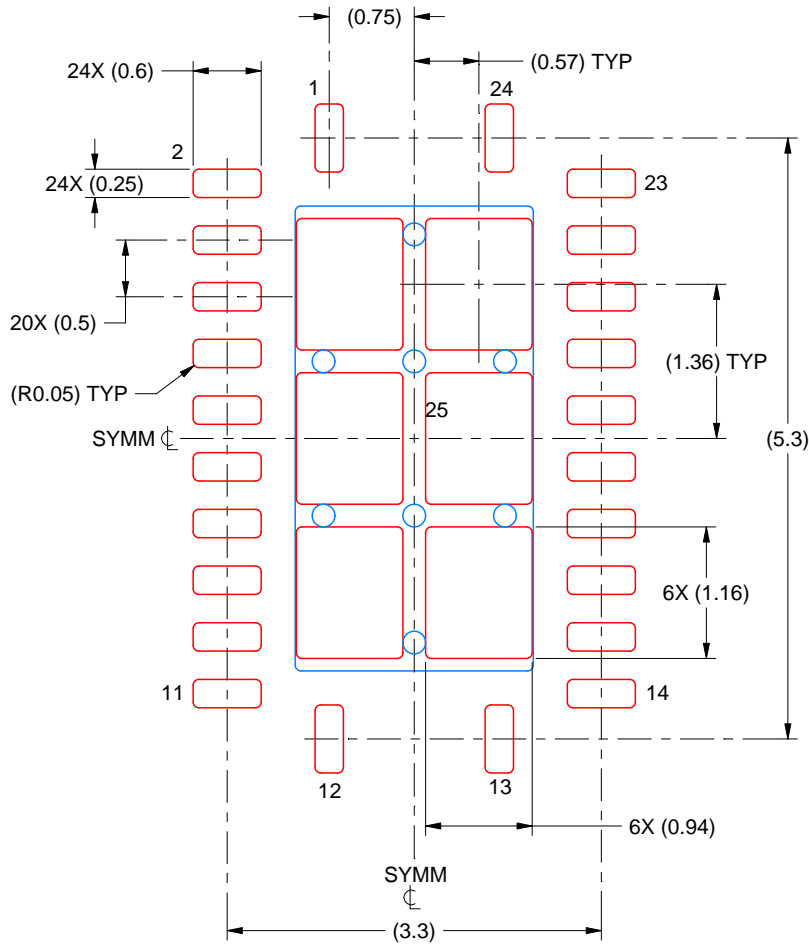
SOLDER PASTE EXAMPLE
BASED ON 0.125 MM THICK STENCIL
SCALE: 15X

EXPOSED PAD 25
76% PRINTED SOLDER COVERAGE BY AREA UNDER PACKAGE

4227032/A   08/2021

NOTES: (continued)

6. Laser cutting apertures with trapezoidal walls and rounded corners may offer better paste release. IPC-7525 may have alternate design recommendations.

重要なお知らせと免責事項

TI は、技術データと信頼性データ (データシートを含みます)、設計リソース (リファレンス・デザインを含みます)、アプリケーションや設計に関する各種アドバイス、Web ツール、安全性情報、その他のリソースを、欠陥が存在する可能性のある「現状のまま」提供しており、商品性および特定目的に対する適合性の黙示保証、第三者の知的財産権の非侵害保証を含むいかなる保証も、明示的または黙示的にかかわらず拒否します。

これらのリソースは、TI 製品を使用する設計の経験を積んだ開発者への提供を意図したものです。(1) お客様のアプリケーションに適した TI 製品の選定、(2) お客様のアプリケーションの設計、検証、試験、(3) お客様のアプリケーションに該当する各種規格や、その他のあらゆる安全性、セキュリティ、規制、または他の要件への確実な適合に関する責任を、お客様のみが単独で負うものとします。

上記の各種リソースは、予告なく変更される可能性があります。これらのリソースは、リソースで説明されている TI 製品を使用するアプリケーションの開発の目的でのみ、TI はその使用をお客様に許諾します。これらのリソースに関して、他の目的で複製することや掲載することは禁止されています。TI や第三者の知的財産権のライセンスが付与されている訳ではありません。お客様は、これらのリソースを自身で使用した結果発生するあらゆる申し立て、損害、費用、損失、責任について、TI およびその代理人を完全に補償するものとし、TI は一切の責任を拒否します。

TI の製品は、TI の販売条件、または ti.com やかかる TI 製品の関連資料などのいずれかを通じて提供する適用可能な条項の下で提供されています。TI がこれらのリソースを提供することは、適用される TI の保証または他の保証の放棄の拡大や変更を意味するものではありません。

お客様がいかなる追加条項または代替条項を提案した場合でも、TI はそれらに異議を唱え、拒否します。